TECHNICAL REPORT GL-83-1

CAVITY DETECTION AND DELINEATION RESEARCH

Report 5
ELECTROMAGNETIC (RADAR) TECHNIQUES APPLIED TO CAVITY DETECTION

by

Robert F. Ballard, Jr.

Geotechnical Laboratory
U. S. Army Engineer Waterways Experiment Station
P. O. Box 631, Vicksburg, Miss. 39180

July 1983

Report 5 of a Series

Prepared for Office, Chief of Engineers, U. S. Army
Washington, D. C. 20314

Under CWIS Work Unit No. 31150

Unclassified

SECURITY CLASSIFICATION OF THIS PAGE *(When Data Entered)*

REPORT DOCUMENTATION PAGE

READ INSTRUCTIONS BEFORE COMPLETING FORM

1. REPORT NUMBER
Technical Report GL-83-1

2. GOVT ACCESSION NO.

3. RECIPIENT'S CATALOG NUMBER

4. TITLE *(and Subtitle)*
CAVITY DETECTION AND DELINEATION RESEARCH; Report 5, ELECTROMAGNETIC (RADAR) TECHNIQUES APPLIED TO CAVITY DETECTION

5. TYPE OF REPORT & PERIOD COVERED
Report 5 of a series

6. PERFORMING ORG. REPORT NUMBER

7. AUTHOR(s)
Robert F. Ballard, Jr.

8. CONTRACT OR GRANT NUMBER(s)

9. PERFORMING ORGANIZATION NAME AND ADDRESS
U. S. Army Engineer Waterways Experiment Station
Geotechnical Laboratory
P. O. Box 631, Vicksburg, Miss. 39180

10. PROGRAM ELEMENT, PROJECT, TASK AREA & WORK UNIT NUMBERS
CWIS Work Unit 31150

11. CONTROLLING OFFICE NAME AND ADDRESS
Office, Chief of Engineers, U. S. Army
Washington, D. C. 20314

12. REPORT DATE
July 1983

13. NUMBER OF PAGES
107

14. MONITORING AGENCY NAME & ADDRESS*(if different from Controlling Office)*

15. SECURITY CLASS. *(of this report)*
Unclassified

15a. DECLASSIFICATION/DOWNGRADING SCHEDULE

16. DISTRIBUTION STATEMENT *(of this Report)*
Approved for public release; distribution unlimited.

17. DISTRIBUTION STATEMENT *(of the abstract entered in Block 20, if different from Report)*

18. SUPPLEMENTARY NOTES
Available from National Technical Information Service, 5285 Port Royal Road, Springfield, Va. 22161

19. KEY WORDS *(Continue on reverse side if necessary and identify by block number)*

Cavity detection
Crosshole
Electromagnetics
Geophysical exploration
Karstic
Radar (ground probing)

20. ABSTRACT *(Continue on reverse side if necessary and identify by block number)*
This study evaluated four different radar systems to determine their effectiveness in locating subterranean cavities. Tests were conducted at three well-documented sites: Vicksburg, Miss.; Medford Cave, Fla. (near Ocala); and Manatee Springs, Fla. (near Chiefland). None of the radar systems was effective at the Vicksburg, Miss., site because of extremely high conductivities encountered in the overburden materials which were comprised primarily of silts (loess) and clays. The following radar systems were used in this study:
(Continued)

DD FORM 1 JAN 73 1473 EDITION OF 1 NOV 65 IS OBSOLETE

Unclassified

SECURITY CLASSIFICATION OF THIS PAGE *(When Data Entered)*

20. ABSTRACT (Continued).

a. A pulsed system fabricated and operated by personnel from Texas A&M University.

b. A pulsed system commercially manufactured by GSSI operated by the owners, Technos, Inc.

c. A pulsed system developed, fabricated, and operated by personnel from SwRI.

d. A continuous wave system developed, fabricated, and operated by personnel from LLNL.

Tests were conducted at Vicksburg, Miss., using systems a, b, and c above. Systems b, c, and d were used at the Medford Cave, Fla., site; and systems c and d were used at the Manatee Springs, Fla., site. All of the systems were successful in locating cavities and other anomalous conditions at both Florida test sites. At the time these tests were conducted, only the SwRI system was capable of operating from the ground surface in the reflection mode and also in boreholes in crosshole fashion. (The GSSI system is currently available with borehole transmitter/receiver.)

Air-filled cavities on the order of 3 to 4 ft in diameter were detected and confirmed to depths of more than 20 ft at the Medford Cave site both from the ground surface and by crosshole tests. A cavity zone approximately 6 ft in height was detected by crosshole tests at Manatee Springs. Radar signals were successfully propagated to distances exceeding 100 ft in the crosshole mode at the Medford Cave site.

It was concluded that surface radar can be a very effective tool for locating subsurface anomalous conditions in limestones at sites where overburden materials are absent or have low dielectric and conductivity characteristics. Such sites would typically be comprised of low moisture content sandy materials. Use of surface radar at sites where the overburden is comprised mainly of clays will likely be ineffective. It was also concluded that crosshole radar was an effective tool for cavity detection (between boreholes) in limestone to borehole spacings of at least 30 ft.

PREFACE

The study reported herein was performed by personnel of the Geotechnical Laboratory (GL), U. S. Army Engineer Waterways Experiment Station (WES), during the period 1977 through 1980. The investigation was sponsored by the Office, Chief of Engineers (OCE), U. S. Army, as part of CWIS Work Unit 31150, "Remote Delineation of Cavities and Discontinuities in Rock." The OCE Technical Monitor was Mr. Paul R. Fisher.

Specific tasks were conducted under contract by Texas A&M University, Technos, Inc., Lawrence Livermore National Laboratory, and Southwest Research Institute. The project was conducted under the general supervision of Dr. W. F. Marcuson III, Chief, GL, and Dr. D. C. Banks, Program Manager for CWIS Materials-Rock Research Program, and under the direct supervision of Dr. A. G. Franklin, Chief, Earthquake Engineering and Geophysics Division (EEGD), GL. This report was prepared by Mr. R. F. Ballard, Jr., EEGD, GL. Other EEGD geophysicists actively involved in this and related projects were Messrs. J. R. Curro, Jr., S. S. Cooper, and D. K. Butler.

COL Tilford C. Creel, CE, was Commander and Director of WES during the preparation of this report. Mr. Fred R. Brown was Technical Director.

CONTENTS

CONVERSION FACTORS, U. S. CUSTOMARY TO METRIC (SI)
UNITS OF MEASUREMENT

U. S. customary units of measurement used in this report can be converted to metric (SI) units as follows:

Multiply	By	To Obtain
feet	0.3048	metres
gallons (U. S. liquid)	3.785412	cubic decimetres
inches	2.54	centimetres
miles (U. S. statute)	1.609347	kilometres
square miles	2.589998	square kilometres

CAVITY DETECTION AND DELINEATION RESEARCH

ELECTROMAGNETIC (RADAR) TECHNIQUES APPLIED TO CAVITY DETECTION

PART I: INTRODUCTION

Background

1. Because some U. S. Army Corps of Engineers (CE) projects have been and will be constructed over solutioned rock, a rapid, reliable methodology is needed to detect and delineate cavities and/or discontinuities in rock masses. In some instances, postconstruction leakage through these openings has necessitated extensive repair work. An extremely important prelude to the design of defensive measures against piping in a new dam is the development of an understanding of which formations are solution prone and the extent of solutioning. In the case of remedial measures, of course, the location and geometry of the cavities through which the water is moving is paramount. Presently, close interval drilling or excavation are the only methods which will provide accurate location. Drilling and excavation are direct exploration methods. To drill enough borings to ensure detection and define the extent of all significant cavity systems is too expensive and time-consuming. Excavation is even more costly and even if the excavation is necessary for another reason (for instance, a core trench), the information gained is not available until after construction is in progress, hence, the reason for establishment of this research effort, to evaluate the effectiveness of indirect methods.

2. In the early years of this investigative effort, the primary thrust was directed toward the general improvement of geophysical methods for CE applications. As the cavity detection problem became more clearly defined, an effort was made to determine the state of the art with regard to geophysical methods applicable to the situation and to determine their advantages and limitations when applied to the problem of cavity detection/delineation.

3. In July 1977, a Symposium on the "Detection of Subsurface Cavities" was held in Vicksburg, Miss. Shortly thereafter, a meeting on the state of the art of ground-probing radar was also held at the U. S. Army Engineer Waterways Experiment Station (WES). Both stimulated a great deal of interest in the possible use of electromagnetics (EM) commonly called ground-probing radar. Its operating principles will be discussed later in this report. Earlier (1976), a test site had been constructed on the WES Reservation to simulate underground cavities using polyvinyl chloride (PVC) pipes of varying lengths and diameters buried in loess material at depths of 10 and 20 ft,* respectively (Butler and Murphy, 1980). Ground-probing radar tests (in addition to numerous other geophysical methods) were conducted to determine whether existing radars could be used to successfully detect the man-made anomalies. One series of tests was conducted by Dr. R. R. Unterberger of Texas A&M University (Unterberger, 1978). A second series of tests was conducted by Mr. R. C. Benson of Technos, Inc. (Benson, 1978), and a third series of tests was conducted by the Southwest Research Institute (SwRI) (Duff and Suhler, 1980). Results of all three tests were somewhat disappointing in that the three radar systems were unable to detect cavities buried as shallow as 10 ft or even culverts more than 3 ft deep on the WES Reservation. The reports on the work are on file at WES. However, a great deal was learned with regard to limitations imposed by different earth materials on the penetration of radar signals. It was determined that the conditions of extremely high electrical conductivities** imposed by the test site, which consisted of very moist loess material, were among the worst that could be presented to propagation of EM signals; only a wet clay would have probably been worse. The dielectric constant at the WES site was in the range of 15 to 20. Typical values for limestones range from 6 to 8. In view of the fact that all three contractors were unsuccessful in their attempts to locate the

---

* A table for converting U. S. customary to metric (SI) units of measurement is given on page 3.

** Definitions of pertinent terms used in this report are given on page 7.

simulated cavities at WES with radar, no further discussion regarding EM work at WES will be presented in this report. Since the WES-simulated cavity test site was not representative of the dielectric constants found in limestone and dolomites, it was decided that a well-designed field effort must be made to evaluate the true potential of radar methods.

4. It was decided that two natural test sites located in karstic areas would be used to evaluate radar methods. A number of candidate areas were considered before final selection of two natural sites, located near Ocala and Chiefland, Fla., respectively, was made in early 1979. Most of the field testing was done during the summers of 1979 and 1980. Other cavity detection methods besides radar were evaluated at this site. For the results of these studies, see Ballard (1982); Butler (1983); Butler, Whitten, and Smith (1983); Cooper (1982); and Curro (1983).

Objectives

5. The objectives of this report are to develop and evaluate surface and borehole radar techniques for detecting and delineating (mapping) subsurface cavities and to present and evaluate the results of surface and borehole radar probings performed at the test sites of Medford Cave and Manatee Springs, Fla.

Approach

6. In an effort to reach the stated objectives systematically, the following steps were performed:

a. Select representative test sites for evaluation of the radar systems.

b. Thoroughly document the test sites.

c. Conduct surface radar tests.

d. Conduct cross borehole radar tests.

e. Evaluate and compare test results.

Scope of Report

7. The scope of this report will include a discussion of the background and application of basic EM principles of wave propagation to the problem of cavity detection. The tests conducted by Technos, Inc., SwRI, and the Lawrence Livermore National Laboratory (LLNL) will be evaluated and conclusions and recommendations will be developed from results of the investigations. Appendix A is the report submitted by LLNL documenting their field investigations at both Medford Cave and Manatee Springs, Fla.

Definitions of Pertinent Terms

8. Certain terms used in this report are defined as follows:

a. Absorption coefficient. A signal loss coefficient derived from relationships between frequencies, conductivity, magnetic, and dielectric properties of the material through which the EM wave is propagating.

b. Angle of incidence. The angle between the normal to the surface at the point of incidence and the line of propagation approaching the surface.

c. Antenna gain. For a directonal antenna, the average of the power radiated through the half-power angle of the antenna divided by the power radiated in the direction of maximum radiation by a half-wave dipole.

d. Bandwidth. The difference between the limiting frequencies of a continuous frequency band. The bandwidth of a device is the difference between limiting frequencies where performance falls within specified limits.

e. Conductivity. The electrical conductance of a material having unit length and unit cross section.

f. dbm. Decibel referred to one milliwatt.

g. Decibel (db). A means for expressing the difference in intensity of electric or acoustic signal power at two points. The power intensity in decibels is equal to 10 times the common logarithm of the ratio of the two amounts of power. The abbreviation db is commonly used.

h. Dielectric constant. That property of a material that determines the electrostatic energy stored per unit volume for unit potential gradient; synonymous with permittivity.

i. Loss tangent. The relation between the dielectric constant and conductivity at a given frequency; synonymous with dissipation factor.

j. Microwaves. Radio waves that have wavelengths so short that they exhibit some of the properties of light.

k. Power reflection coefficient. The ratio of the reflected power density at the surface of a material to the incident power density.

PART II: BASIC PRINCIPLES OF EM

Early History

9. In the early 1900's, successful experiments were conducted in the propagation of EM waves, commonly referred to as "radio." These experiments proved the feasibility of generating EM waves, transmitting them through space as a beam, and receiving a reflected signal from an object which interrupted the beam path. During the 1920's and 1930's, a great deal of progress was made in the development of intense sources of EM waves at wavelengths of 10 cm, 3 cm, and shorter with peak powers of radiation energy approaching the megawatt range. During the war years, from 1940 to 1945, technical advances were extremely rapid though primarily for airborne applications. Nevertheless, much of this technology was also applicable to transmission of EM signals through solids, such as soil and rock. Microwave sources have since been routinely employed with appropriate detection circuits for the accurate location of planes, ships, clouds, land forms, and, in fact, any object capable of scattering EM waves. Such systems which were based on the principle of scattering and reflection of EM waves were ultimately given the acronym radar (radio, detection, and ranging).

10. Radar technology has been refined to a degree that will permit not only the detection of objects, but also the recognition of certain details of objects by their characteristic scattering and absorption coefficients. Determination of range is based on the experimental fact that EM waves travel through free space with a constant velocity of 299,792 km/sec. Consequently, the measure of total lapsed time of flight in air from the instant the wave leaves an antenna, strikes a target, and returns is the measure of distance to the target.

11. In the early 1950's, experiments were conducted using the radar as a means of probing through solids. It was quickly recognized that the wave speed and its amplitude as a function of distance through the solid could vary drastically from one material to another.

Wave Velocity and Absorption

12. A number of factors control the velocity and absorption characteristics of a radar wave. Consider that the attenuation of a propagating plane EM wave in a dielectric medium such as the earth is given by the expression

$$E = E_o e^{-\alpha x} \tag{1}$$

where

E_o = the initial EM field intensity, v/m
α = the absorption coefficient, m^{-1}
x = the propagation distance, m

13. Generally, absorption is expressed in terms of decibels per metre. The absorption loss, A , is given by

$$A = 20\alpha/2.3 = 8.7\alpha \text{ db/m} \tag{2}$$

then

$$E = E_o e^{-0.115Ax} \tag{3}$$

14. The absorption coefficient is strongly frequency-dependent and is a function of the electrical conductivity, the magnetic susceptibility or permeability, and the relative dielectric constant of the medium. For a medium of negligible magnetic permeability, such as soils, this relationship is given by

$$\alpha = 0.014f\sqrt{K}\left(\sqrt{1 + \tan^2 \delta} - 1\right)^{1/2}{}_m{}^{-1} \tag{4}$$

where

$\tan \delta$ (the loss tangent) = $18\beta/Kf$
β = the conductivity of the medium, millimhos/m
K = the relative dielectric constant, dimensionless
f = frequency, MHz

15. The moisture content of the earth material is the single most important factor affecting EM absorption loss. An increase in moisture content of the soil or other earth material greatly increases both the electrical conductivity and the dielectric constant of the earth. The magnitude of the effect of moisture depends on the composition and porosity of the ground material. The dielectric constant at normally used ground-penetrating radar frequencies is generally in the range of 3 to 30 as illustrated in Figure 1. The dielectric constant of most dry soils or rocks is in the range 3 to 10. The dielectric constant of pure water is 81.

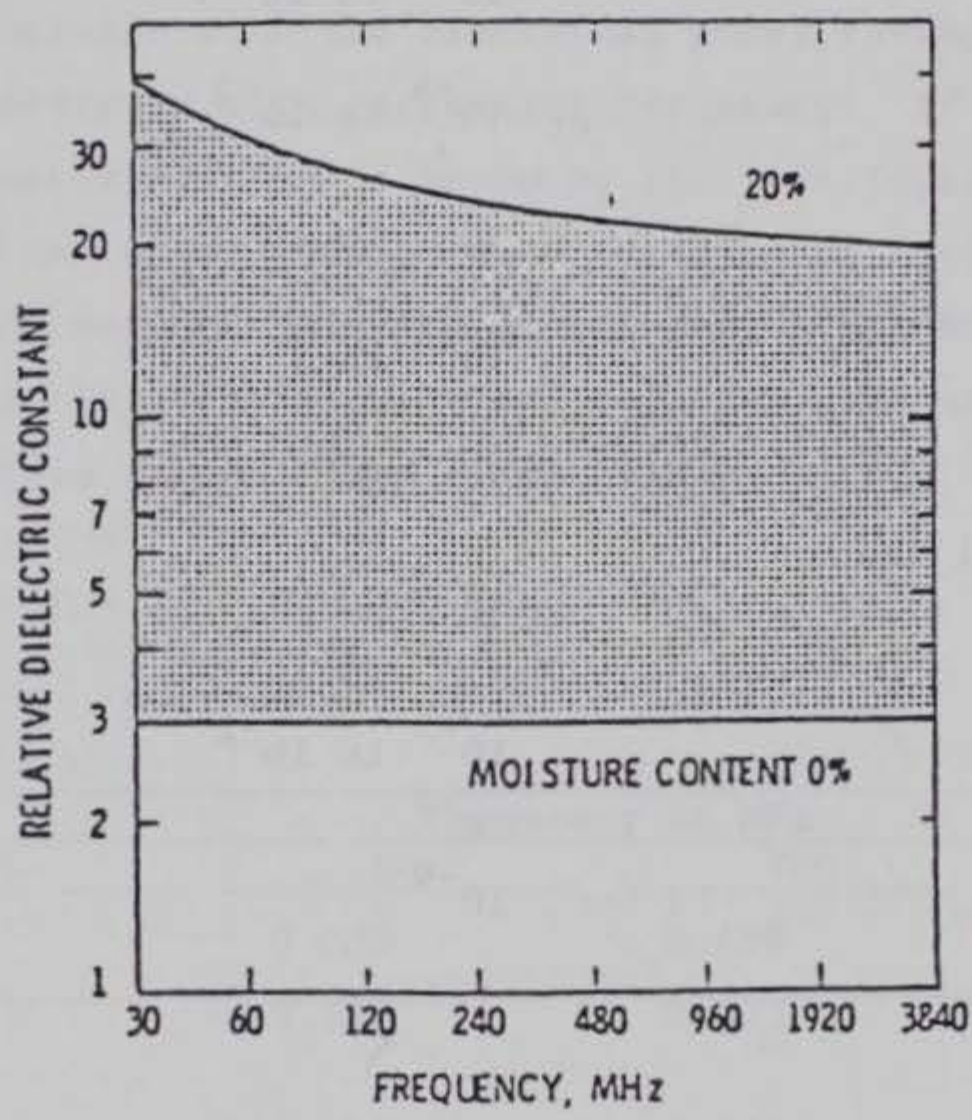

Figure 1. The relative dielectric constant of typical soils for moisture content in the range 0 to 20 percent by weight (20 percent corresponds to saturated soil) (from Battelle Laboratories, 1981)

16. To provide the reader with a feel for approximate values of conductivity and dielectric constants of various materials as determined by various investigators (Kraichmann, 1970; Wait, 1971; Von Hippel, 1954; Lundien, 1966), Table 1 is included.

Table 1

Approximate VHF Electromagnetic Parameters of Typical Earth Materials

Material	Approximate Conductivity σ (mho/m)	Approximate Dielectric Constant ε_r
Air	0	1
Fresh water	10^{-4} to 3×10^{-2}	81
Sea water	4	81
Sand "dry"	10^{-7} to 10^{-3}	4 to 6
Sand, saturated (fresh water)	10^{-4} to 10^{-2}	20
Silt, saturated (fresh water)	10^{-3} to 10^{-1}	30
Clay, saturated (fresh water)	10^{-1} to 1	40
Dry, sandy, flat coastal land	2×10^{-3}	10
Rich agricultural land low hills	10^{-2}	15
Fresh water ice	10^{-4} to 10^{-2}	4
Permafrost	10^{-5} to 10^{-2}	4 to 8
Granite (dry)	10^{-8}	5
Limestone (dry)	10^{-9}	7

17. Additional loss factors which affect the performance or effectiveness of a given ground-penetrating radar system include reflective losses at the air-ground interface, geometrical spreading of the transmitted radar beam, the effective backscattering cross section of the reflective target, and the spreading of the reflected signal. A positive factor is a refractive gain due to the focusing effect of the dielectric medium (Battelle Laboratories, 1981).

18. In order to achieve adequate propagation distances in solids, such as the earth, radar wavelengths on the order of 10 m must be used

(Equation 4). Because many ground materials are highly absorbant of short wavelength EM energy, a tradeoff between resolution and penetration must be realized. In reality, the absorption characteristics of subsurface materials are such that radar wavelengths greater than about 0.5 m will be required to gain appreciable penetration (Battelle Laboratories, 1981).

19. Since penetration depth or distance is generally one of the first questions addressed by the user, it must be realized that it is quite difficult to estimate a radar system's capability to penetrate to a certain depth before the survey is actually run. Obviously, penetration depth will increase with the electrical power rating of the system. Penetration will decrease with increasing frequency. If beforehand knowledge of the material type is known by the investigator, however, attenuation rates can be calculated as a function of frequency if the dielectric constant and conductivity of the medium are known. Table 2 can be used (Morey, 1974) as a guide for relative attenuations of the EM signals in certain common types of materials.

Table 2*

Attenuation in Decibels/Metre

Material	Frequency in MHz			
	1	10	100	500
Pure water	0.025	0.039	0.408	16.191
Sandy soil (moist)	0.471	0.513	0.773	4.047
Clay soil (dry)	0.013	0.075	0.425	1.649
Clay soil (moist)	0.780	3.803	17.93	53.75
Sea water	34.50	108.54	326.54	592.03
Granite (dry)	0.732×10^{5}	0.732×10^{-5}	0.732×10^{-5}	0.732×10^{-5}

* From Morey (1974).

20. Several investigators have reported maximum depths of penetration achieved while conducting tests under a wide variety of conditions. Table 3 (Bowders, Lord, and Koerner, 1982) is a recently published summary. Most of the radar systems in use today use peak pulsed powers and the order of watts to hundreds of watts.

Table 3*

Details of GPR Methods

Investigator(s)	Approximate Frequency Range, MHz	Maximum Depth, m	Major Application Area
Cook	1-100	225	Locating faults, walls, holes
Rosetta	100-200	15	Locating faults, caverns, water, utilities
Morey	100-200	15	Locating faults, caverns, water, utilities
Dolphin et al.	15-50	40	Locating rock cavities
Unterberger	230	500	Salt thickness measurement
Harrison	35	2000	Determining ice thickness
Rubin et al.	100-200	10	Detecting subway tunnels
Rubin and Fowler	100-200	15	Drilling guidance, subway tunnel monitoring, coal thickness
Benson and Glaccum	100-200	10	General subsurface probing, locate and follow pollutants in ground, detection of buried containers of industrial wastes
Sandness et al.	100-200	10	General subsurface probing as described above
Alongi	1000	3	Locating mines, pavement thickness, shallow voids, pipelines
Moffatt and Puskar	6000	3	Locating faults, joints, cavities, pipelines

* From Bowders, Lord, and Koerner (1982).

Future Development

21. An attempt has been made by Cook (1981) to describe ultimate depth penetration and resolution capabilities of a state-of-the-art EM system. Cook also attempts to extrapolate to systems that might be developed in the future. In so doing, he used several combinations of parameters; namely, wavelengths of 1 and 3 m, and distances or depths of penetration of 30, 100, and 300 m. He graphically portrayed the results in the form of a calculated round-trip amplitude loss versus wave type and rock type. He concluded that many of today's ground-penetrating radars have a "performance figure" or signal recovery range in the vicinity of 110 db, and at least one system is estimated to be capable of a "performance figure" of 140 db, the latter producing pulses of 2 megawatts peak power.

22. In Cook's opinion, improved pulsed radar systems of the future probably would not exceed a peak transmitter power greater than 20 megawatts thereby improving the performance figures by only 10 db. He further states that by combining all foreseeable improvements, a radar having a performance figure of 200 db may eventually become feasible. With a performance figure such as this, a radar would then be able to detect voids on the order of 1 to 3 m in diameter at a maximum depth of 200 m in granites.

Types of Radar Systems

23. Several types of radar systems have been and are currently used for ground-probing applications. Some of these are the pulse, short pulse, continuous wave (CW), and frequency modulated-continuous wave (FM-CW). Each of these has specific advantages but inherent disadvantages. The pulse radar has been successfully used by Unterberger (1978) to penetrate to several hundred feet in salt formations. This device has not achieved any success in soil materials. A conventional pulse system has a relatively high power output and its inherent long pulse length, several hundred nanoseconds, consists of many cycles of

the carrier frequency, thus causing dead times greater than the total possible propagation in soil materials; i.e., the transmit pulse is still ringing when the reflected signal is returning.

24. Another type of radar system is the short pulse consisting of a single cycle of a sine wave. It has broad bandwidth but also a generally lower power output. Typically, pulse widths used are from 1 to 10 nsec and, in some instances, are capable of penetrating to depths of 100 ft in earth materials with high resolution. Both long and short pulse systems operate on the principle of inducing a single pulse, then abruptly ceasing transmission, followed by a dead time in which reflected signals would be returned to the receiver.

25. A third system operates by transmitting a continuous signal at a single frequency and is commonly called a CW radar. This type system has been used by the LLNL with transmitter and receiver displaced in different boreholes. It is not designed nor intended for ground surface use.

26. A fourth system is the swept frequency radar, which is commonly called the FM-CW system. It operates principally in the reflection mode transmitting a swept frequency signal which becomes mixed with the received signal. The data are analyzed on a real-time basis using a Fourier spectrum analyzer. This type system is inherently narrow band and ordinarily requires a great deal of hardware and associated software, thus making it rather difficult and expensive to use as a portable-type system.

27. A fifth, and relatively new system, described by Lundien (1978) and Fowler, Rubin, and Sill (1980) is called a synthetic pulse radar. It differs from the short pulse system in that instead of transmitting a single broad band pulse, it transmits the frequency spectrum of that pulse. Amplitude and phase data are acquired, and a reflection received from a target is generated by performing an inverse Fourier transform on the data. It appears that the synthetic pulse system might have operational advantages over the other systems previously described. Its concept dictates that only one frequency is transmitted at a time and the system can operate in a high-gain, narrow-band mode, similar to

a CW system. It can also be described as a "swept pulse" because a wide band of discrete frequencies is used during a single test. Only milliseconds are spent at each frequency of a test run, thus allowing a complete sweep to be performed very rapidly. Disadvantages are that the electronics package required is more complicated than that used in conventional short pulse systems. Also, since data are recorded in the frequency rather than the time domain format, an appreciable amount of processing is required even before preliminary data interpretation can be done. Consequently, extra equipment is needed in the field. Another complication is associated with the expanded dynamic range of the equipment; inherently, it must be able to recognize small signals recorded in the presence of large ones. According to Fowler, Rubin, and Sill (1980), advantages far outweigh limitations. Successful tests have been conducted through 200 ft of coal, and future refinements on units operating on the synthetic pulse concept may well represent the foundation for an evolution resulting in the ultimate radar of the future. Table 4 is a comparison of the WES-developed synthetic pulse system (Lundien, 1978) and a commercially available pulse system.

Table 4*

Comparison of Synthetic Pulse WES-Developed System and the Short Pulse System Manufactured by GSSI

	WES	GSSI
Pulse repetition frequency (PRF), pulses/sec	100	50,000
Measurement sweep time, sec	0.01	0.06
Wave form repetition rate, pulses/sec	2.5	16
Average transmitter power, mw	10	5.2
Effective peak power, w	60,000	35
Effective pulse width, nsec	1.67	3-8.3
Transmitter bandwidth, MHz	10-8400 500-2000	100±60 300±150

* From Lundien (1978).

Texas A&M radar system

28. The ground-probing radar system used by Professor R. R. Unterberger of Texas A&M University to conduct tests at the WES site in Vicksburg, Miss., was described in detail in a report by Unterberger (1977). Professor Unterberger stated that the equipment is essentially a modified airborne radar altimeter ordinarily used to measure the airplane's altitude above the earth. It is an FM-CW radar system. The radar energy has been concentrated by the use of horns on both the transmitter and receiver. In operation, the FM-CW radar is linearly swept through a frequency range by modulating a microwave magnetron. The transmitter emits signals at all times (hence, the CW), but is frequency-modulated in a linear fashion. Radar echoes (reflections) are received from dielectric discontinuities in the earth at some later time when the transmitter is operating at another frequency. The beat frequency of the received signal and the portion of the instantaneous transmitted signal is a measure of the range to the target when the radar wave speed in the medium through which the signal has been transmitted is known. Figure 2 is a block diagram of the Texas A&M (Echo II) radar system. Figure 3a is a photo of the Echo II equipment in operation, and Figure 3b is a photo of the Echo II horns probing horizontally.

Technos radar system

29. The ground-probing radar system used by Technos, Inc., was suited only for surface use. It is a commercially available unit, manufactured by Geophysical Survey Systems, Inc. (GSSI), designated as Model No. 4700P (see Table 4). This unit is a pulsed system used with two antennas and consists of a radar set, a prerecord/playback unit, a magnetic tape recorder, a graphic recorder output display, and a portable generator power source. Either a single antenna or separate antennas can be used for transmit and receive when connected to the radar unit by cables up to 200 ft long. The transmitter is built into the transmit antenna housing and a preamplifier is built into the receive antenna housing for dual antenna operation. This reduces impedance matching and signal loss problems encountered when long transmission lines are used. Separate transmitting and receiving antennas

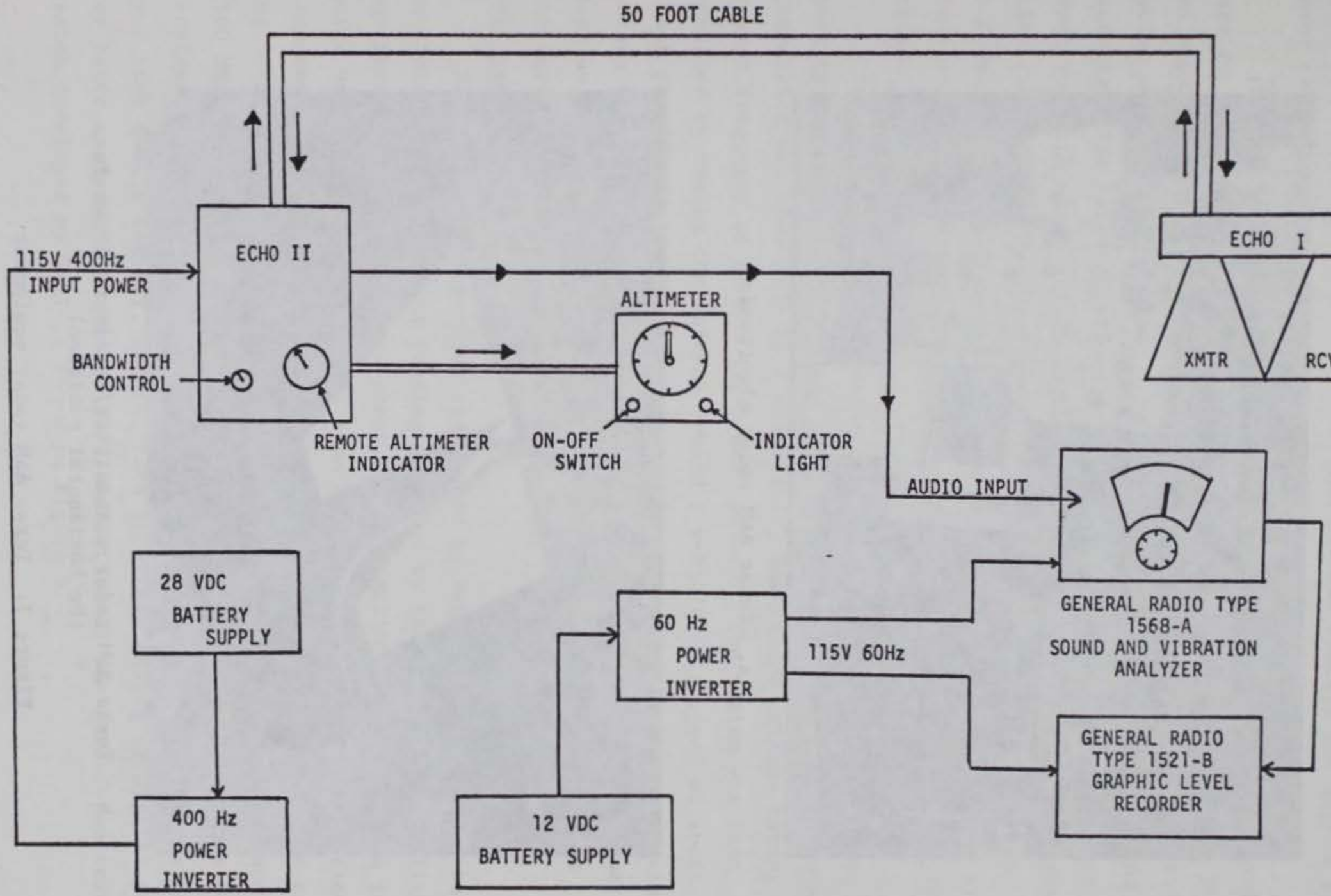

Figure 2. Block diagram of Echo II radar system
(furnished by Texas A&M)

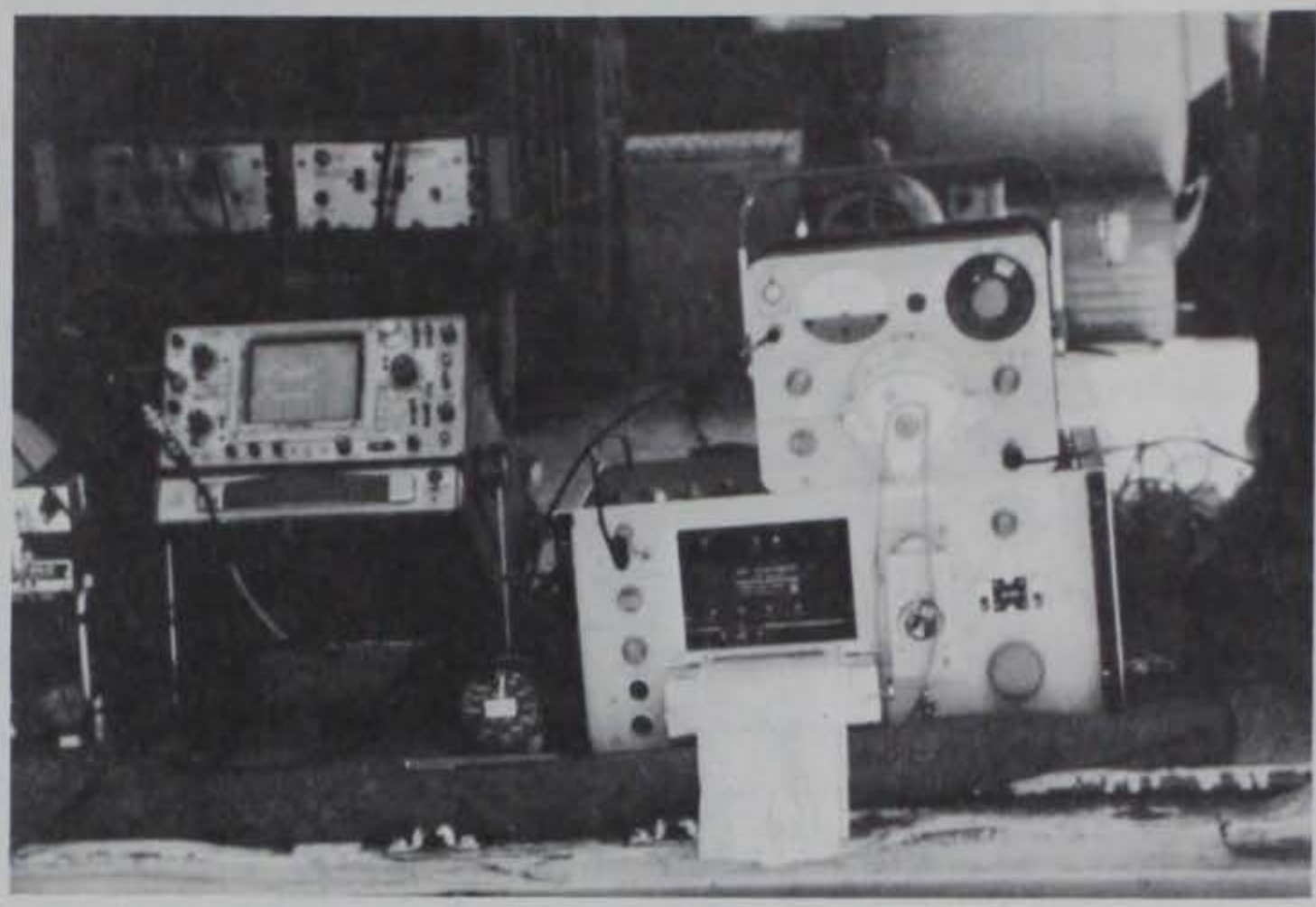

a. Texas A&M radar electronics

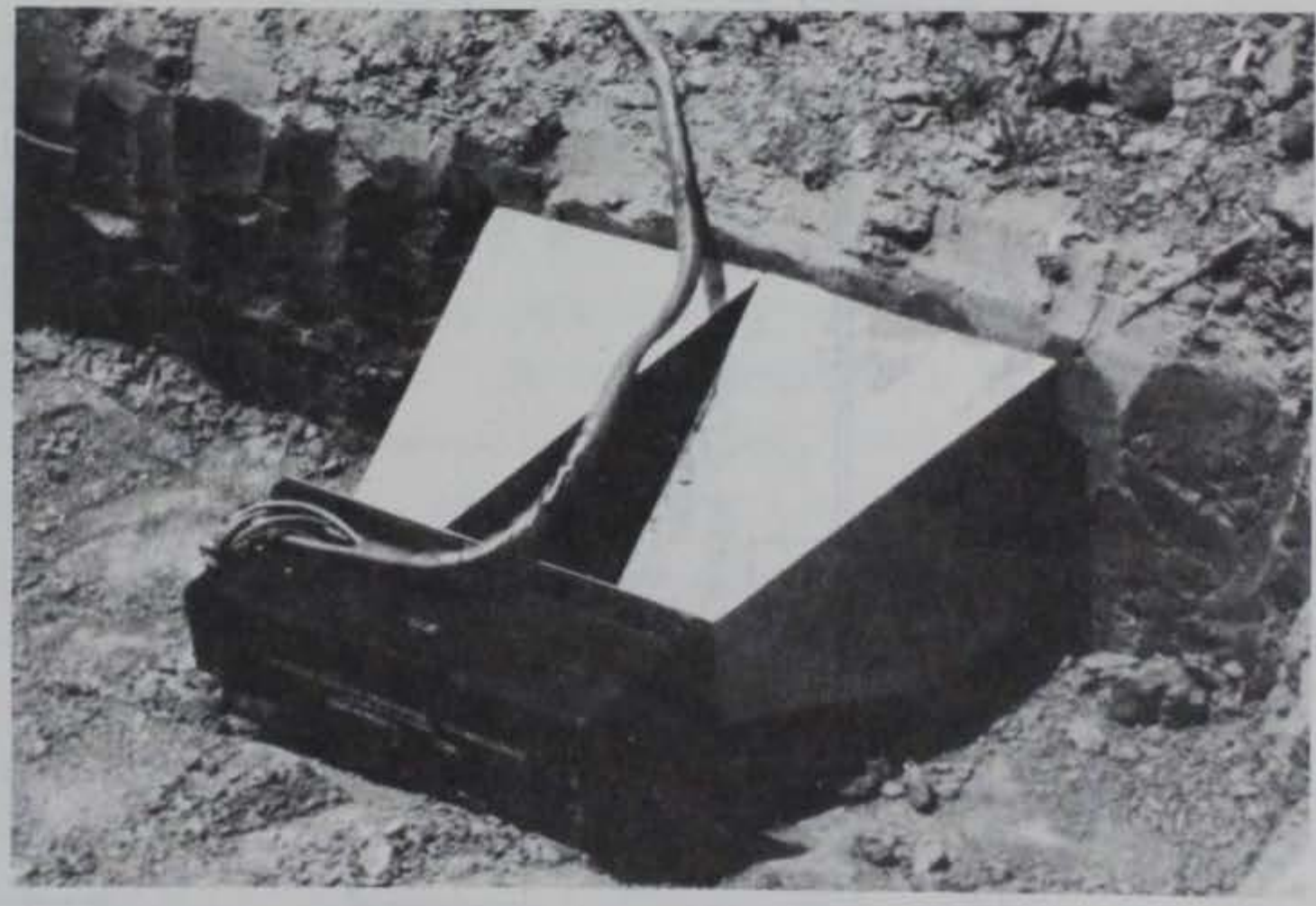

b. Texas A&M radar transmitter/receiver (shown in the horizontal position)

Figure 3. Texas A&M radar equipment

allow a greater pulse power to be used without concern for signal feed-over or overloading the receiver circuit.

30. In operation, a power supply furnishes a regulated DC voltage to the transmitter, which when triggered, generates a voltage pulse of approximately 3 nsec in time duration. The resulting quasigaussian pulse wave form is radiated into the earth by means of a broad band antenna. The radiated signal is an EM transient having a frequency spectrum with -3 db points at about 30 and 120 MHz. The pulse repetition rate is 500 MHz, peak power is 35 watts, and average power is 5.2 mw. A two-way transmission loss of 110 db is claimed for the system indicating the ratio of peak radiated power to minimum detectable received signal power.

31. When the test sequence started at the Medford Cave site, data quality was recognized as being extremely poor with the 300-MHz antenna. Conversion was then made to a monostatic, unshielded antenna having a center frequency of 80 MHz (12.5-nsec pulse). The system was then operated by towing the antenna behind a vehicle at a speed of about 2 mph providing a near real-time graphic record as the antenna scanned across the surface of the ground. Data were also recorded on magnetic tape on most of the traverses for later processing. Figure 4 is a photograph of the Technos radar equipment.

SwRI radar system

32. The ground-probing radar used by SwRI was designed and built in their laboratory using funding provided by the U. S. Army Mobility Equipment Research and Development Command (MERADCOM). The system is quite versatile and can be used from the ground surface in the reflection mode or in a borehole-to-borehole configuration for crosshole testing. In operation, the SwRI system emits 10-nsec duration EM pulses (100 MHz) from the transmitter. The full wave form of the impulse is received, converted to a low-frequency replica of the real-time pulse by a time domain sampler, and recorded in either analog or digital form for later analysis. A conceptual illustration of the ground-penetrating system developed by SwRI is shown in Figure 5.

Figure 4. Technos radar system

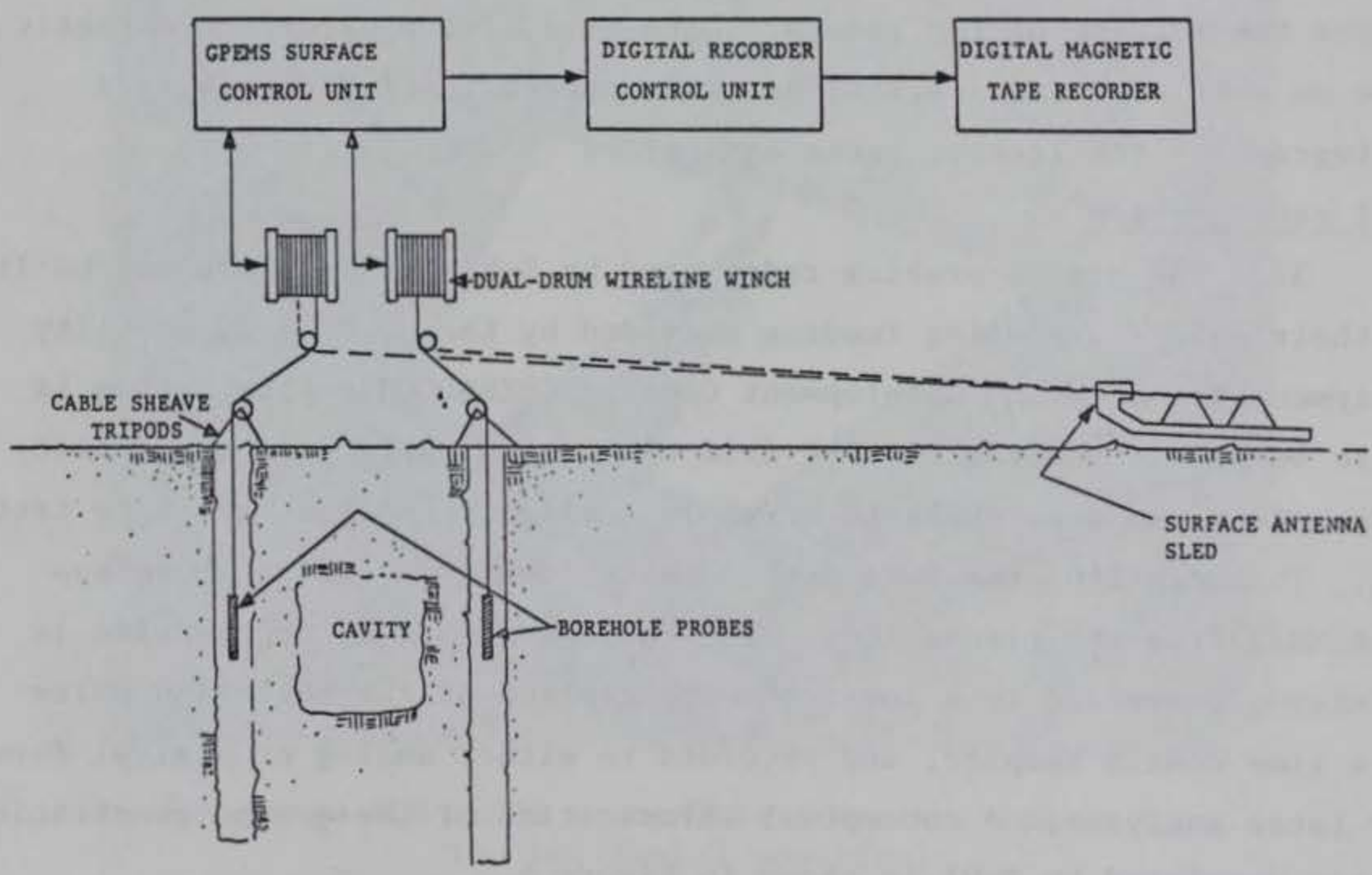

Figure 5. SwRI radar concept schematic

LLNL radar system

33. The LLNL ground-probing radar equipment operates on a slightly different principle than that used by SwRI or Technos. Where the SwRI and GSSI systems use a short rise-time pulse and a receiver which monitors the transmission time of the pulse and its signature, the LLNL approach is to use a frequency scan to determine that discrete frequency best suited for probing the area between boreholes. Ideally, the chosen frequency will be the highest (shortest wavelength) frequency that can be received with confidence. The swept frequency concept is not ordinarily used by LLNL because it requires considerably more time to conduct the tests. Rather, the single frequency restrictive to a narrow bandwidth, typically 1 kHz, is used because it brings system noise levels down to the point where signals as low as -110 dbm can be analyzed.

34. In practice, once a frequency has been chosen, the LLNL transmitter is carefully controlled to provide a constant power output. The receiver signal is then observed for the appearance of prominent nulls or minima in the signal level as a function of depth. One mechanism of signal interaction with cavities as observed by LLNL seems to be diffraction in addition to refraction or reflection. Consequently, as the transmitter and receiver are moved simultaneously in different boreholes, a distinct signal null (minima) may appear at both the top and the bottom of the anomaly. If the cavity is fully or partially filled with a soil material, the maximum signal loss may occur at the widest point of the cavity. When signal losses are observed at a particular depth, transmitter and receiver can be offset (held at different depths) so that a "skewed run" can be made to determine the geometry of the anomaly in two dimensions.

PART III: SITE DESCRIPTIONS AND TESTS CONDUCTED

Medford Cave, Florida

35. Medford Cave test site is located approximately 12 miles north of Ocala, Fla., in an area of karst topography and has been a local spelunker attraction for a number of years. The cave system exists in limestone covered by 3 to 6 ft of soil (primarily silty sands averaging about 8 percent moisture content) and has known passageways whose roofs range from 10 to 22 ft below the ground surface. Figure 6 is a plan view of the Medford Cave system as mapped by personnel of the SwRI showing the grid system used for geophysical surveys and the location of exploratory borings placed at the site. The general geology of the area and of Medford Cave site in particular is covered in a report by Mr. William D. Reves, which is included as Appendix A in Butler (1983).

Technos tests

36. The surface ground-probing radar investigation conducted at Medford Cave by Technos used the GSSI Model 4700P radar system previously described. Technos used two different antenna systems. The first was a bistatic shielded antenna having a center frequency of about 300 MHz (3-nsec pulse). At the beginning of the test program, data quality obtained with this antenna was recognized as being extremely poor and conversion was made to a monostatic, nonshielded antenna having a center frequency of about 80 MHz (12.5-nsec pulse). The system was deployed in the towed traverse mode providing a continuous near real-time graphic record by scanning the antenna across the surface of the ground. The locations of the radar traverses were chosen by CE representatives on-site. Both Technos and SwRI conducted the majority of their tests along the same traverses. In the course of testing, Technos recorded data on magnetic tape on most of the traverses for later processing.

37. Some sampling was done with the antenna stationary providing a static record of reflecting horizons. This technique was used to

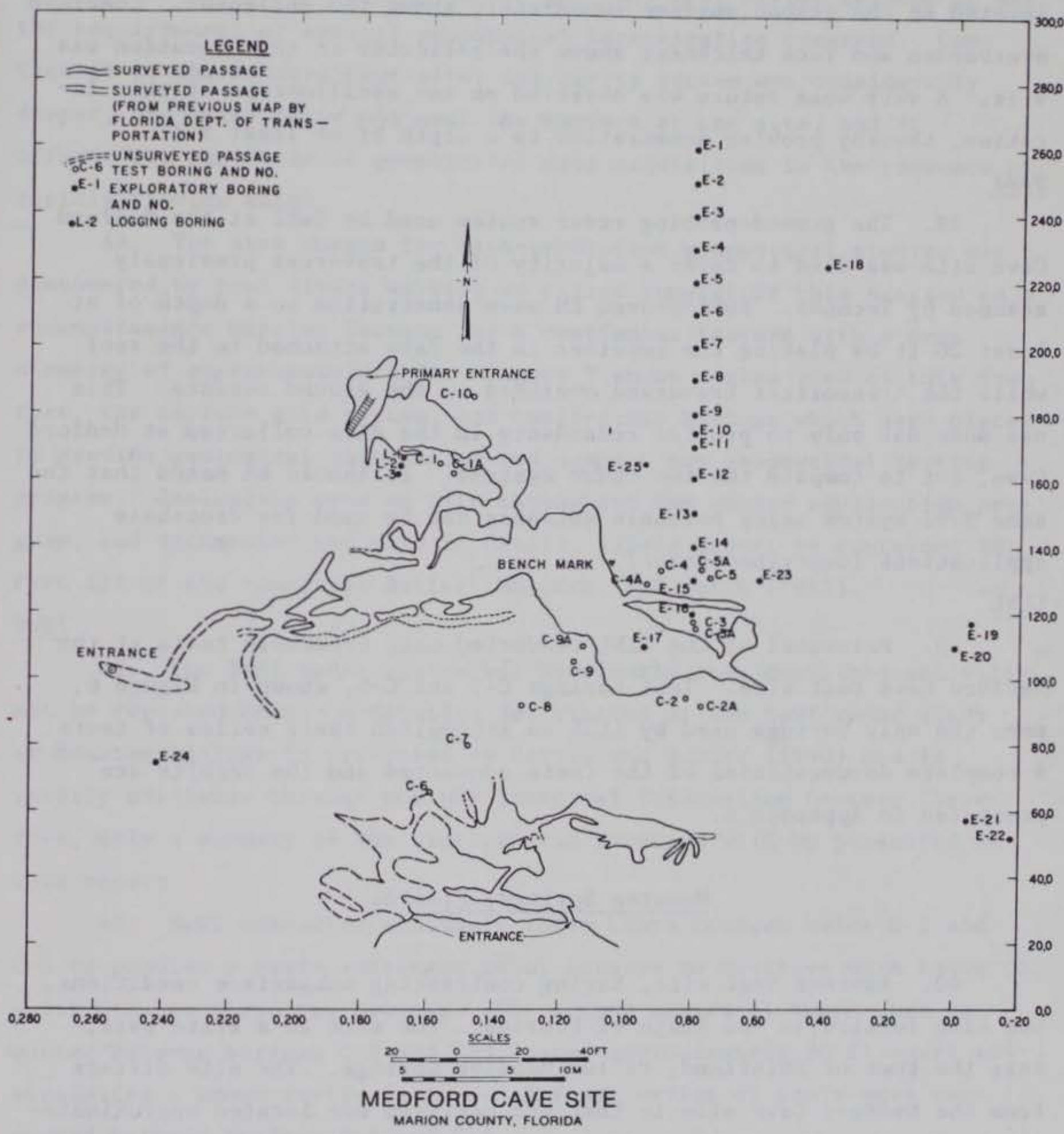

Figure 6. Medford Cave site map and locations of borings

calibrate the data interpretation for the site. In one instance, a metal foil reflector was placed inside the secondary entrance and attached to the roof of the cave. The radar transmitter/receiver was then located on the ground surface immediately above the reflector. Combined overburden and rock thickness above the reflector at this location was 9 ft. A very weak return was observed on the oscilloscope at this location, thereby proving penetration to a depth of at least 9 ft.

SwRI

38. The ground-probing radar system used by SwRI at the Medford Cave site was used to cover a majority of the traverses previously scanned by Technos. SwRI proved EM wave penetration to a depth of at least 20 ft by placing the receiver in the cave attached to the roof while the transmitter traversed overhead on the ground surface. This was done not only to provide redundancy in the data collected at Medford Cave, but to compare the two radar systems. It should be noted that the same SwRI system using borehole antennas can be used for crosshole applications (described later).

LLNL

39. Personnel of the LLNL conducted only crosshole tests at the Medford Cave test site. Test borings C-3 and C-5, shown in Figure 6, were the only borings used by LLNL to accomplish their series of tests. A complete documentation of the tests conducted and the results are presented in Appendix A.

Manatee Springs, Florida

40. Another test site, having contrasting subsurface conditions, was also located in the State of Florida. The site is a state park, near the town of Chiefland, called Manatee Springs. The site differs from the Medford Cave site in that the cavities are located approximately 100 ft below the ground surface, are water-filled, and were mapped by cave divers. Overburden materials were primarily silty sands. The cave system extends several miles to the southeast of its mouth, at which the volume of flow is approximately 82,000 gpm. The actual test

locations were near the mouth of the subterranean system. The system has been mapped by the Cave Diving Section of the National Speleological Society. Manatee Springs was chosen for this test series because it met the requirements of several geophysical investigation programs. Contrasted to the Medford Cave site, its cavity system was considerably deeper, the water table was near the surface at the site, and it offered the challenge of geophysical data acquisition in the presence of rapidly flowing water.

41. The area chosen for high-resolution geophysical studies was discovered by cave divers working in direct support of this program on a reconnaissance mission looking for a continuous feature with a mean diameter of approximately 6 ft. Figure 7 shows a plan view of this feature, the surface grid system, and exploratory borings which were placed to provide geological information and support the geophysical testing program. Geologists were on site throughout the entire exploration program, and documented the site in detail. Their report is contained in Part III of the report by Butler, Whitten, and Smith (1983).

SwRI

42. The SwRI radar system has previously been described and will not be repeated here. A detailed description of the SwRI radar study at Manatee Springs is presented by Herzig and Suhler (1980) and is readily available through the WES Technical Information Center; therefore, only a summary of the test program findings will be presented in this report.

43. SwRI conducted crosshole radar tests between holes C-2 and C-5 to provide a basic reference point because no cavities were known to exist between these two borings. The second series of tests were conducted between borings C-2 and C-3 spaced approximately 30 ft apart and straddling a known cavity feature. A final series of tests were conducted between borings C-3 and C-4.

LLNL

44. Crosshole radar tests were conducted by the LLNL during the summer of 1980 and are contained in their entirety herein as Appendix A. Radar scans were made between holes C-3 and C-2 with the transmitter in

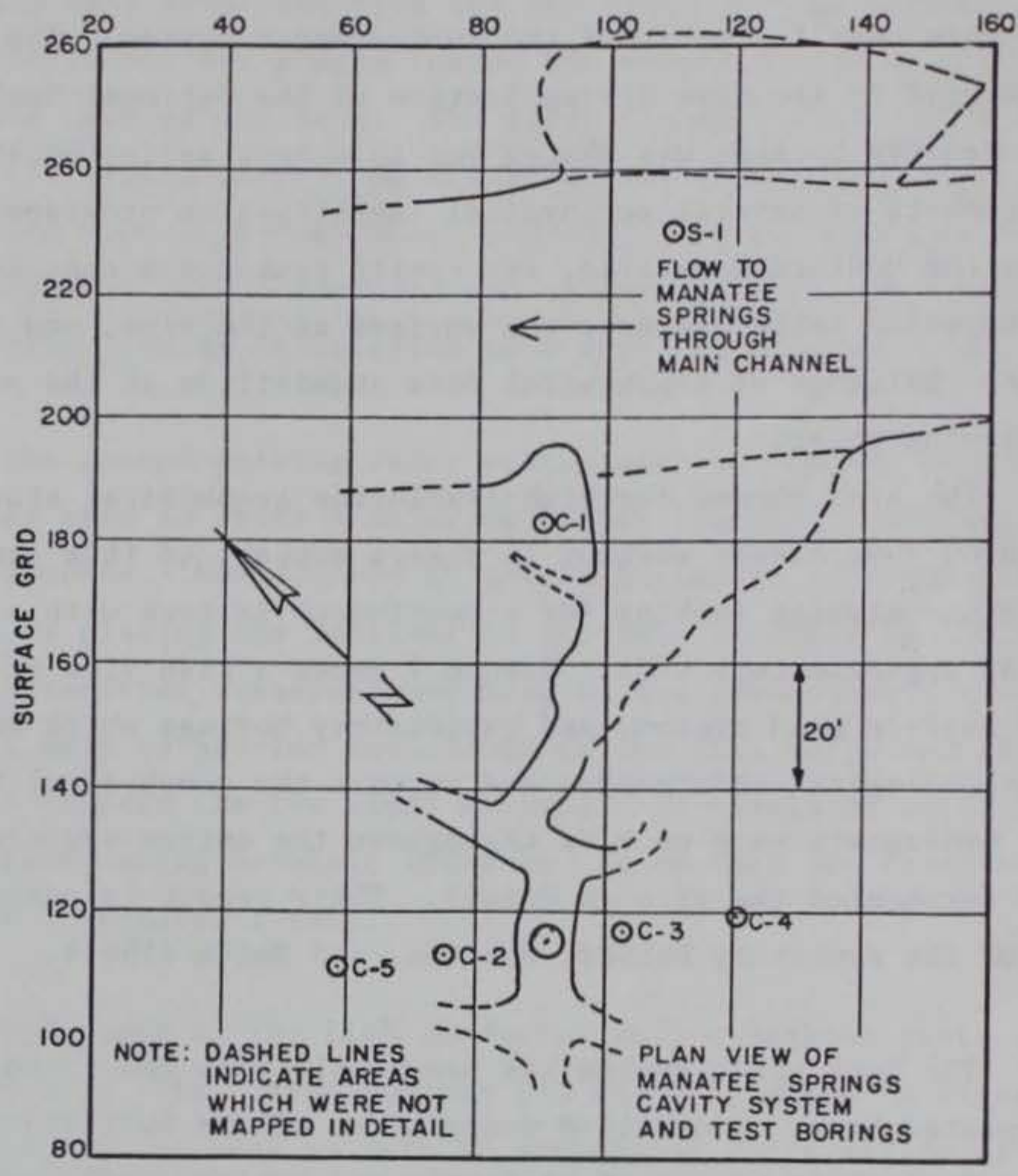

Figure 7. Plan view of Manatee Springs site

C-3 and receiver in C-2. Other cross borehole testing was done with the transmitter in hole C-4 and receivers in holes C-3 and C-2. In this particular case, receiver C-2 was used as a reference for the spectrum analyzer and receiver C-2 as the test input. By so doing, phase changes representative of the change in relative dielectric constant of the media provided the means for determining the dielectric constant of the formations at Manatee Springs. This procedure is described in Appendix A.

PART IV: TEST RESULTS

Medford Cave, Florida

Technos

45. A report documenting the investigation conducted by Technos at Medford Cave is available through the WES Technical Information Center (Benson and Glaccum, 1980). Their findings, which fall within the scope of this report, will be discussed in detail.

46. Technos conducted tests along some 17 selected traverse lines located in areas where known cavities existed and in unmapped areas where the presence of cavities was unknown. Figure 8 shows the location of the Technos radar traverses. Prior to the conduct of the radar investigation, Technos personnel performed a brief conductivity survey to determine the range of conductivities present at the test site in an effort to determine the likelihood of effectiveness (in terms of penetration) of the radar. Based on previous experience gained in the State of Florida and the relatively low average conductivities (about 5 millimhos per metre), Technos concluded that the site would be acceptable for a radar survey. Figure 9 is a plot of conductivity traverse which was conducted along the north-south 0,100 grid line crossing some of the known cave features. The higher conductivities observed at sta 220,100 and extending farther north toward sta 260,100 were later proven to be related to the fairly thick zones of clay that were found in this area when exploratory borings were conducted after radar testing was completed. In the areas of low conductivity (low clay content of the near-surface), radar profiles produced numerous clear anomalies over mapped cave areas as well as over unmapped areas. In those areas of higher conductivity, the anomalies became less distinct. The 80-MHz antenna achieved much better results than a 300-MHz antenna because of the greater depth of penetration and amplification of the lower frequency antenna. At the beginning of the survey, calibration of the system was accomplished with a small, accessible, horizontal cave whose roof was about 9 ft below the ground surface. An aluminum foil reflector was used

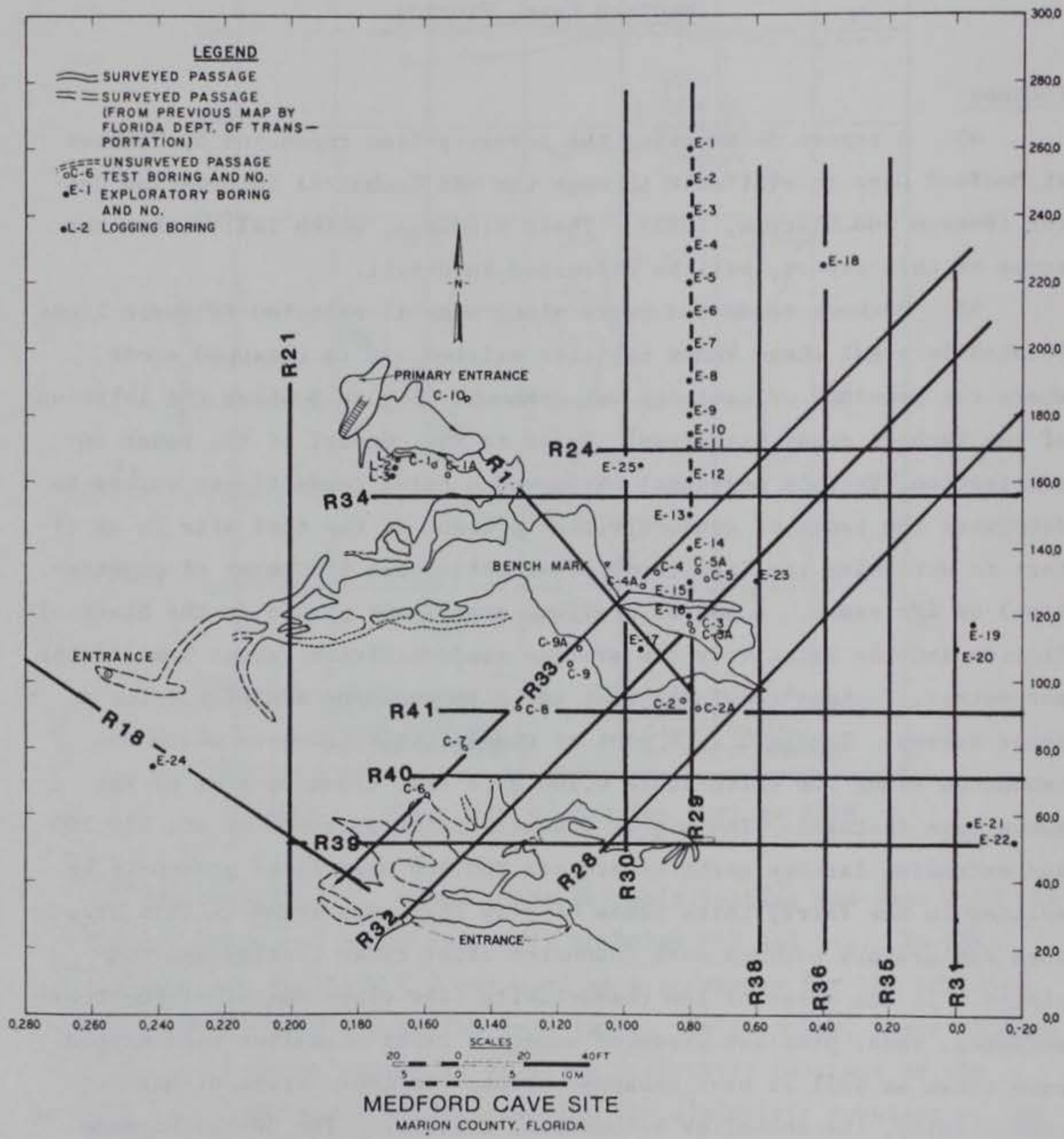

MEDFORD CAVE SITE
MARION COUNTY, FLORIDA

Figure 8. Location of Technos radar traverses

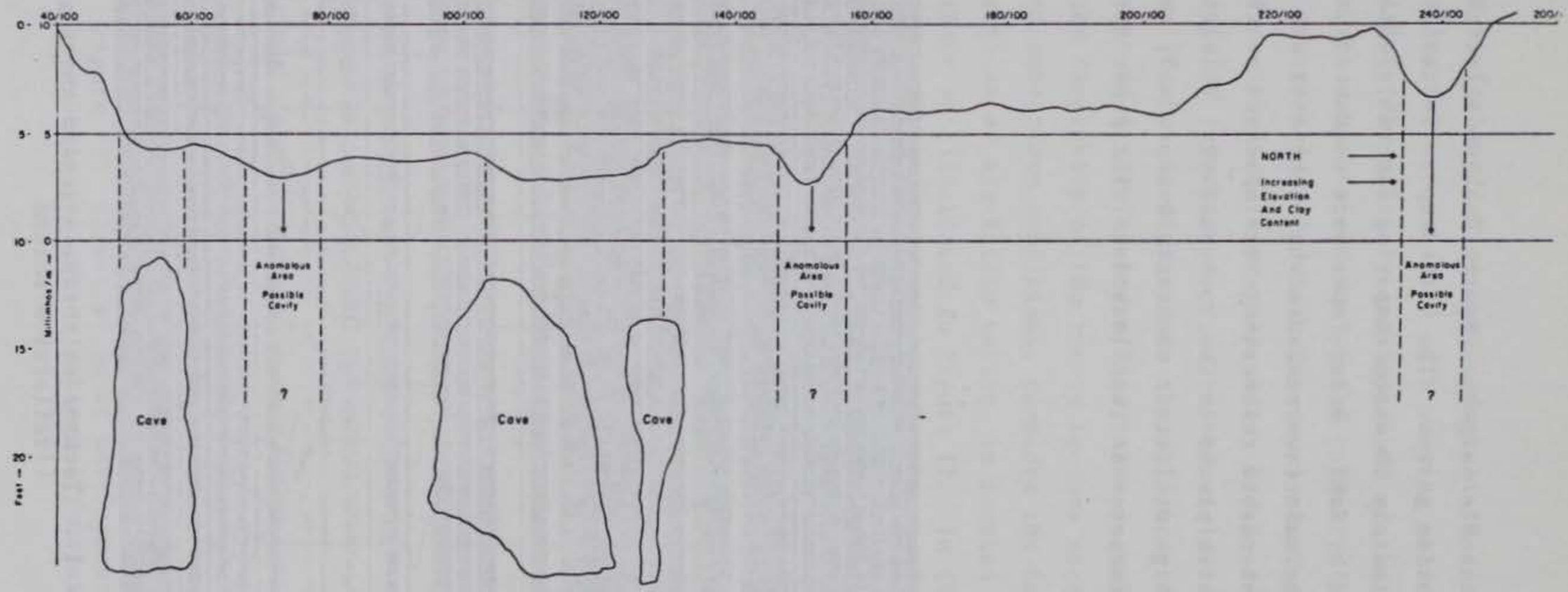

Figure 9. Conductivity traverse conducted by Technos

to provide a recognizable target. Figure 10 shows a record obtained during this calibration series. The 9-ft-deep reflector produced a response at approximately 50 nsec, comparing favorably with data which were later obtained by SwRI. Other tests were conducted using an aluminum reflector in the main cave entrance where the roof was approximately 22 ft thick. No detectable reflections were observed at this site. An auger boring was later placed in the rock surface. This concentration of clay, having a high dielectric constant, was probably responsible for lack of radar response at this location. The paper strip recorder,

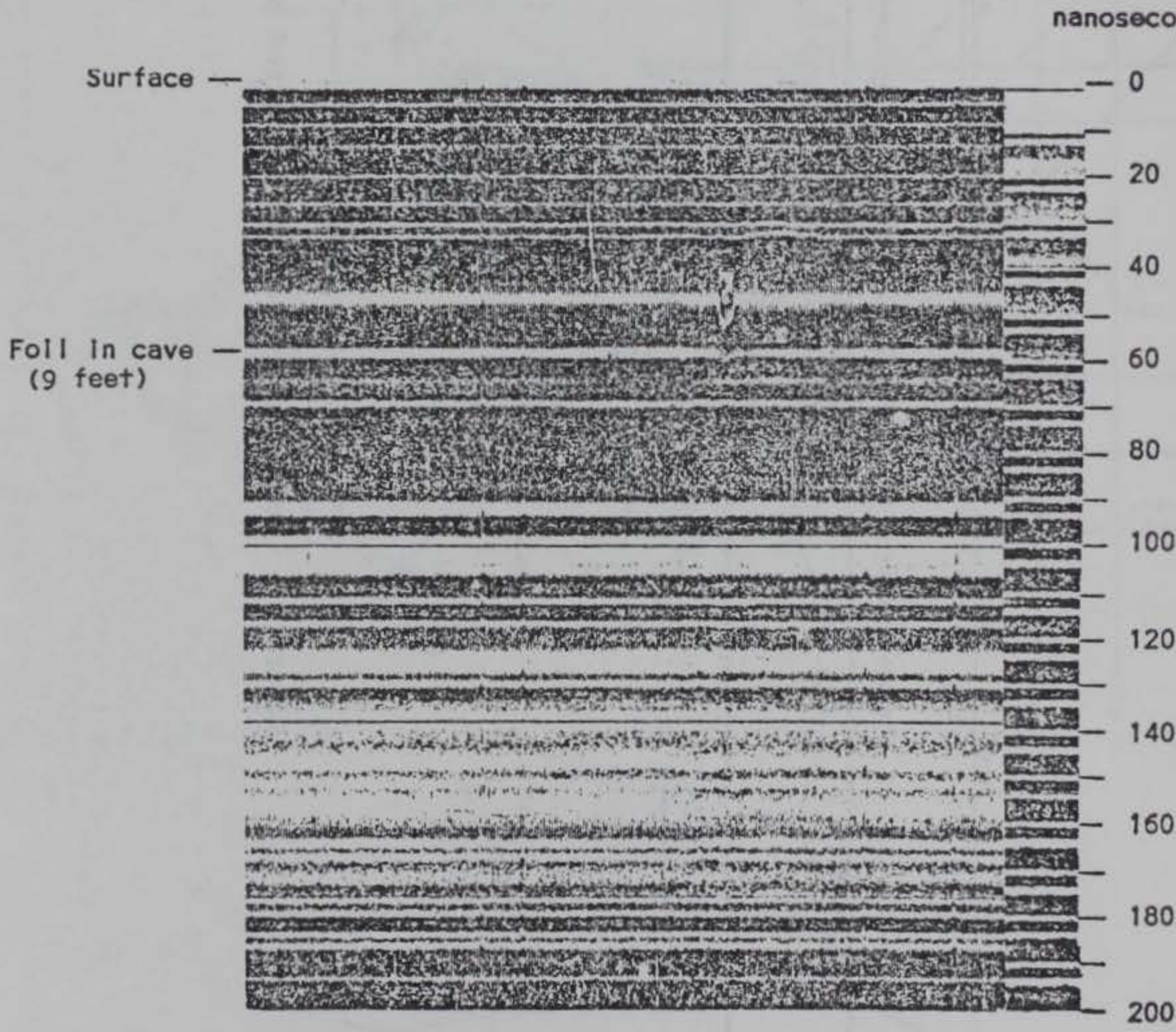

Figure 10. Technos calibration record showing reflection return

which was used by Technos during the conduct of these tests, provided a convenient display for use on-site. Its varying shades of gray are directly related to the polarity and amplitude of the returning signal.

47. The records obtained during the conduct of a radar traverse incorporate a horizontal scale which is comprised of grid coordinates and a vertical scale which is elapsed time. In the case of a relatively uniform horizontally layered system, a record would look similar to that shown in Figure 10, but as distance to the reflectors begins to vary, as would be the case of irregular bedrock or other anomalous features, such as cavities, the complexity of the record becomes more apparent. Under reasonably good subsurface conditions, consider the case where a reflective object, such as an air-filled cavity, is located at a point beneath the ground surface as illustrated in Figure 11. In this illustration, the antenna (transmitter and receiver) is initially located on the ground surface at some point well away from the reflective object. As

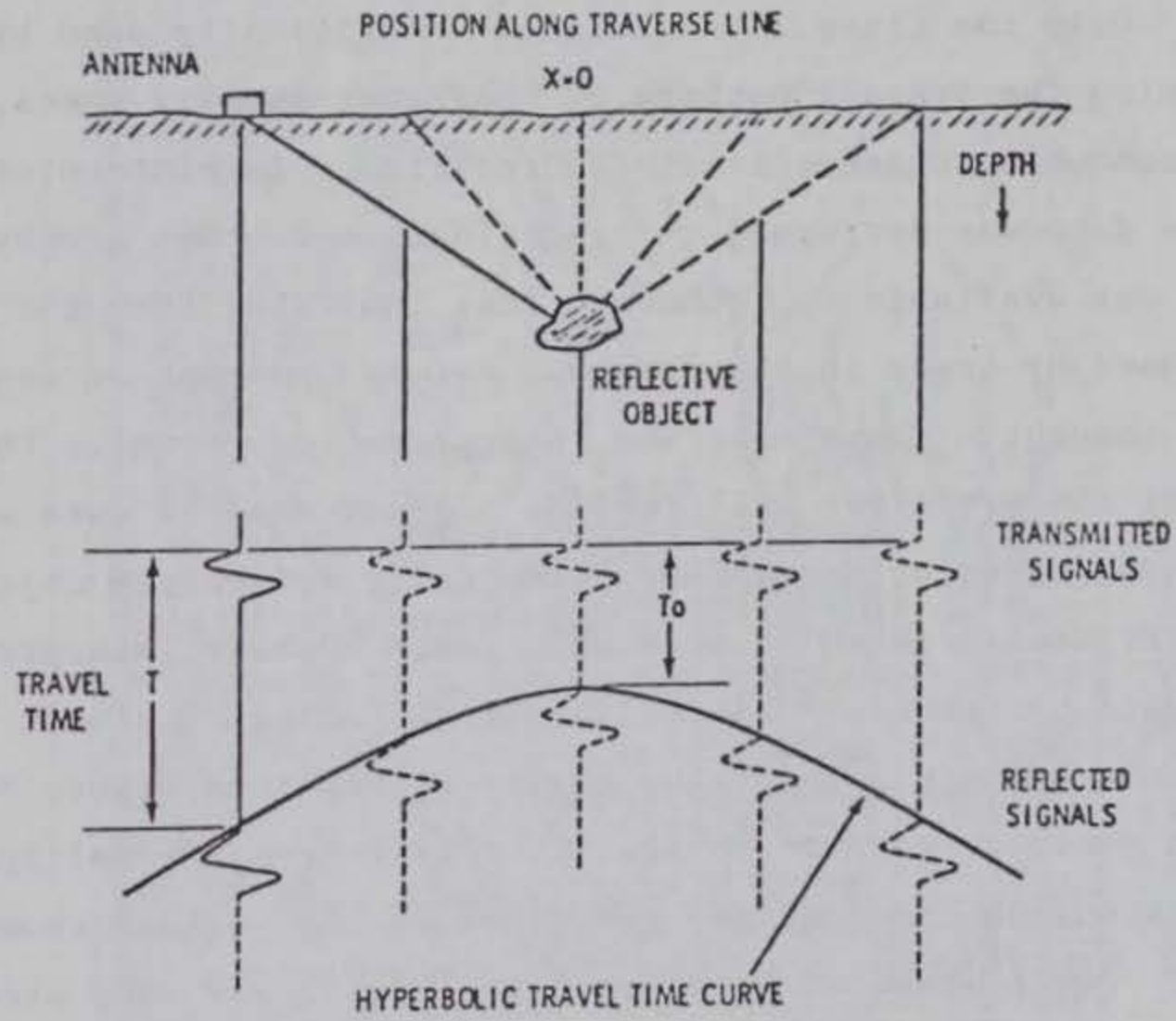

Figure 11. Illustration of development of hyperbolic reflection pattern (from Battelle Laboratories, 1981)

the antenna changes its position along the traverse line moving closer to the target, the time of arrival of the reflected signal becomes progressively shorter until it reaches its minimum directly above the reflective object. Once passing over the object, the time of arrival then begins to increase until signals can no longer be received. A continuous record obtained in this manner will exhibit a hyperbolic travel time curve. This effect is readily apparent in some of the records which will be shown.

48. Figures 12-33 are copies of records obtained by Technos along each of the traverses. The line numbering sequence devised by Technos does not indicate the order in which the lines were run or that lines might be missing because the numerical sequence at times skips certain numbers. In their original report, Benson and Glaccum (1980) classified anomalies detected in two categories: Class I, those which were clearly independent of any EM noise; and Class II, those which were present in zones of backscatter noise (particularly overhead noise possibly caused by trees). Only the Class I anomalies were originally used by Technos in determining the overall pattern of the radar anomaly zones, thus presenting a somewhat conservative interpretation. A reinterpretation of the Technos data was performed using geologic and other geophysical data which were not available to Technos. This indicated that the backscatter caused by trees in the area was not as apparent or degrading as originally thought. Therefore, the interpretation shown in this report, though still conservative, will include a great deal of data which were obtained under trees or near other potentially reflective objects.

49. Figure 12 is an example of a radar anomaly interpretation which was made by Technos. Since line R1 was oriented almost exclusively over the primary axis of the cavity system (see Figure 8), the entire line exhibits erratic data which result from the multiple reflections received from the roof and the floor of the various rooms of the known cave. One feature at grid location 120,100 was very prominent and was probably caused by in-phase reflections converging at the approximate center of the largest room in the mapped cave system.

50. Figures 13 and 14 show the results obtained while traversing

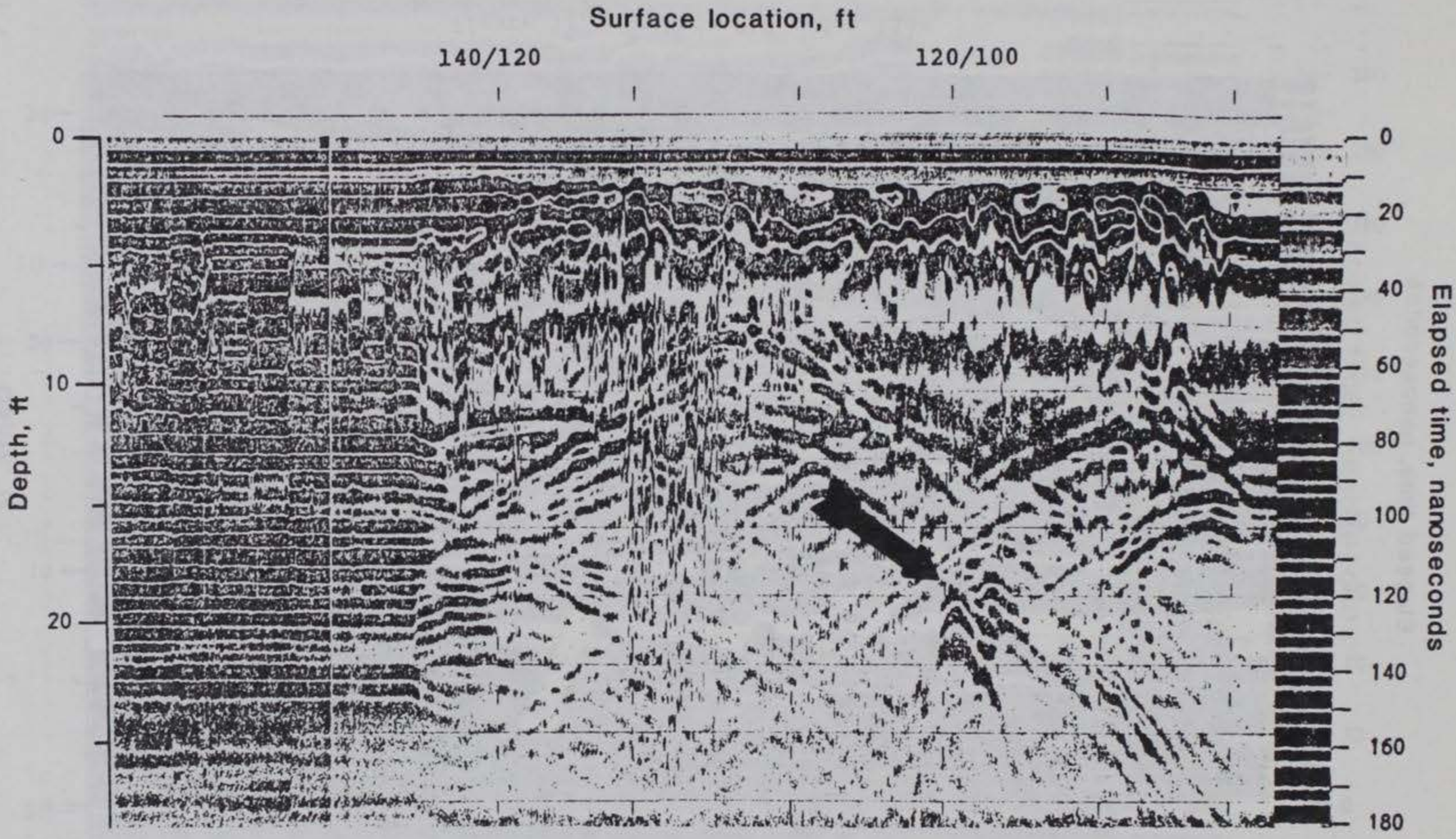

Figure 12. R1 radar line

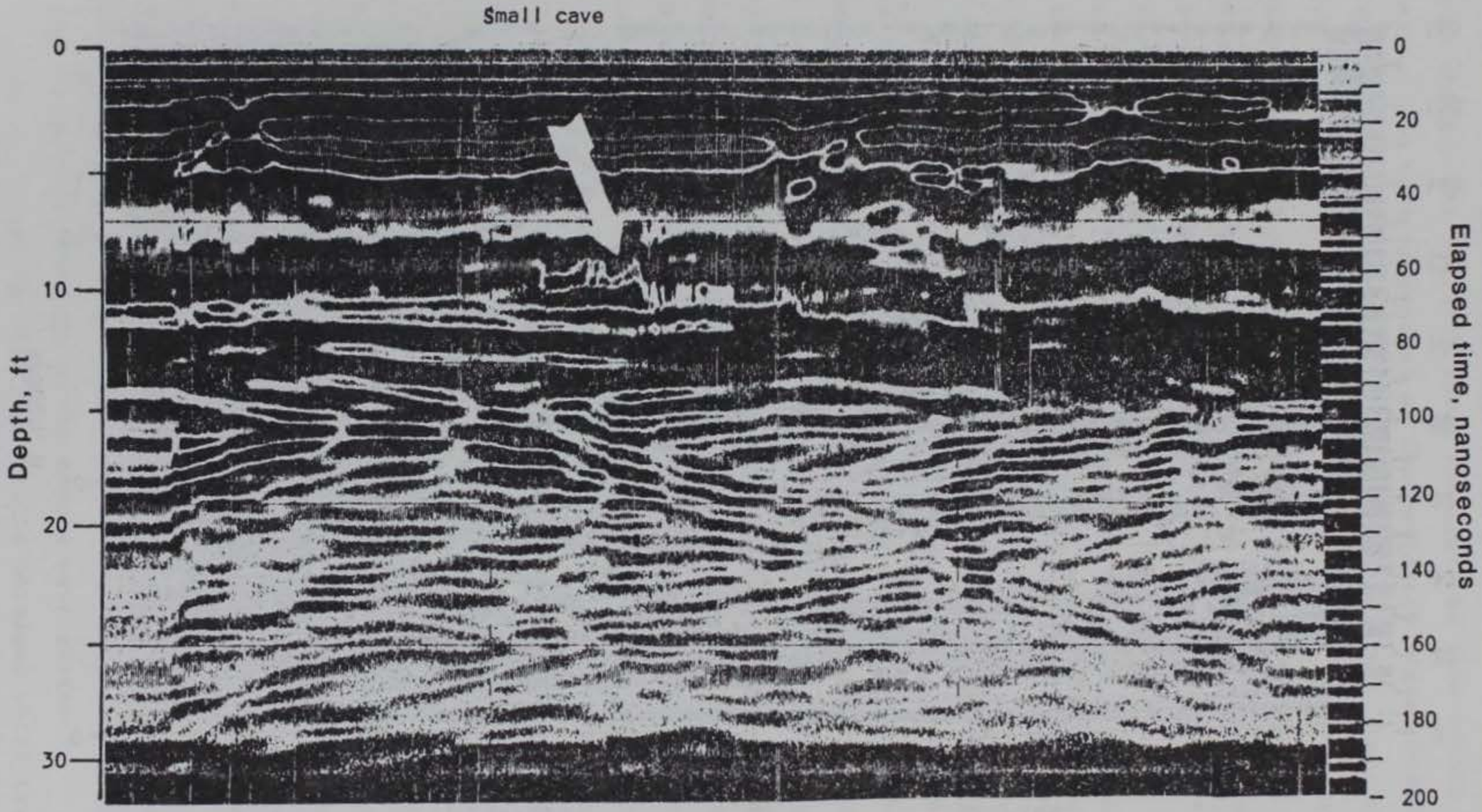

Figure 13. Technos R18 radar line

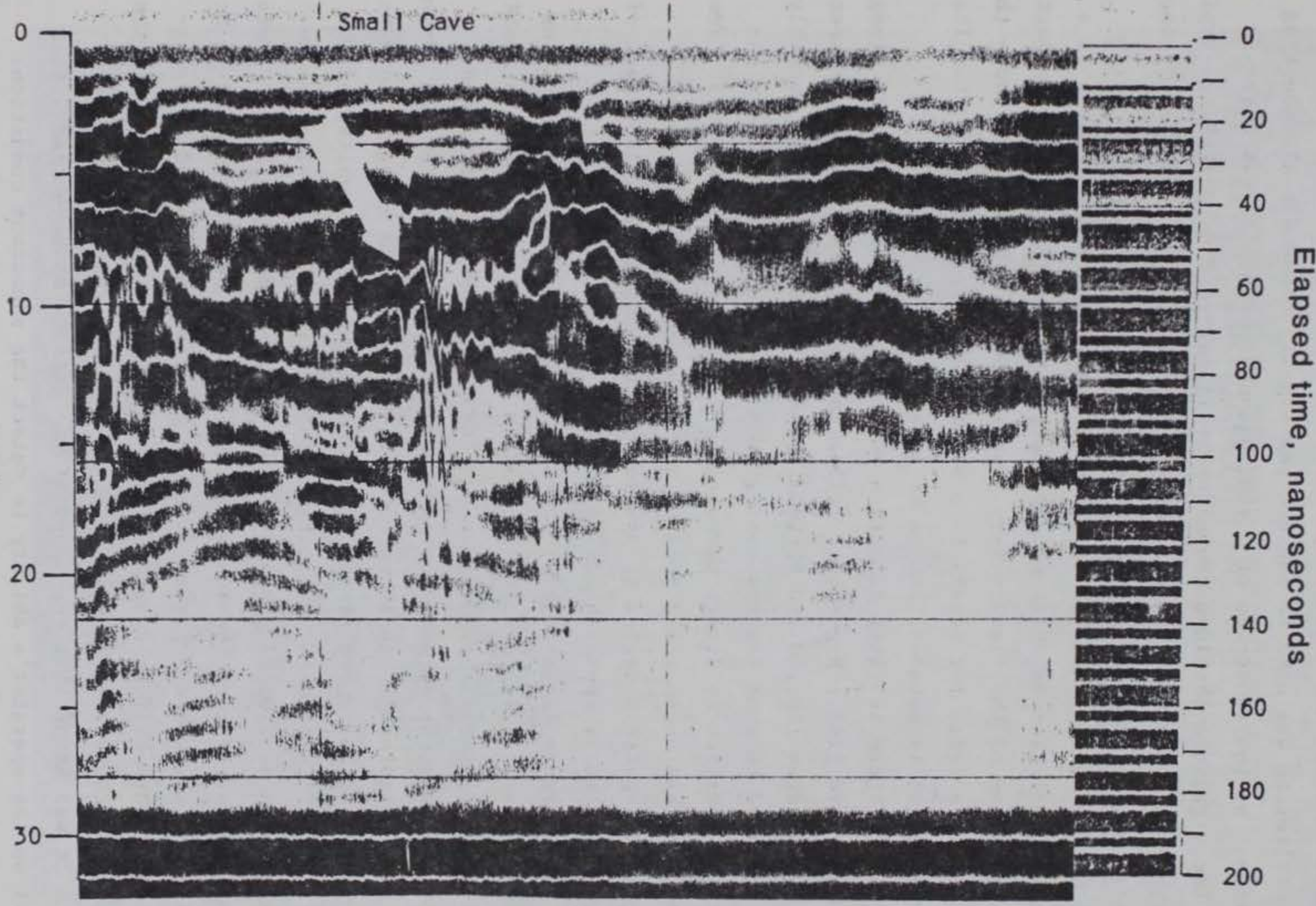

Figure 14. Technos R18 radar line showing effect of filtering

over the secondary entrance to the small cave system where velocity calibration data were taken. Figure 14 is an example of signal-processing where filtering was used to enhance the signal. Some signal smoothing is evident by the reduction of high-frequency noise. It was observed that the signature obtained above the small cave did not exhibit a typical hyperbolic pattern. This important observation is explained by the geometry of the interior of the secondary cave system. Figure 15, a photo of the interior of the cave, shows that the primary feature is a sharp vertical fissure which extends deep into the interior of the earth. The dimensions of the fissure vary from a width of about 6 in. (note the oak leaf on a ledge for scale) to a maximum of approximately 1 ft. Its overall height is unknown, but is at least 6 ft.

51. Figure 16 (line R21) is a north-south traverse located along the 0,200 grid line. Hyperbolic reflection patterns were noted between grid coordinates 180,200 and 80,200. This broad expanse could possibly be attributed to some returns coming from the area of the primary entrance in addition to direct passage over some of the mapped area. Few reflections are encountered from 80,200 to 40,200. At this point, a hyperbolic pattern begins to develop as the southernmost labyrinth of the cave system is approached.

52. Figure 17 (line R24) showed strong returns at the beginning of the line near grid location 170,120. These reflections were probably due to backscatter occurring from the known cave system. A second strong return occurred near the unmapped eastern edge of the grid system.

53. Figures 18 and 19 were additional runs made along R1 to determine the effect of speed of the antenna movement on the quality of the data. The original data were obtained along line R1 by towing the antenna by hand at a walking speed of approximately 1-1/2 to 2 mph. Data shown in Figure 18 are the result of the fast tow speed estimated to be about 2 ft/sec, whereas Figure 19 shows the results obtained using approximately one-half this speed (1 ft/sec). Both runs were made in the vicinity of the strong anomaly detected near the center of the large room. It was found that the speed of the antenna movement had little effect on the operator's ability to detect the anomalous condition.

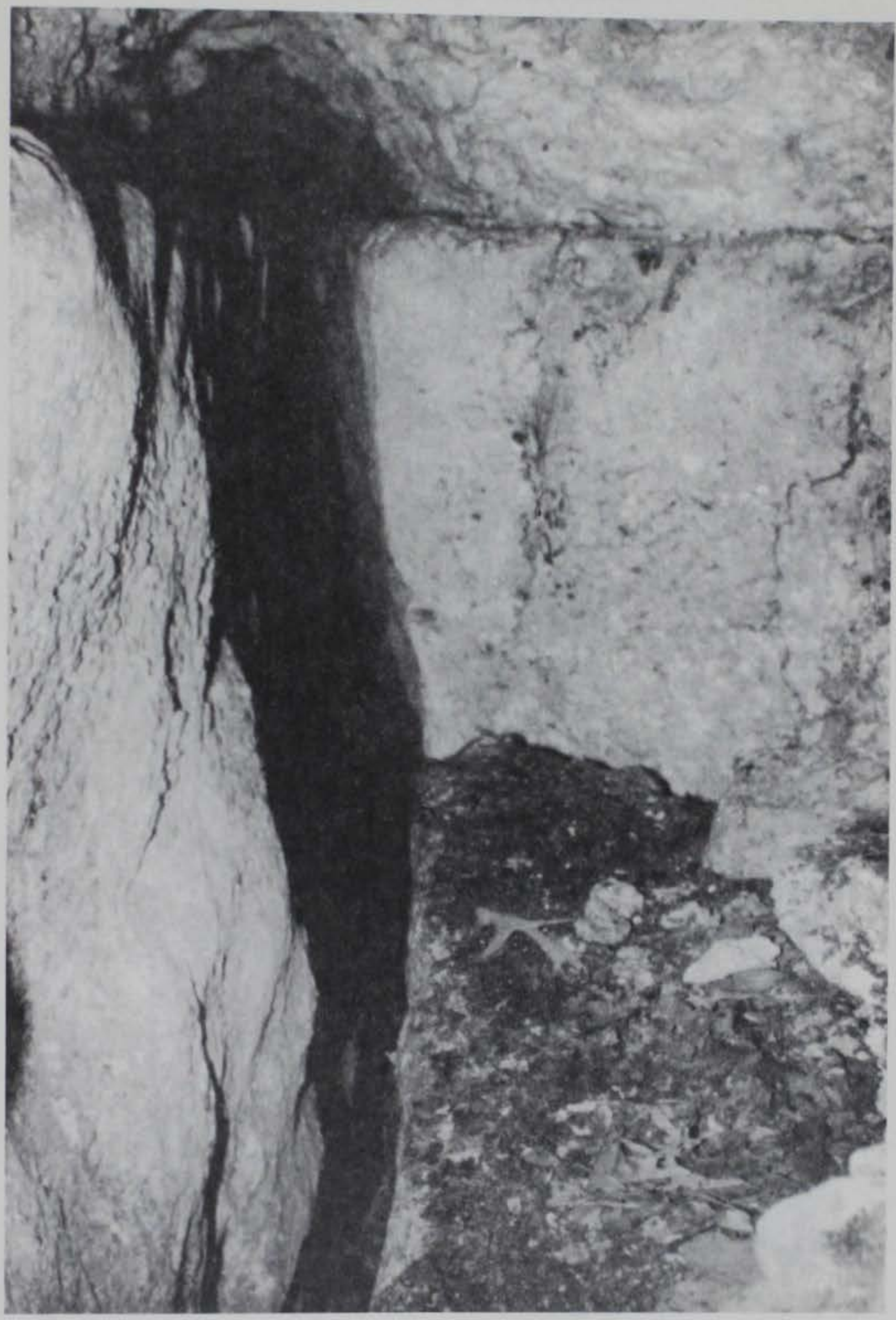

Figure 15. Interior of Technos calibration cave

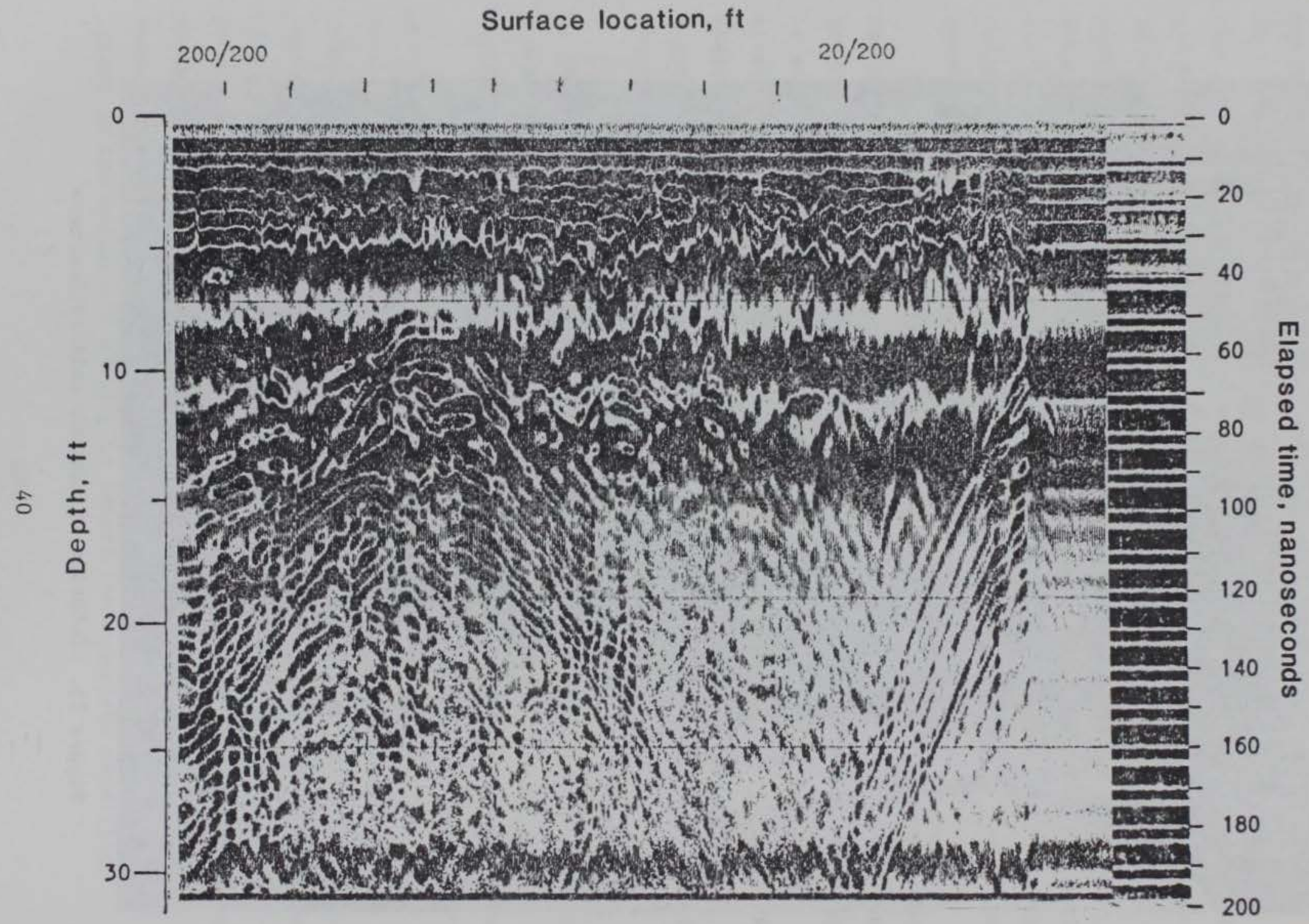

Figure 16. Technos R21 radar line

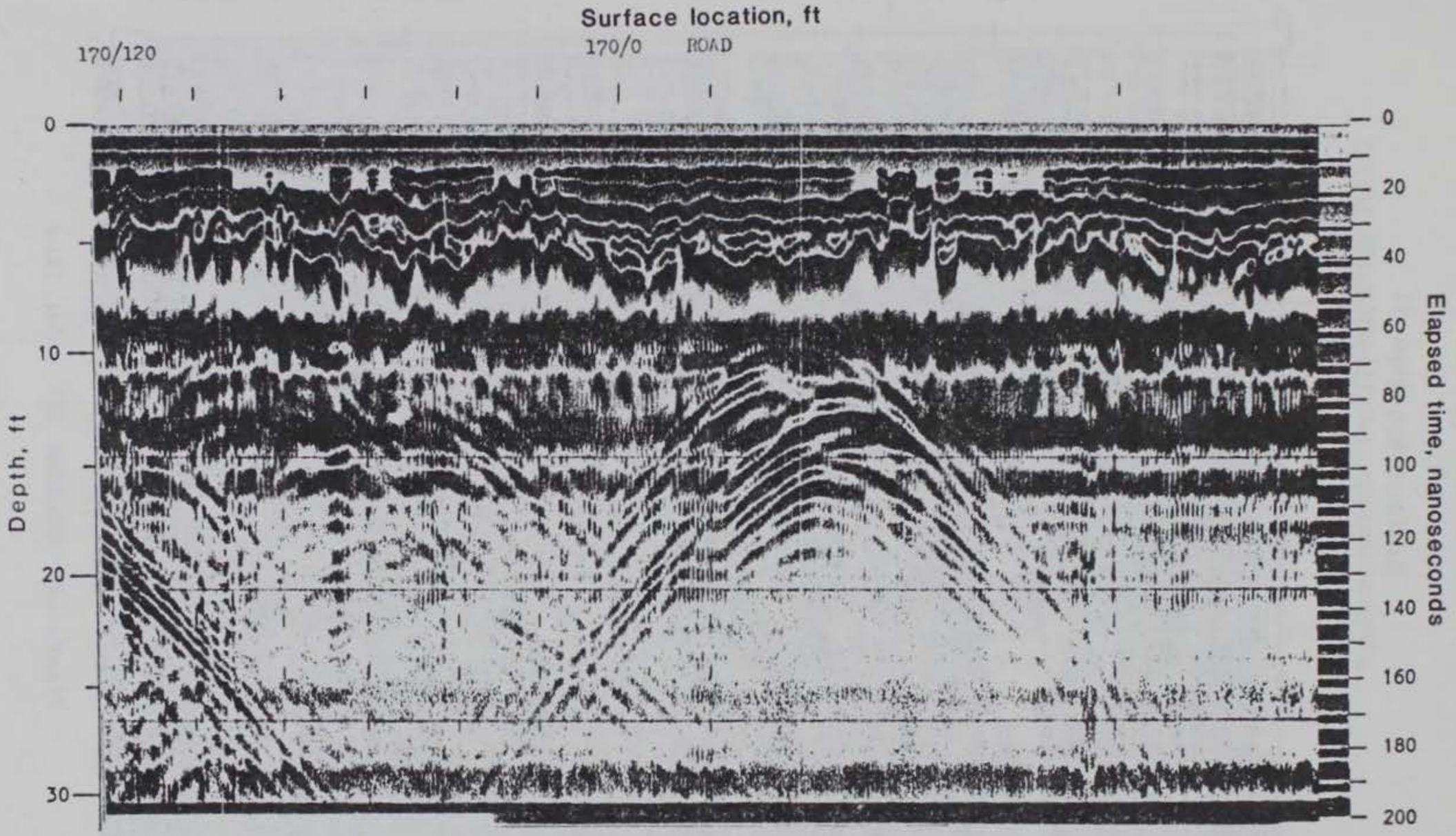

Figure 17. Technos R24 radar line

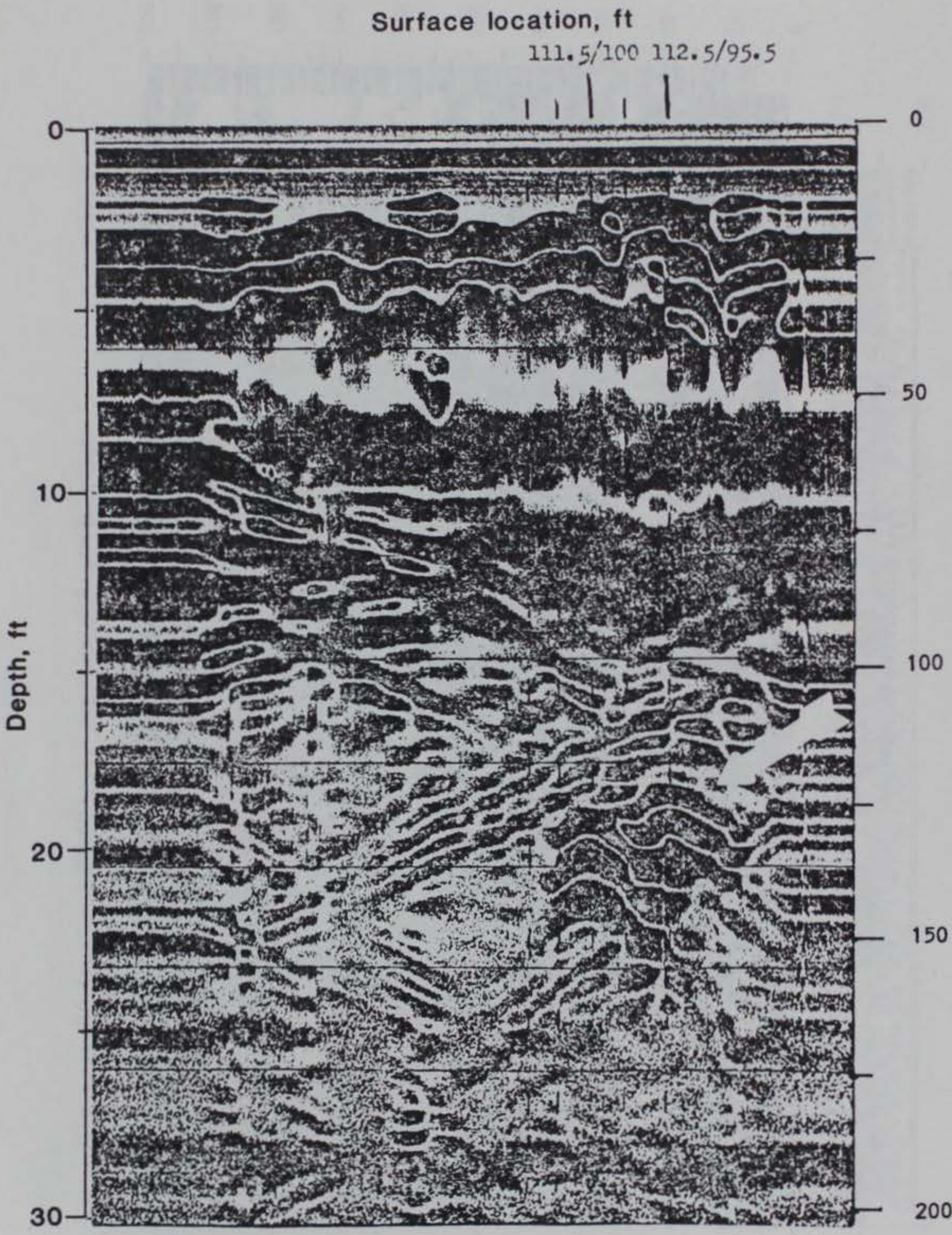

Figure 18. Technos R25 radar line

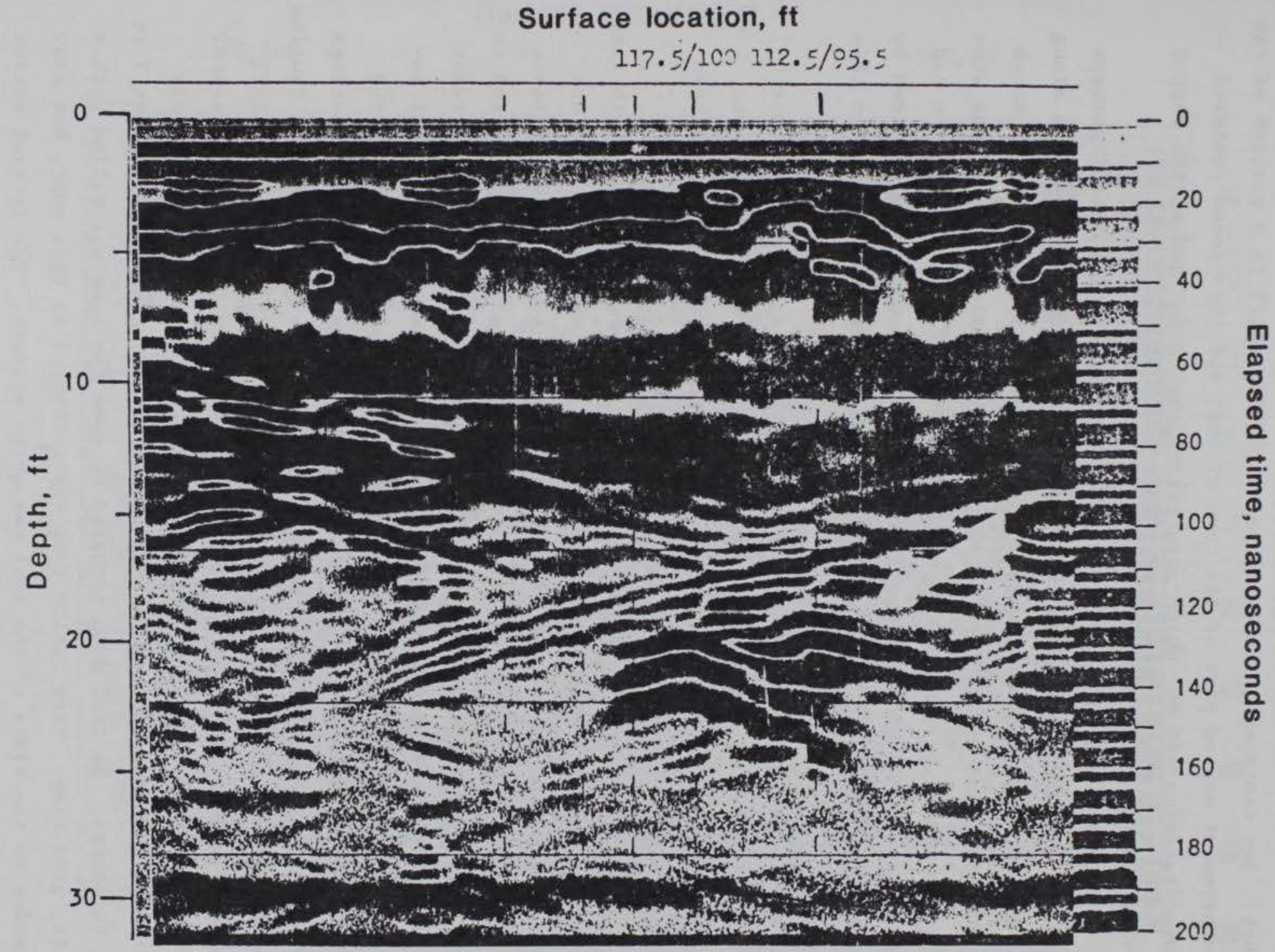

Figure 19. Technos R26 radar line

However, the slow speed did provide better resolution of the reflections.

54. Line R28, shown in Figure 20, exhibits two distinct reflection zones: one centered around grid point 60,100, which is a portion of the southernmost mapped part of the cave system; and the second centered around location 100,60, which also passes over a portion of the mapped cavity system.

55. Traverse R29 (Figure 21), one of the most important surveys from the standpoint of known conditions, was oriented north-south along the 80 grid line. Numerous prominent reflectors appear over the known cave system, and it was also noted that fairly shallow reflections were severely masked by the clay pocket, discovered at the far northern end of the line. Additional comparisons will be made with data obtained by other contractors and known conditions using traverse R29 later in this report.

56. Traverse R30 (Figure 22) was located parallel to the north-south 80 grid line. Again, prominent reflections occurred over the mapped portions of the cave system and at other areas in the northern section of the grid where no known cavities existed.

57. Traverse R31 (Figure 23) was the easternmost north-south line surveyed by ground-penetrating radar. The location of this line was specifically chosen because of the lack of known subsurface conditions prior to the survey. It was planned that if anomalies were detected in this area, every effort would be made to confirm or disprove the radar data. When the survey was made along line R31, two very prominent reflectors became the targets of interest. These were located at grid points 60,0 and 117.5,-5. Technos recommended that exploratory borings be placed at these locations to describe the subsurface condition causing the localized reflections. At a later date, exploratory borings E-21 and E-19 were placed near these locations, and cavities were confirmed. Boring E-19 encountered the first cavity at a depth of approximately 10 ft after having passed through a soft limestone, which was about 7 ft in thickness. No tool drop occurred because the zone was filled with a soft, gray clay. Very little core was recovered in this zone, but clay residue on the sides of the tool was quite evident. The lateral extent

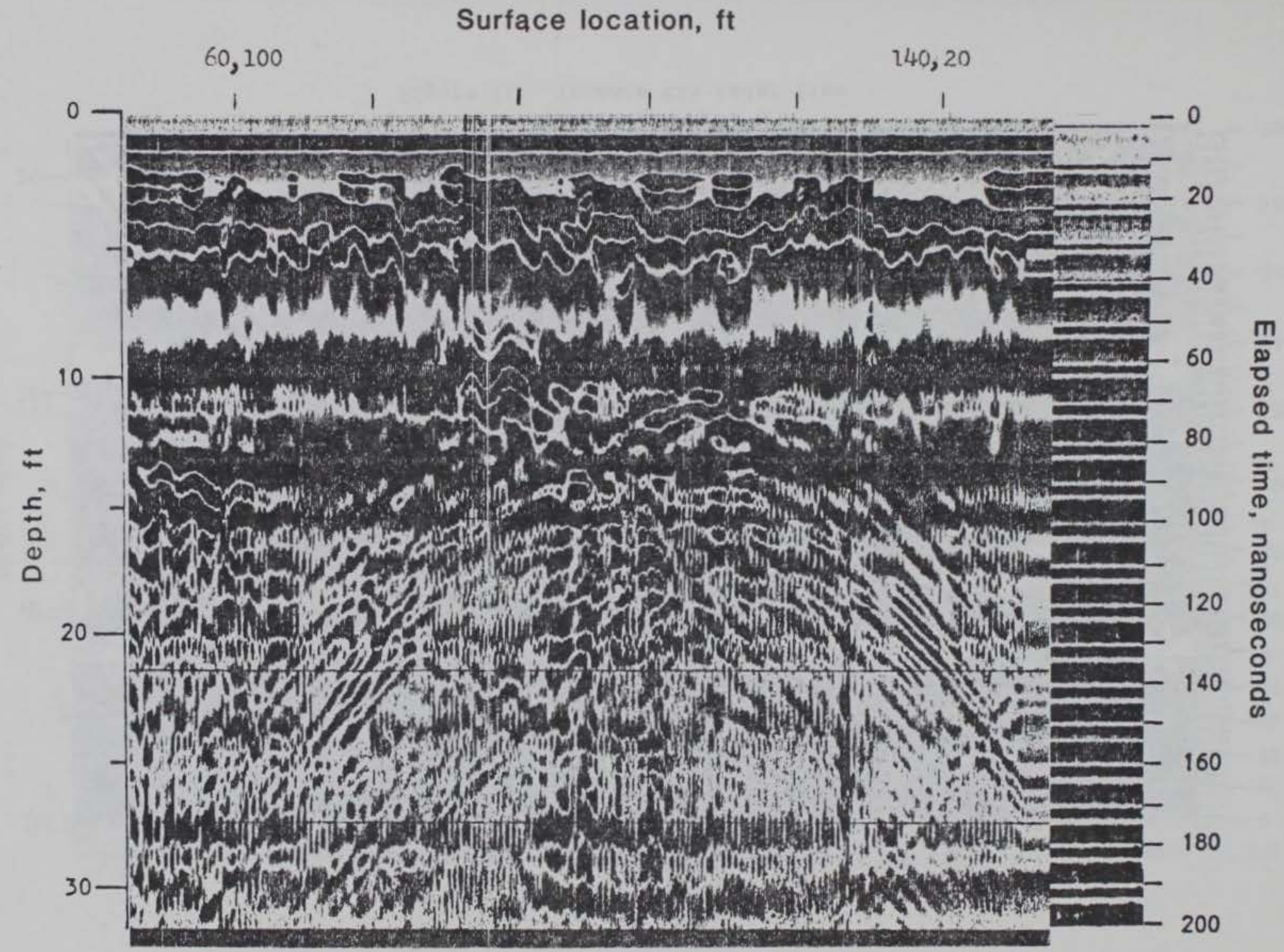

Figure 20. Technos R28 radar line

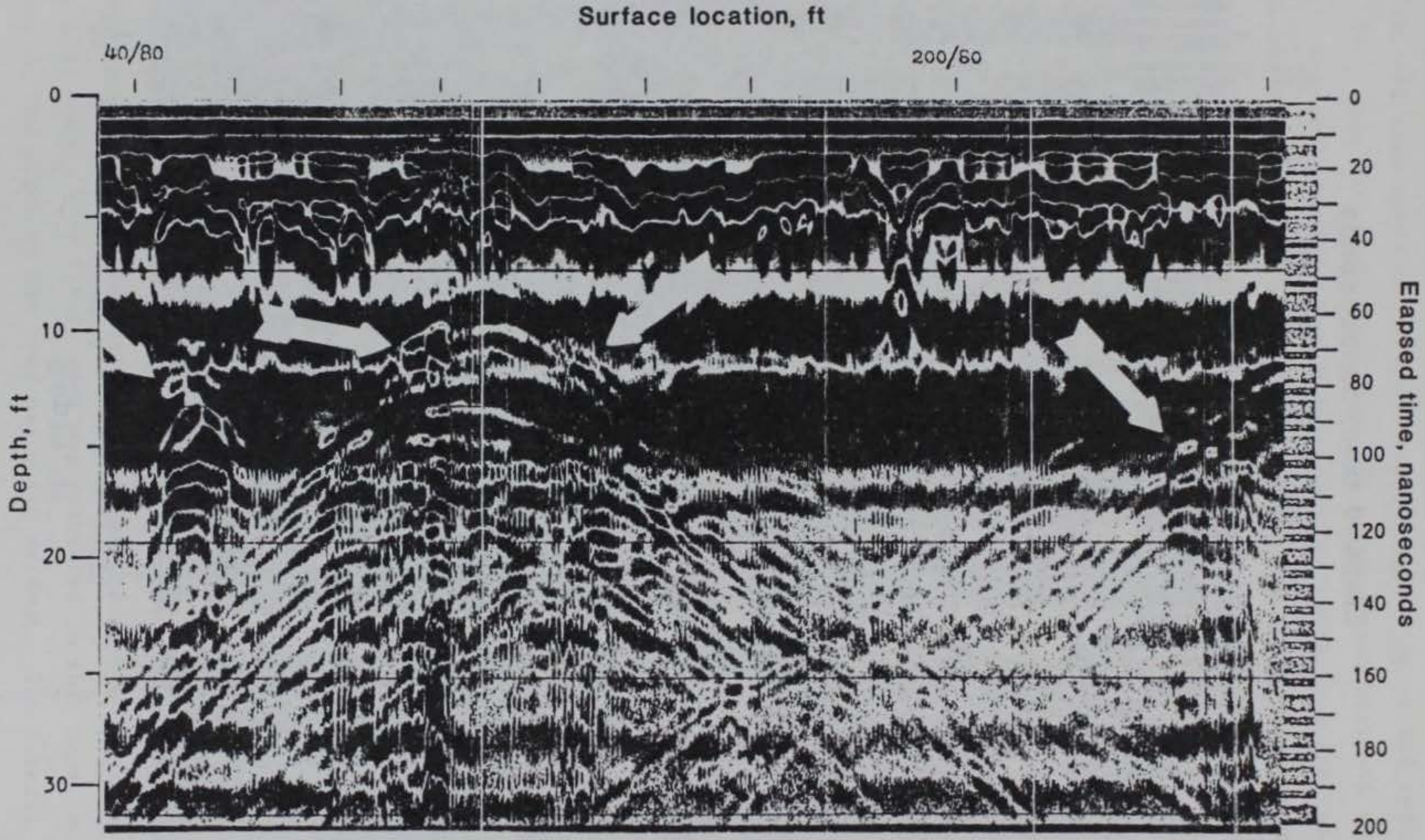

Figure 21. Technos R29 radar line

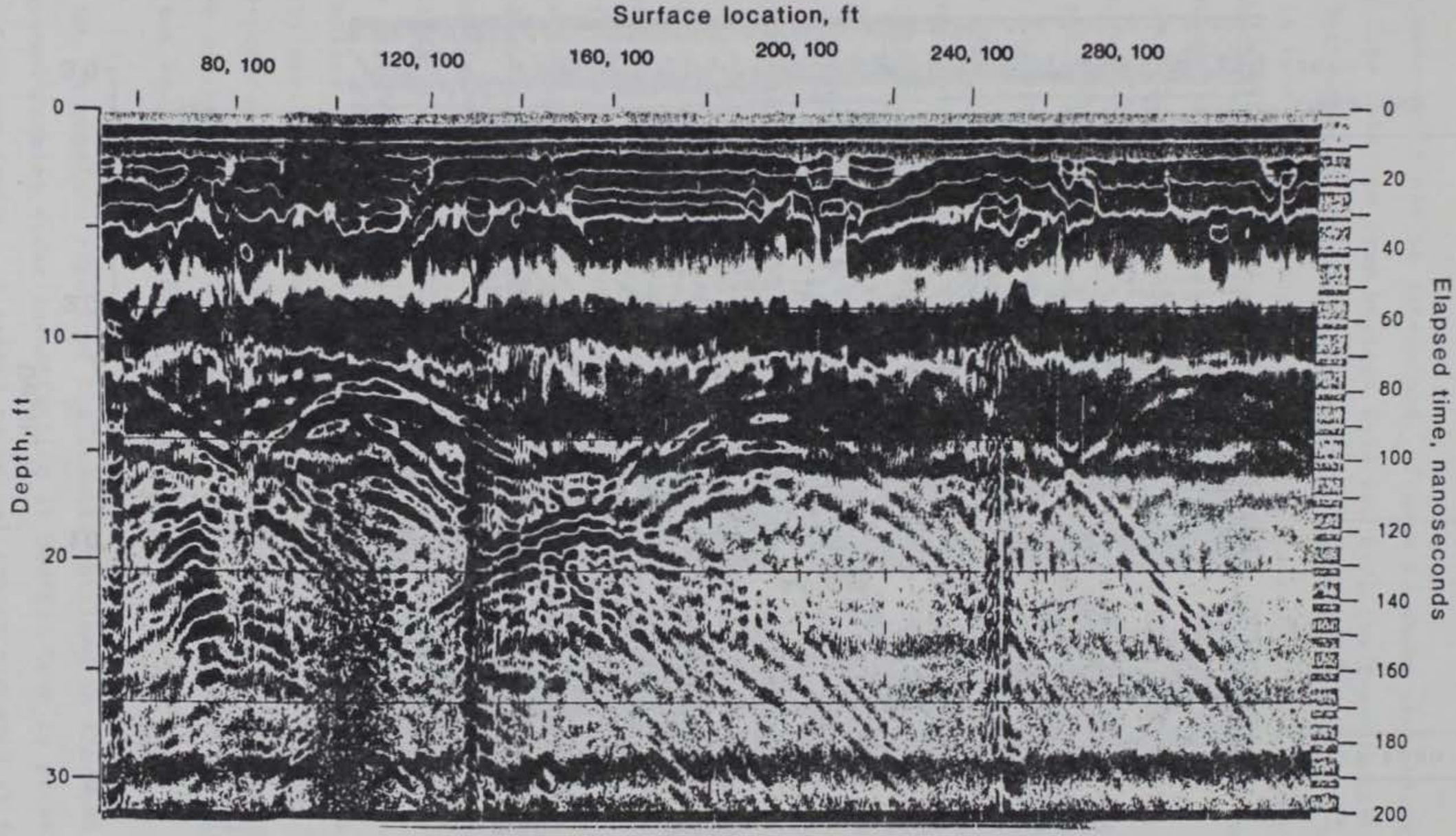

Figure 22. Technos R30 radar line

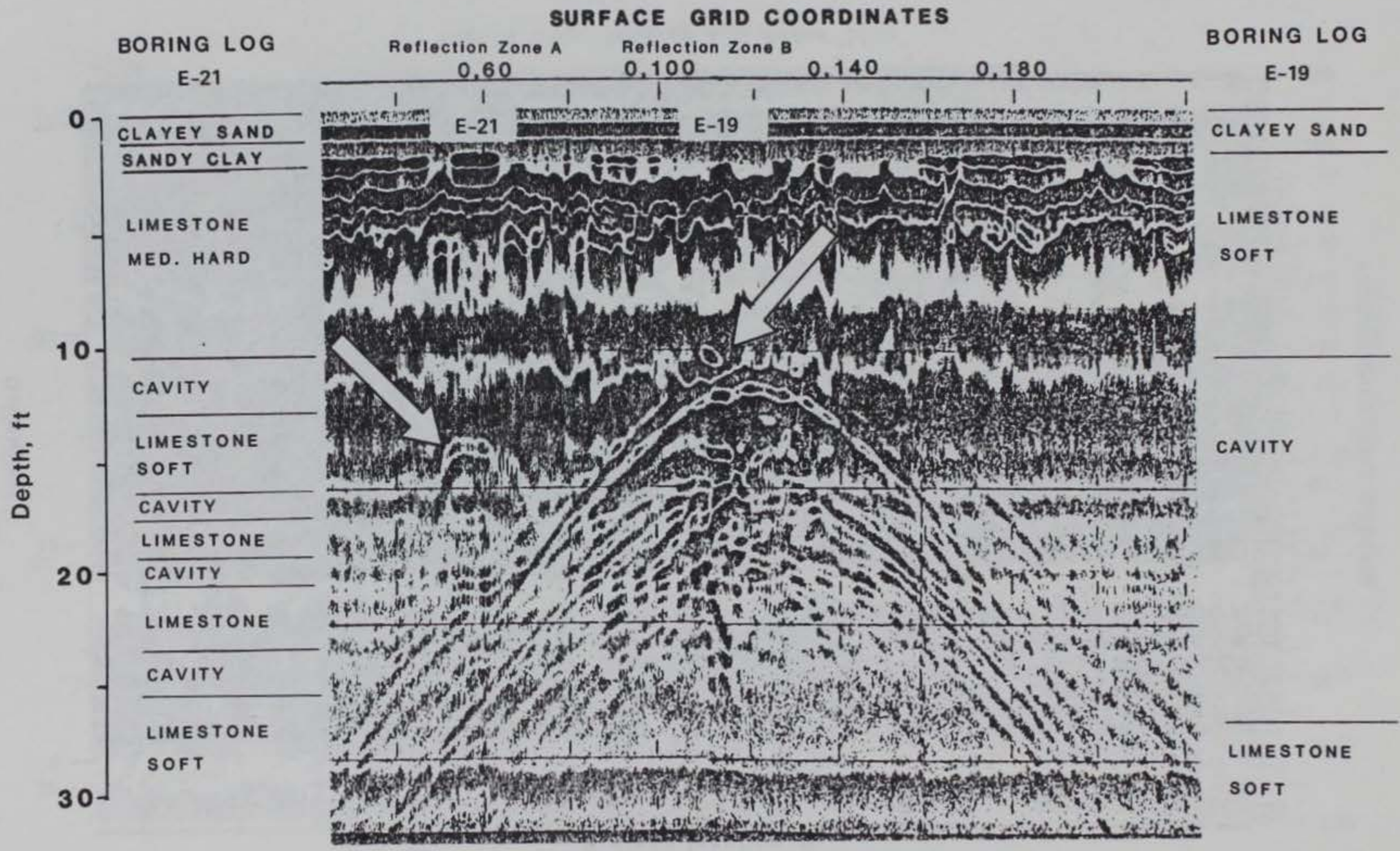

Figure 23. Technos R31 radar line

of the zone could not be determined. Figure 23 shows the abbreviated boring logs obtained from borings E-19 and E-21 for convenient comparison. Both show the excellent correlation which was obtained. Boring E-21, in contrast to boring E-19, encountered several thin cavity zones, each about 1 to 2 ft in thickness, rather than a single large zone as encountered in E-19.

58. The remaining traverses, R32 through R36 and R38 through R41, are shown in Figures 24-33. The anomalous zones which were detected along all of the traverses investigated by Technos are indicated in Figure 34. It is interesting to note that the extension of the anomalies in the easterly direction along the axis of the two main mapped cave sections may be simply an unmapped extension of the primary cave system or incipient cavities or fractured rock zones.

59. A large concentration of radar anomalies occurred in the vicinity of the east-west 110 grid line. The final recommendation by Technos was that exploratory borings be placed at grid coordinates 110,0; 117.5,-5; 60,0; and 165,95. Borings E-20, E-19, E-21, and E-25 accomplished this purpose. In each case, the boring logs indicated the presence of cavities or other anomalous features, such as soft zones. Some of the more meaningful boring logs are shown in Figures 35 and 36. The results of ground-probing radar tests conducted by Technos at the Medford Cave site indicate that radar can be a viable tool for the detection of cavities confirmed to be as deep as 25 ft and other anomalous conditions at sites where the electrical characteristics of the overburden materials are compatible with ground-probing radar. Basically, this implies that sites with sandy or silty overburden materials, which normally exhibit low conductivities, would be likely candidates for ground-probing radar investigations. Conversely, sites which are known to have overburdens comprised mainly of clays (high conductivities) would not be likely candidates for radar investigations.

SwRI

60. A complete report of the results obtained in the SwRI surface ground-probing radar investigation at Medford Cave is presented by Duff and Suhler (1980). A second technical report prepared at SwRI by

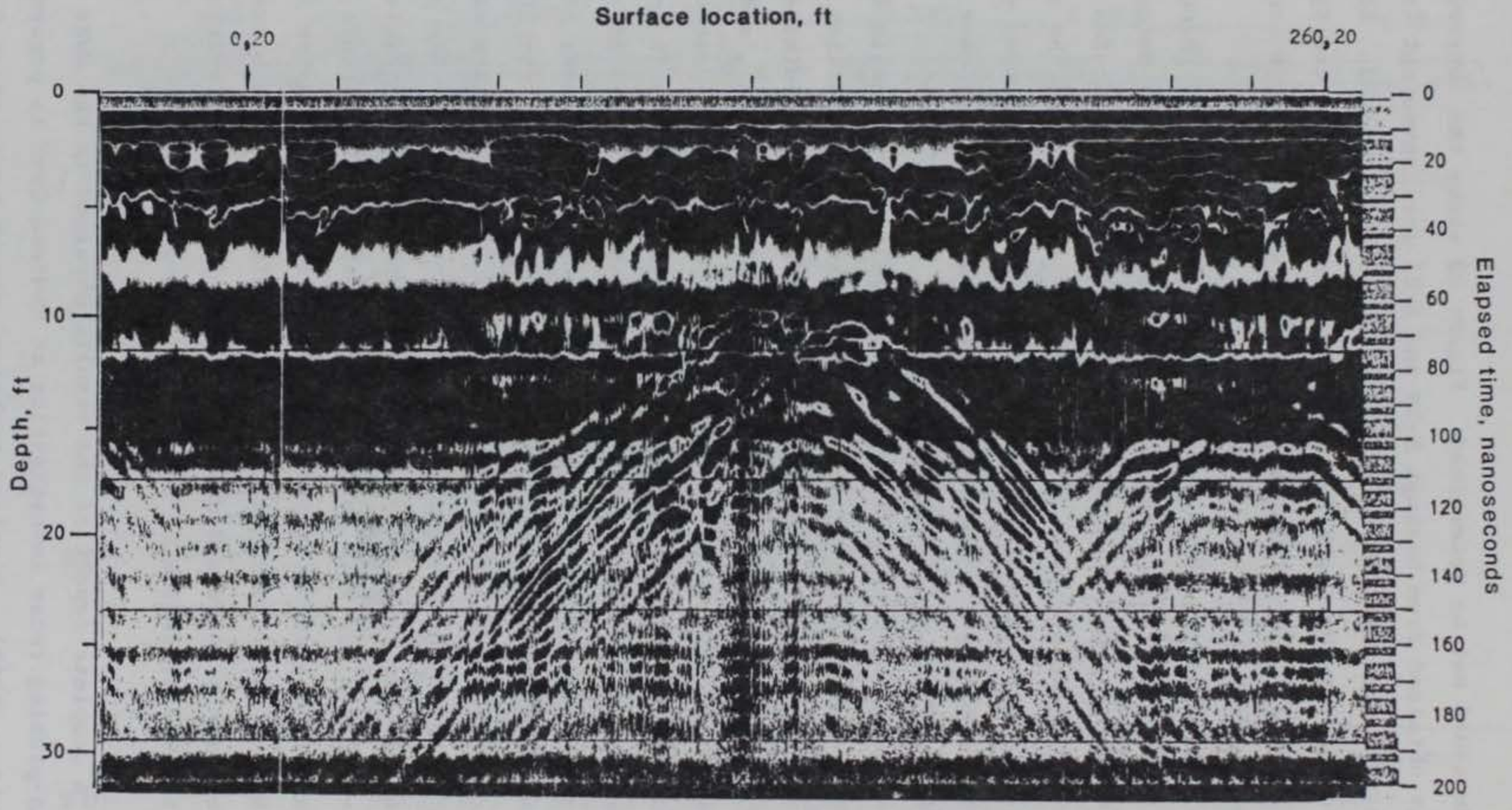

Figure 24. Technos R35 radar line

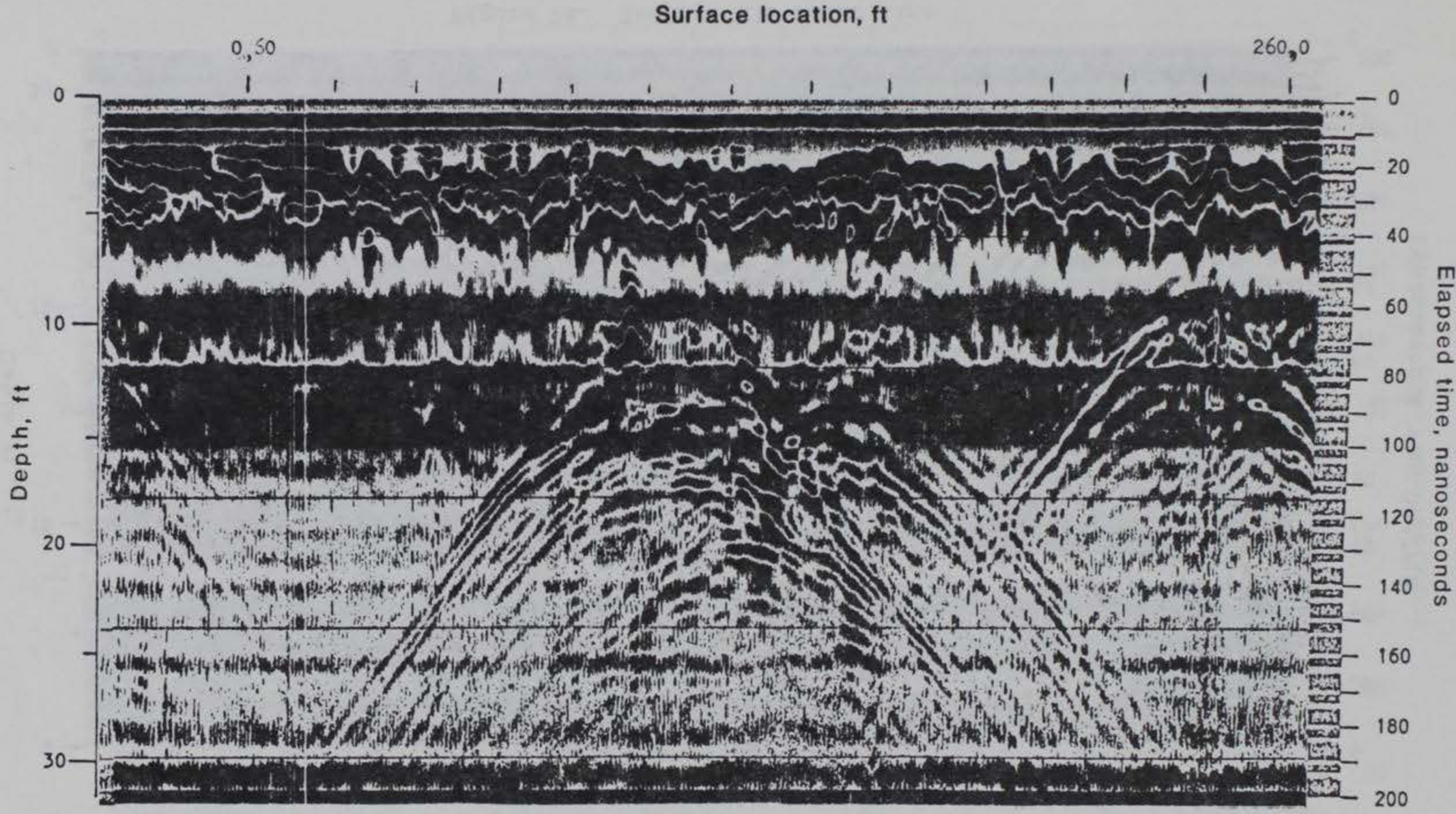

Figure 25. Technos R38 radar line

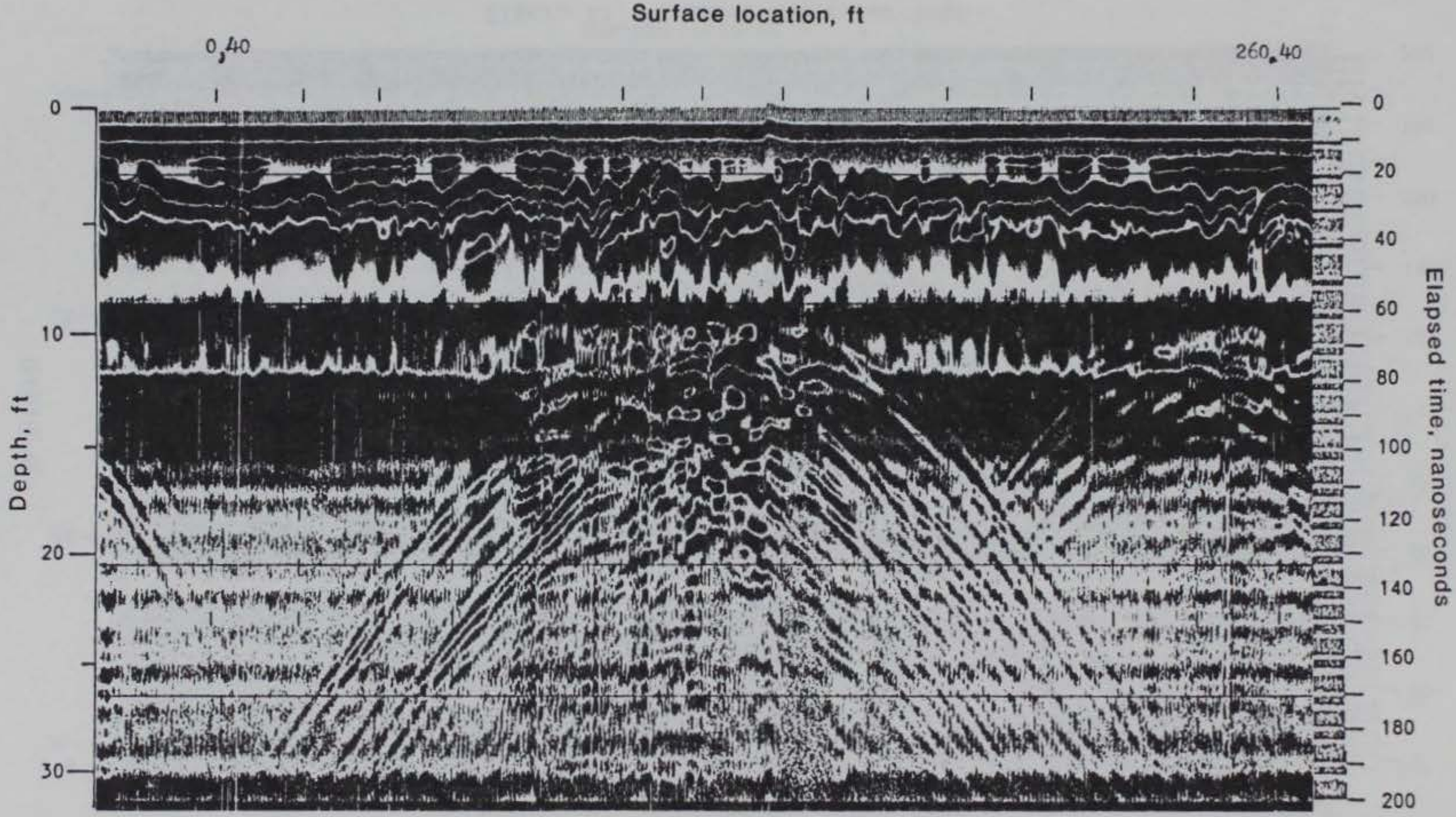

Figure 26. Technos R36 radar line

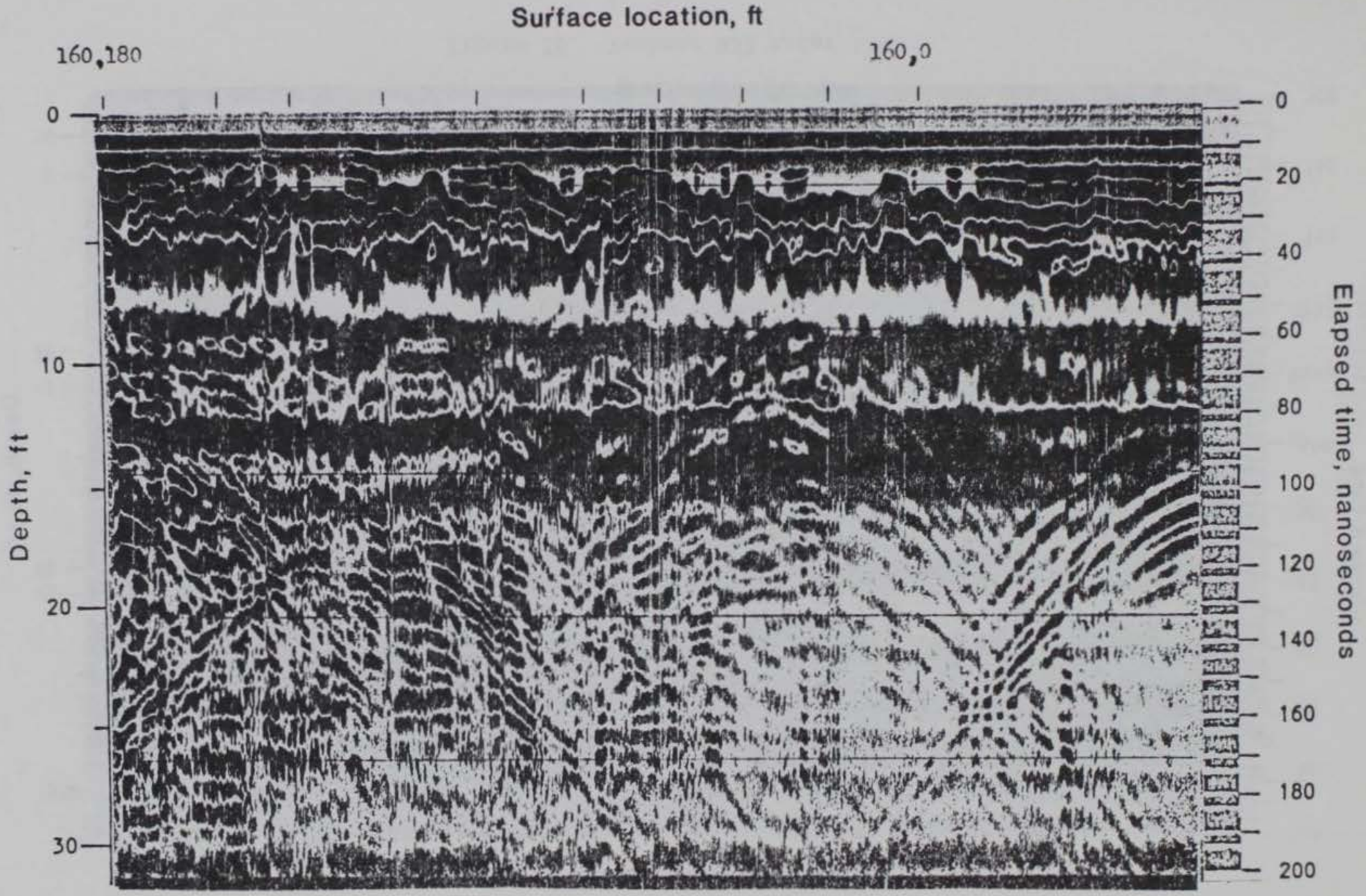

Figure 27. Technos R34 radar line

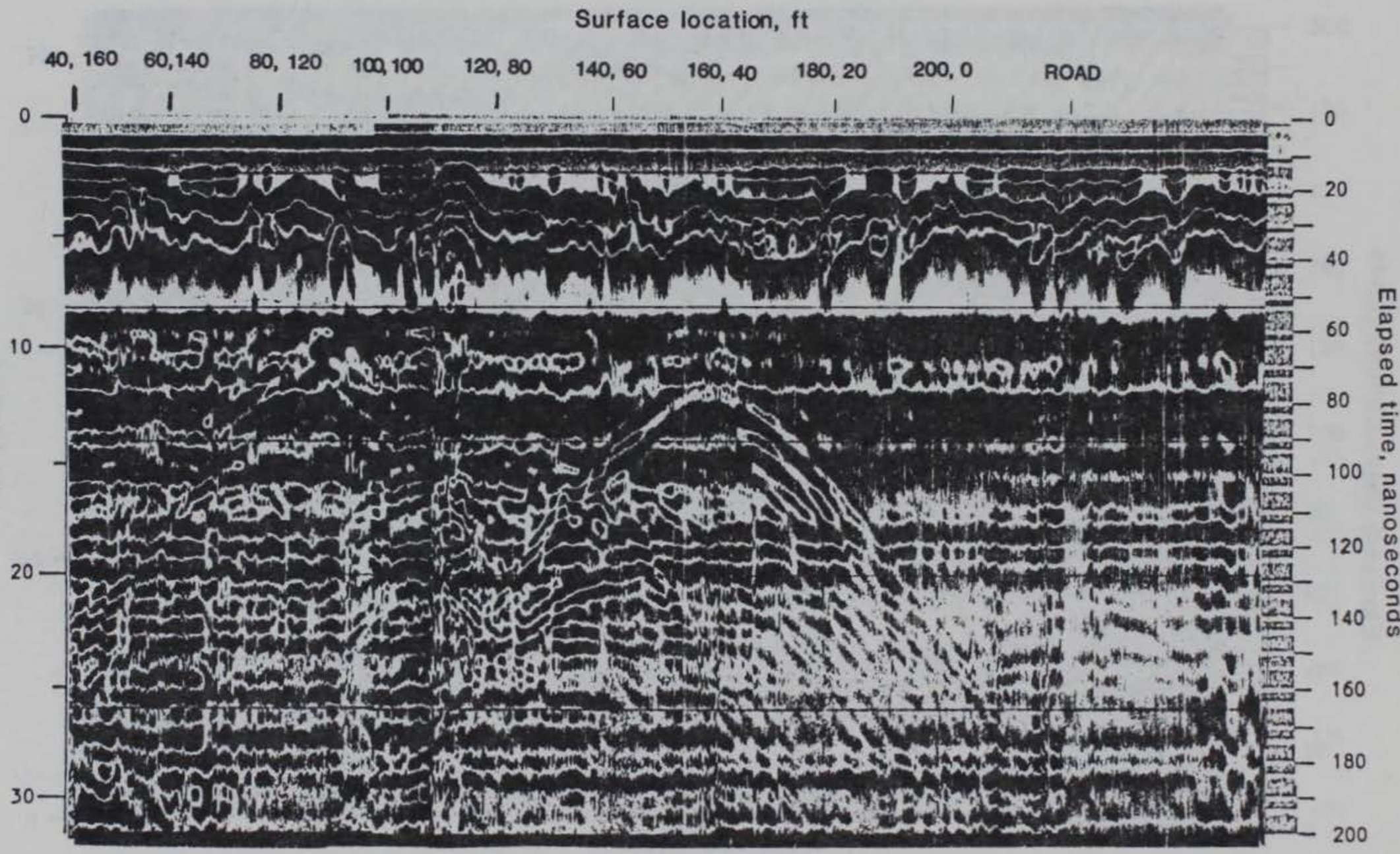

Figure 28. Technos R32 radar line

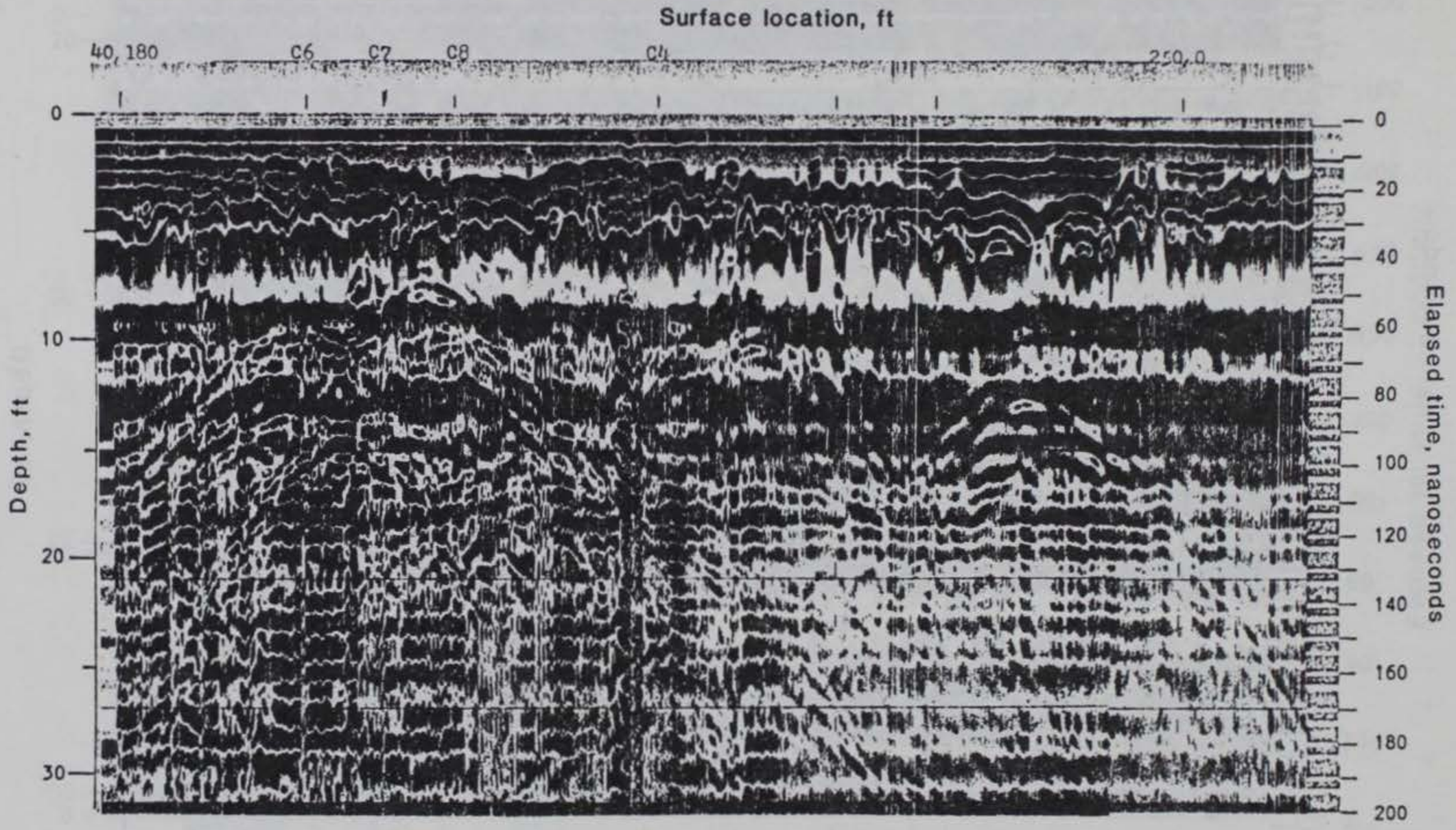

Figure 29. Technos R33 radar line

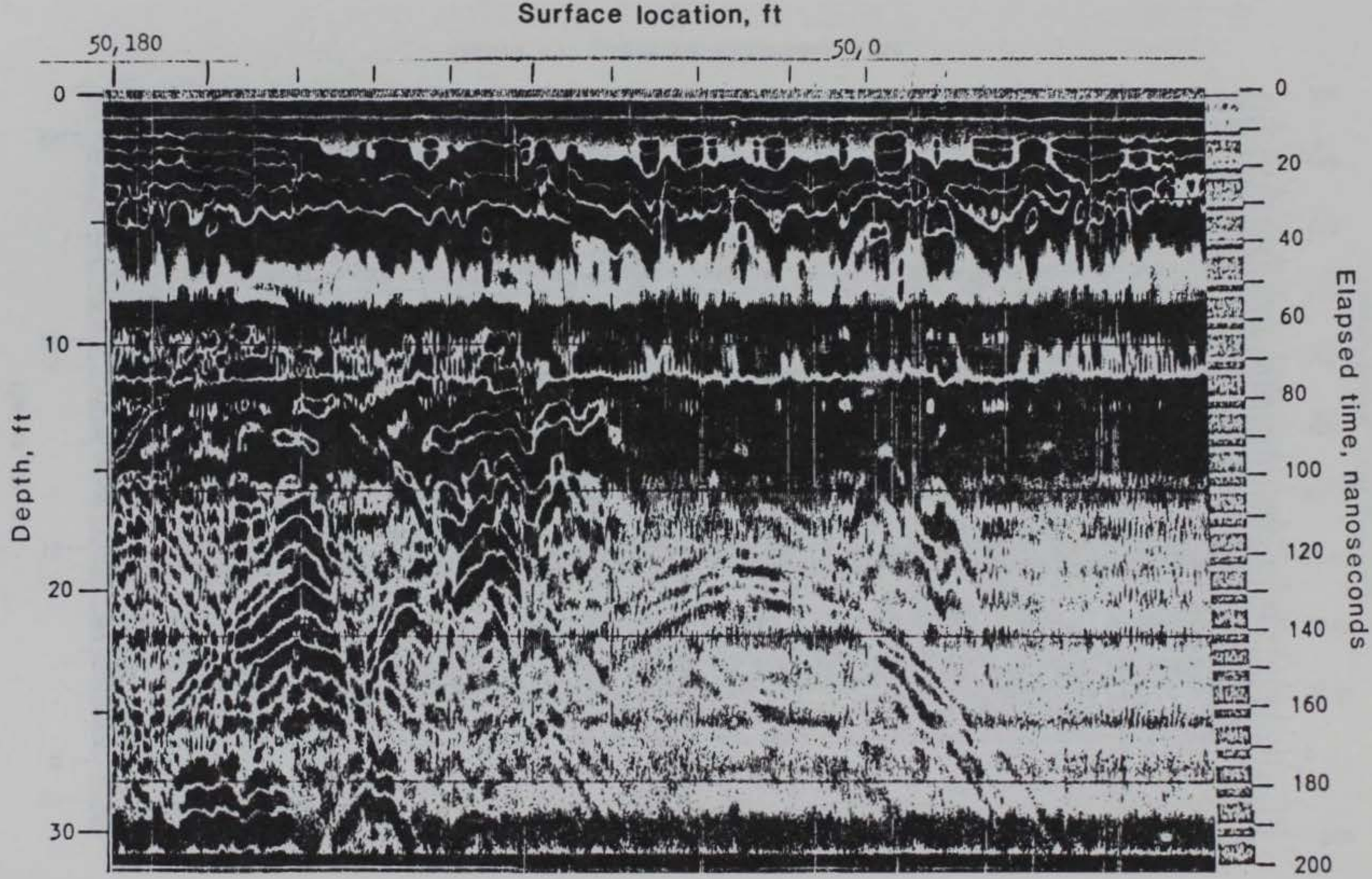

Figure 30. Technos R39 radar line

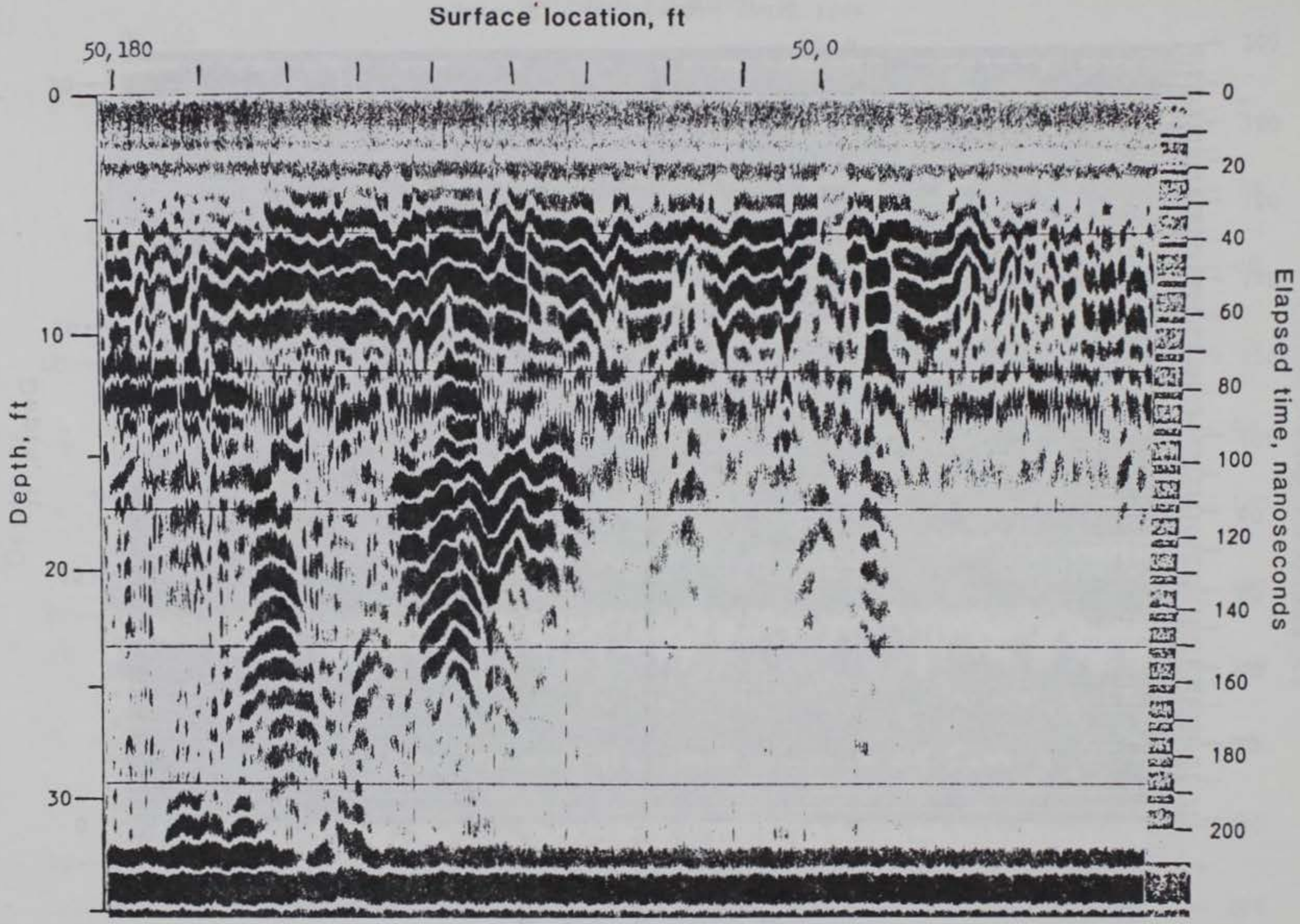

Figure 31. Technos R39 radar line (filtered data)

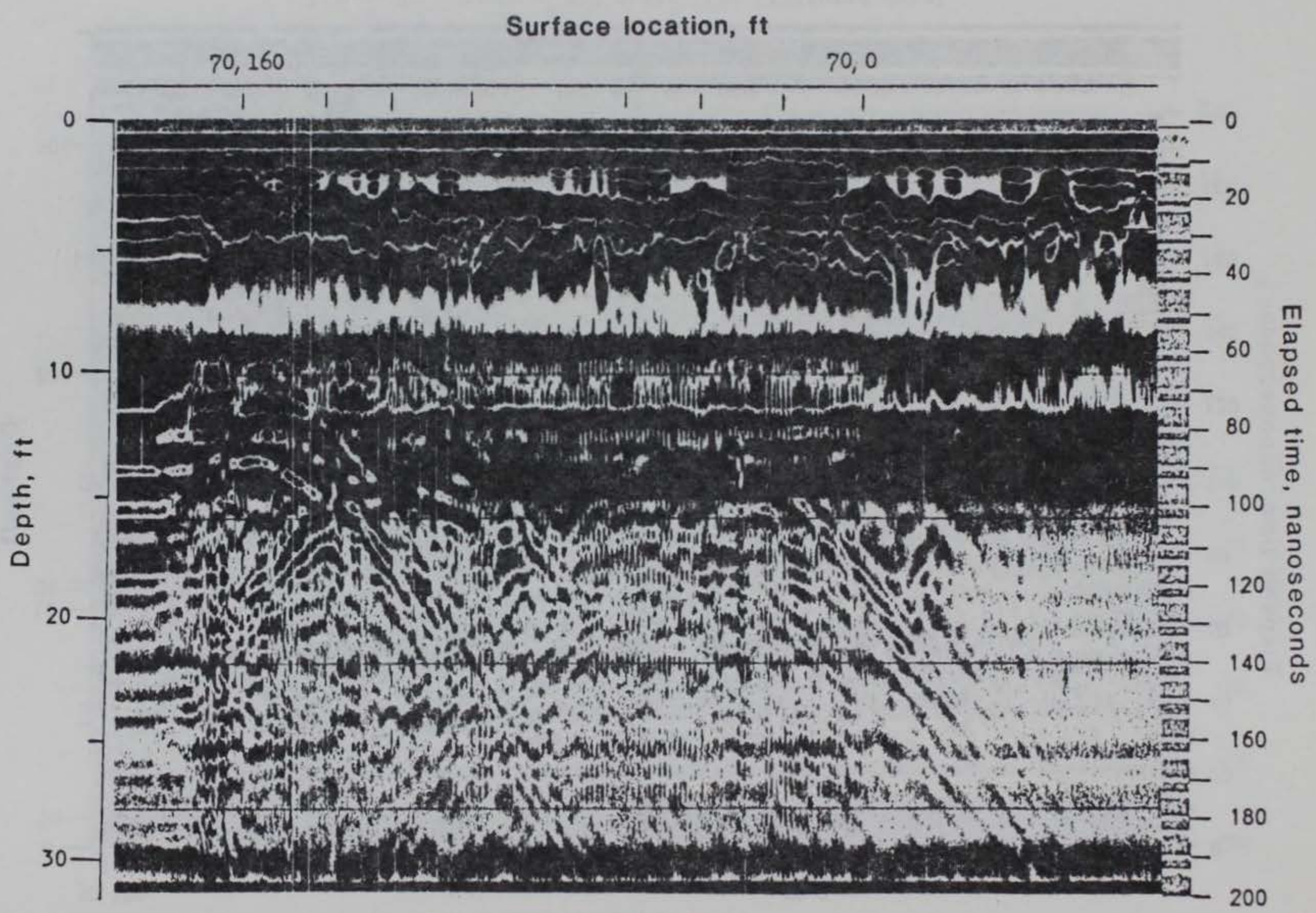

Figure 32. Technos R40 radar line

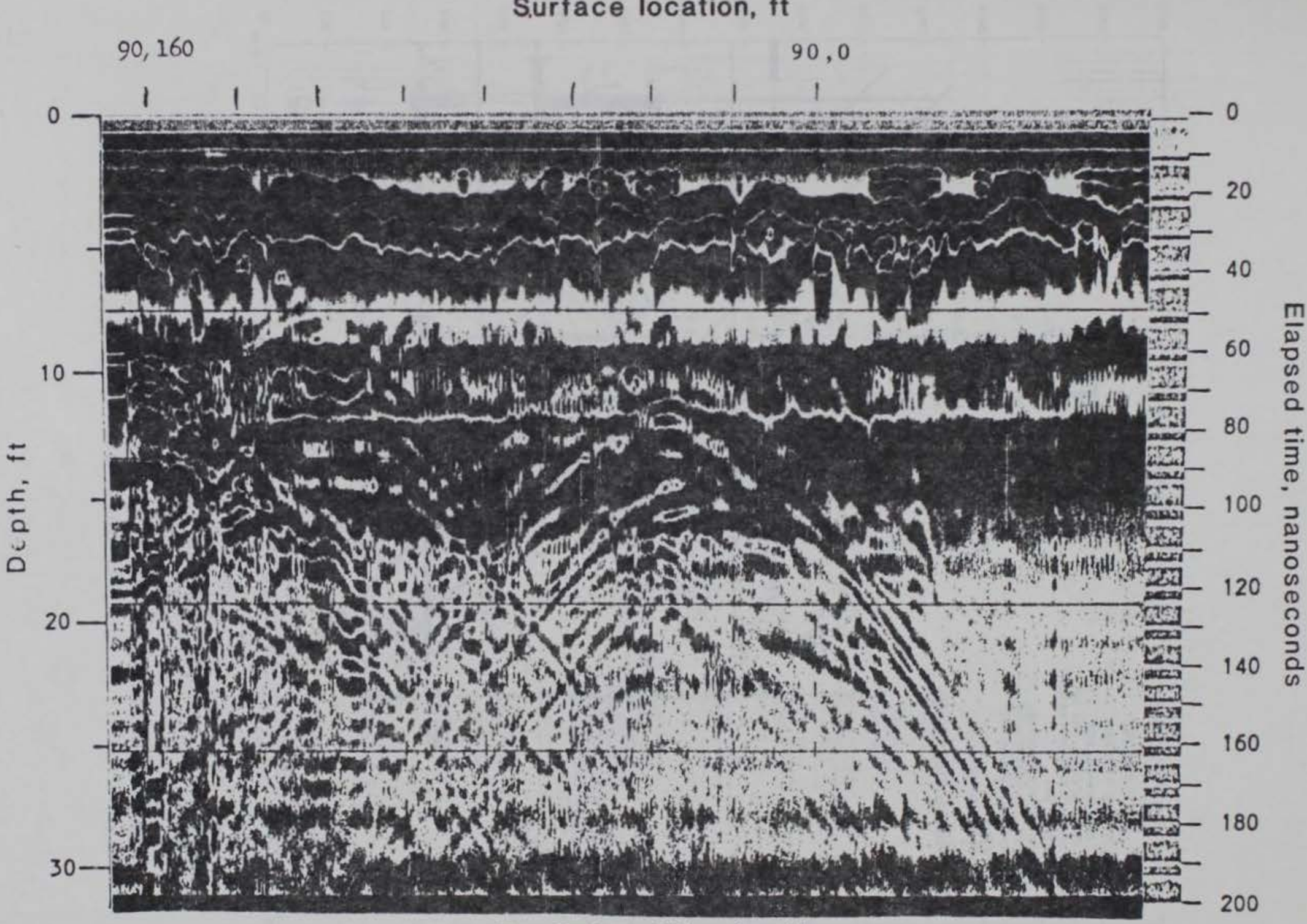

Figure 33. Technos R41 radar line

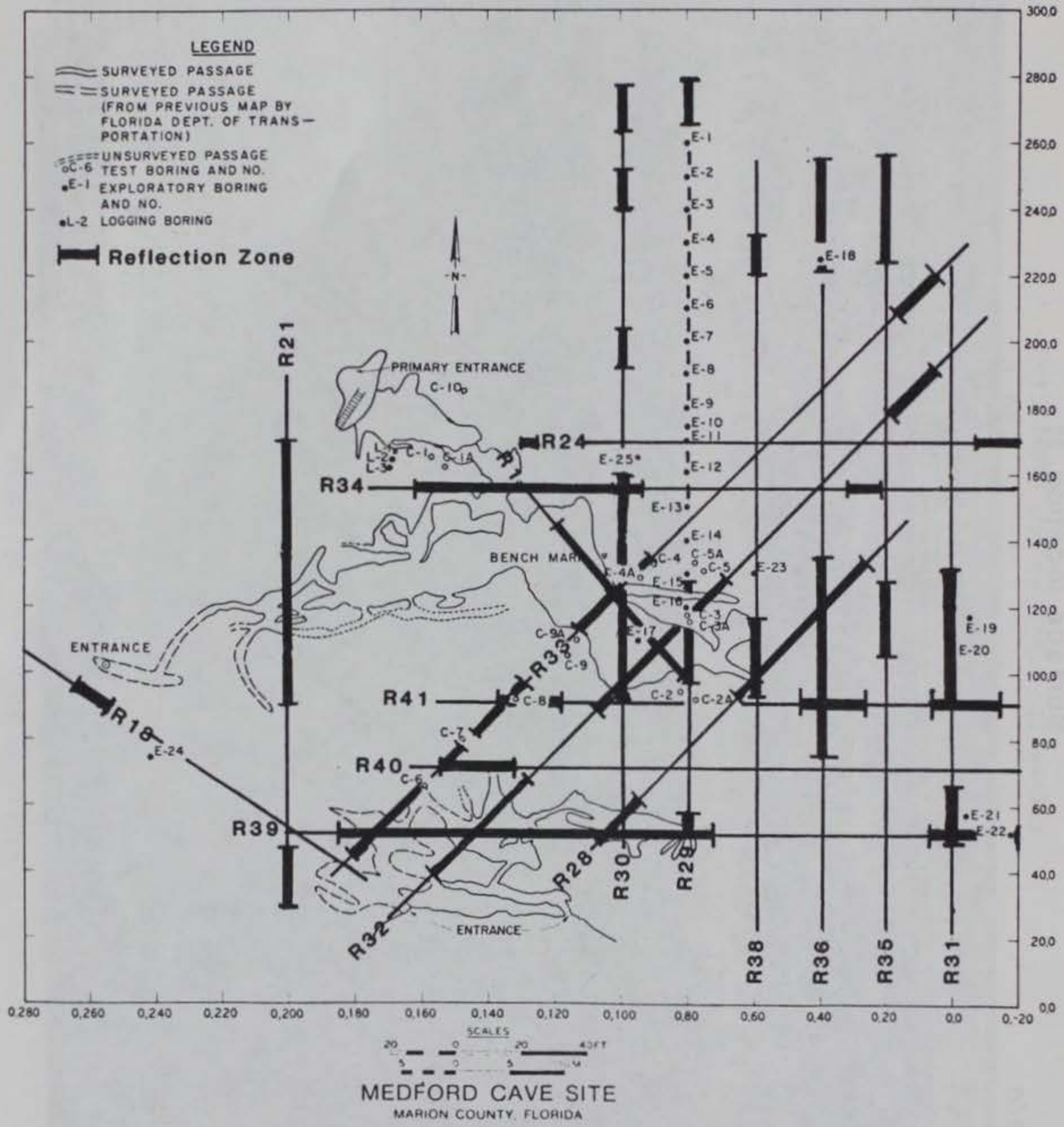

MEDFORD CAVE SITE
MARION COUNTY, FLORIDA

Figure 34. Location of radar reflections interpreted from Technos data

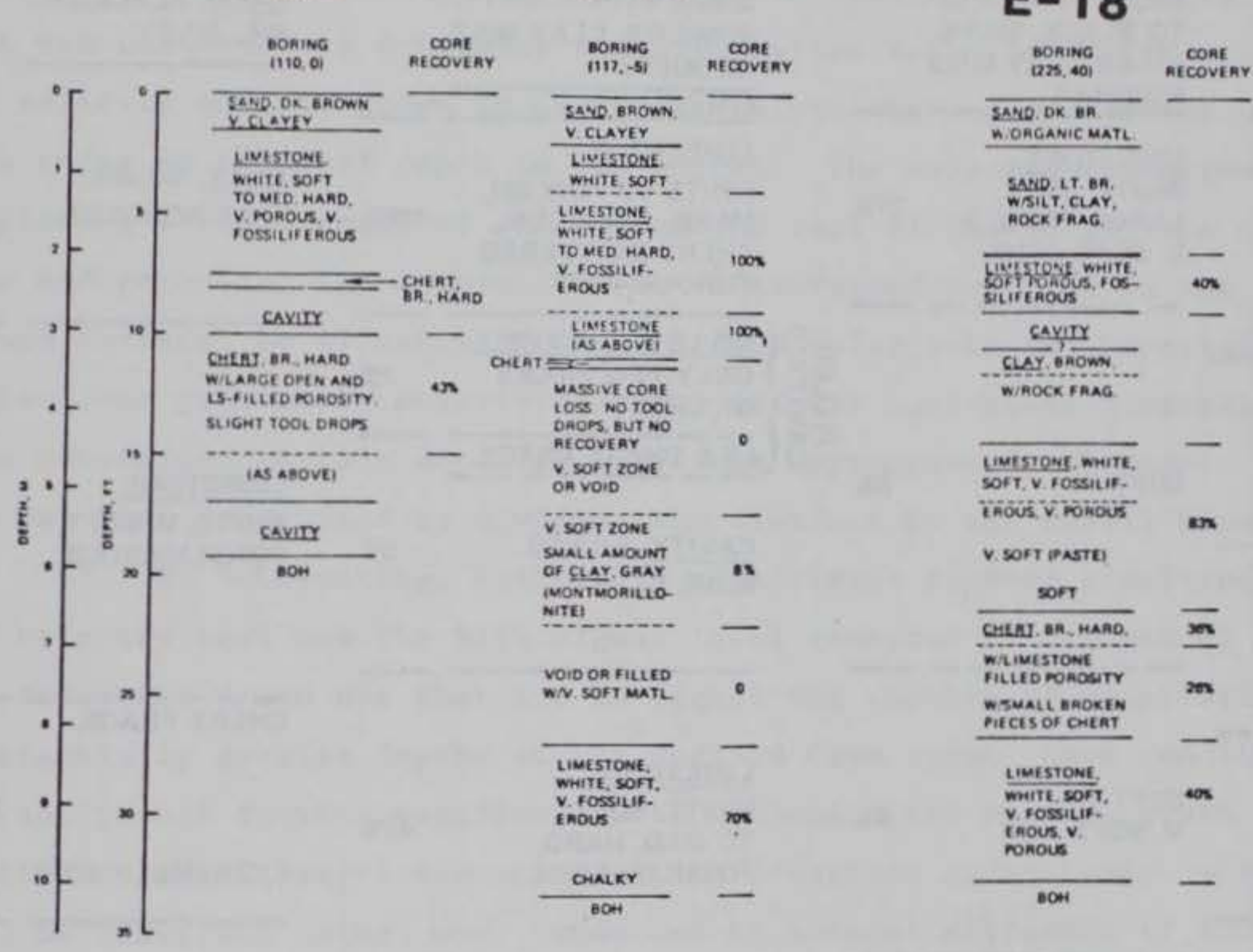

Figure 35. Logs obtained from borings E-20, E-19, and E-18

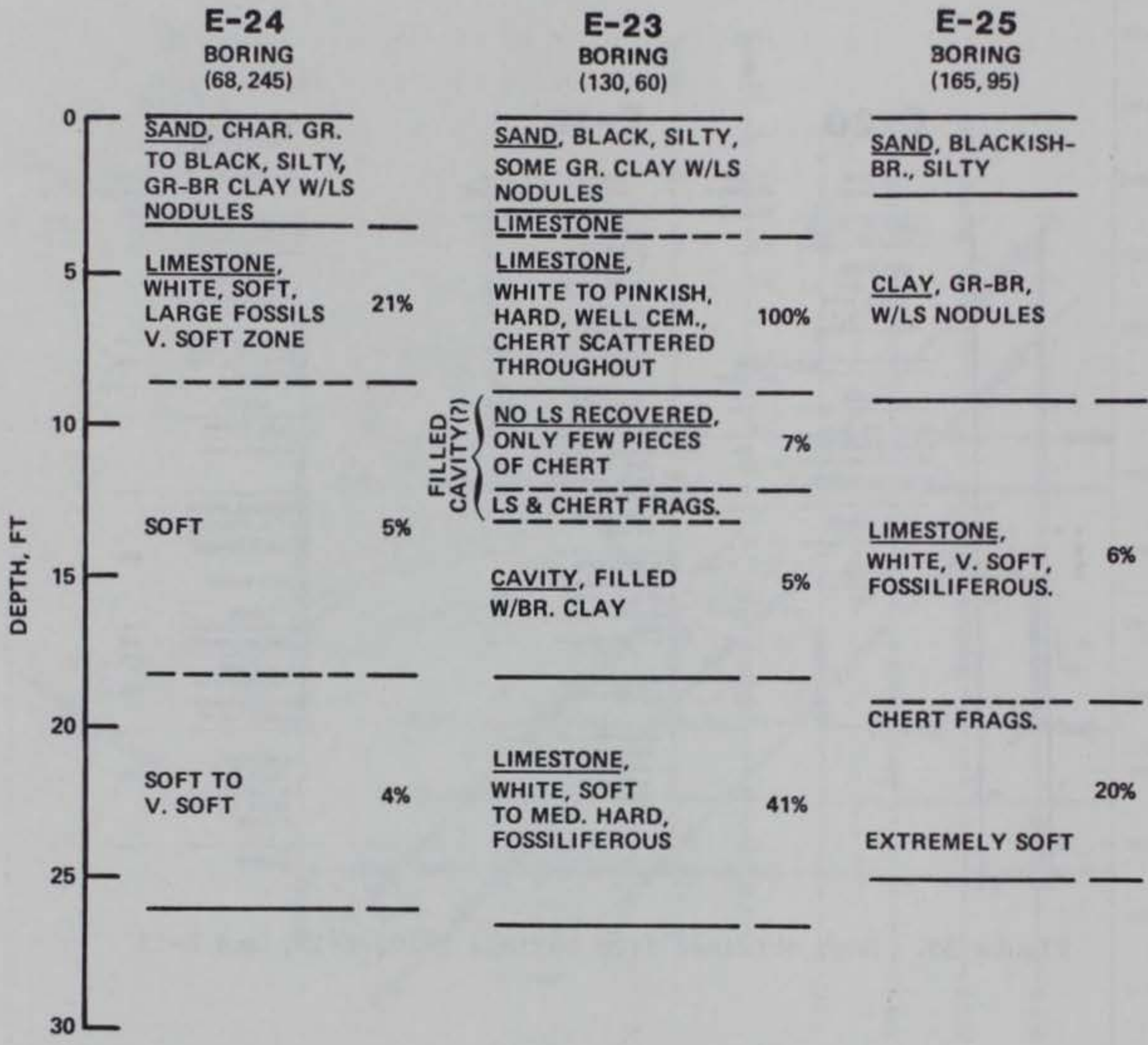

Figure 36. Logs obtained from borings E-24, E-23, and E-25

Fountain and Herzig (1980) documents the crosshole EM tests conducted at Medford Cave site. Both of these reports are available through the WES Technical Information Center and SwRI.

61. Tests were conducted by SwRI along 11 tranverse lines, all of which overlapped test areas previously investigated by Technos. The lines were chosen to be representative of cavity areas and noncavity areas. Figure 37 is a map of the Medford Cave site showing the location of SwRI's 11 radar traverse lines. Prior to running the traverses, one test was conducted to determine the propagation velocity of the medium. The velocity must be known in order to analyze the returns of the pulse echo radar in terms of depth to the target. The velocity was determined by placing a small receiver antenna on the roof of the large room of the cave and recording the transmitter as it traversed overhead on the ground surface, as illustrated in Figure 38 (also note the hyperbolic reflections previously described). The two-way equivalent propagation time determined at this depth of 12 ft was approximately 65 nsec. Velocity was then determined by dividing the distance by the travel time.

62. An interesting, but highly significant finding resulting from the velocity test was the high signal level recorded at a depth of 12 ft. The inference drawn was that the EM signal was capable of penetrating to substantially greater depths at the Medford Cave site. Cave conditions did not permit further verification to determine the maximum depth limitation of the surface-mounted unit. Crosshole radar tests, which will be described later, were conducted to lateral distances of 100 ft.

63. Data recorded on all 11 traverses were reduced by digital band pass filtering to the time-domain signals and depicted as such on separate plots with identified reflections outlined by SwRI personnel. From these data, most of the reflections, according to SwRI, appear as localized targets. In the regions corresponding to known voids, multiple reflections were seen over an extended portion of the traverse lines. In nearly all cases, anomalies detected by Technos were also detected by the SwRI system. Minor differences involved areal extent of some of the zones where a large number of reflections occurred. One unexplained difference was observed near the eastern end of SwRI's line 21

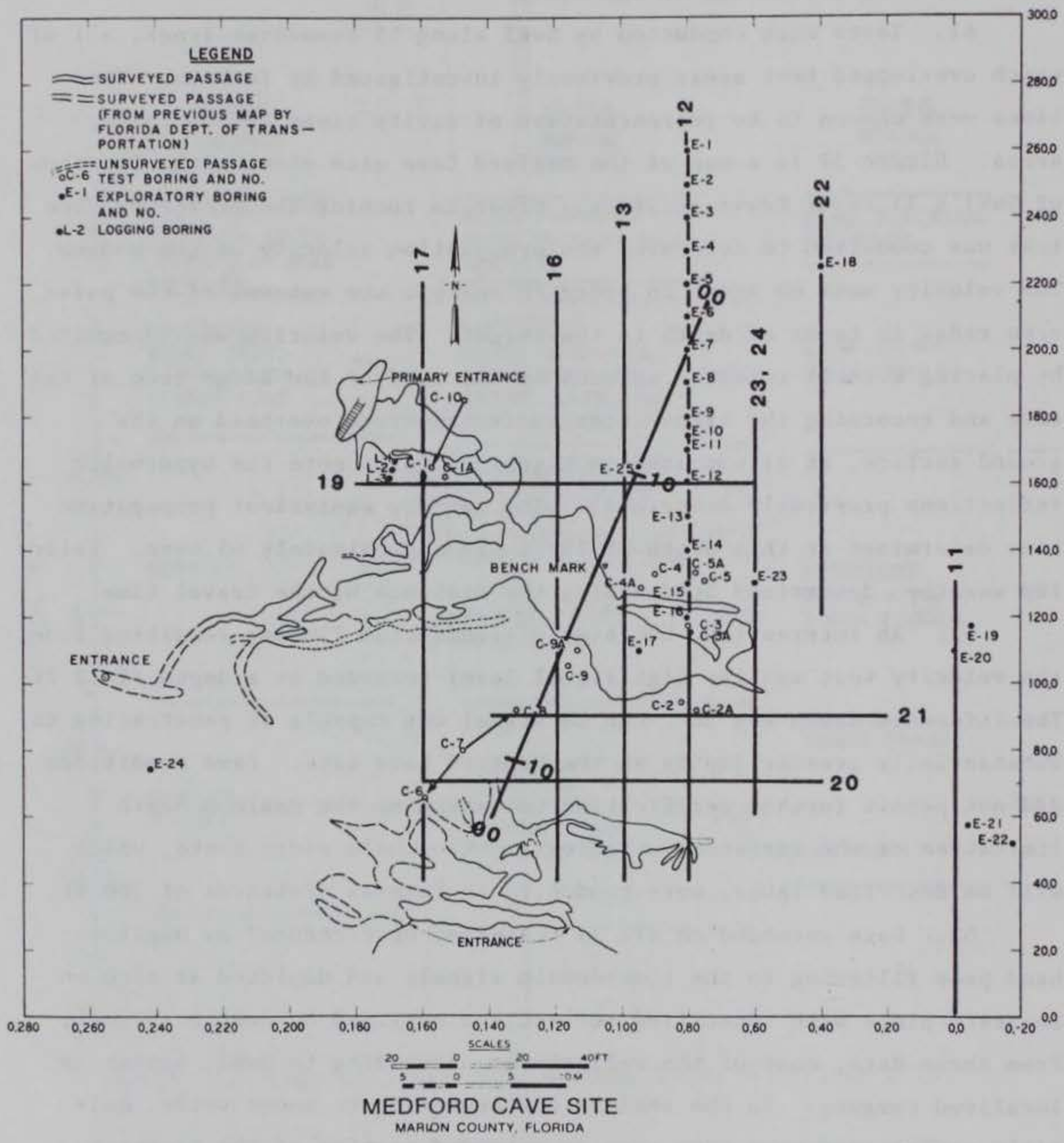

Figure 37. Location of SwRI radar traverses

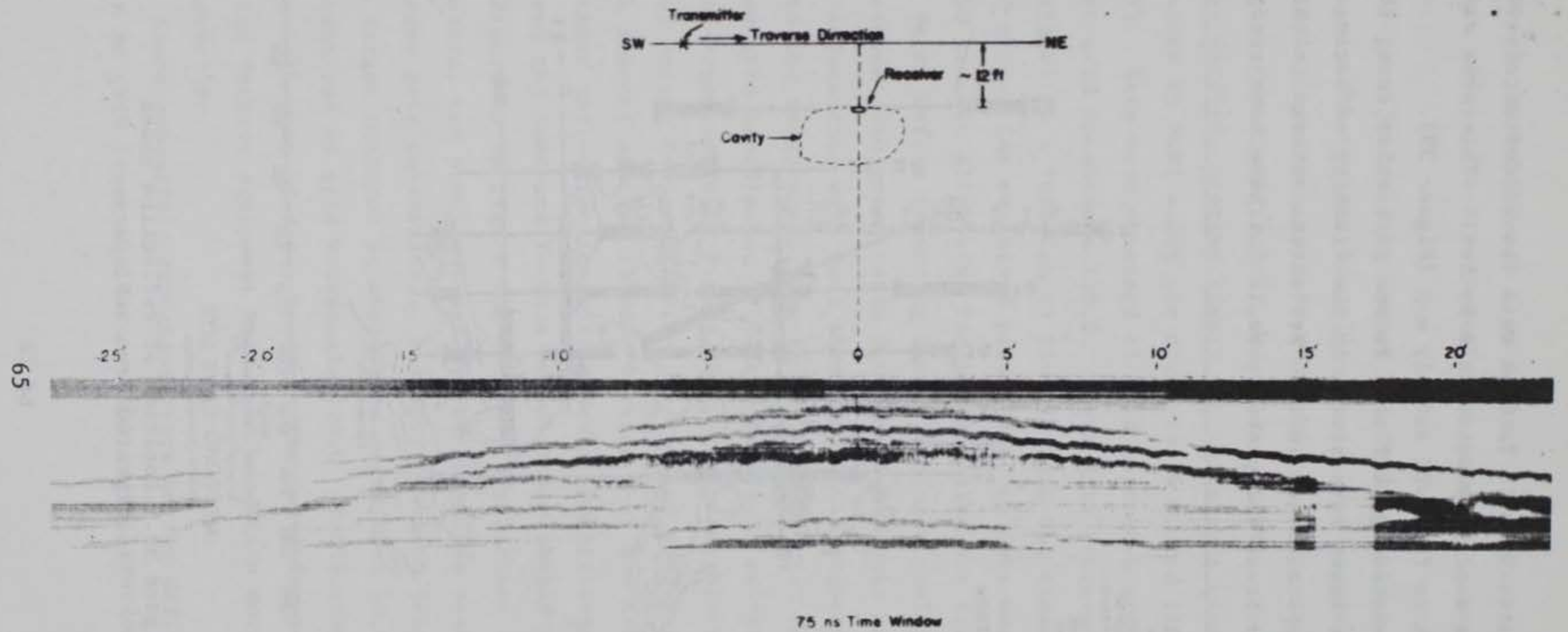

Figure 38. Data obtained during SwRI calibration traverse

near grid coordinates 90,40. Technos data showed definite reflections in this area where none were detectable by SwRI. This area was denoted by a question mark on the SwRI anomaly map (Figure 39).

64. It was noted by SwRI that in one particular case, the depth to the roof of the known cave system in the vicinity of boring E-17 was estimated to be approximately 16 ft. Reflection returns in this area were very weak and broad and probably would not have been recognized had

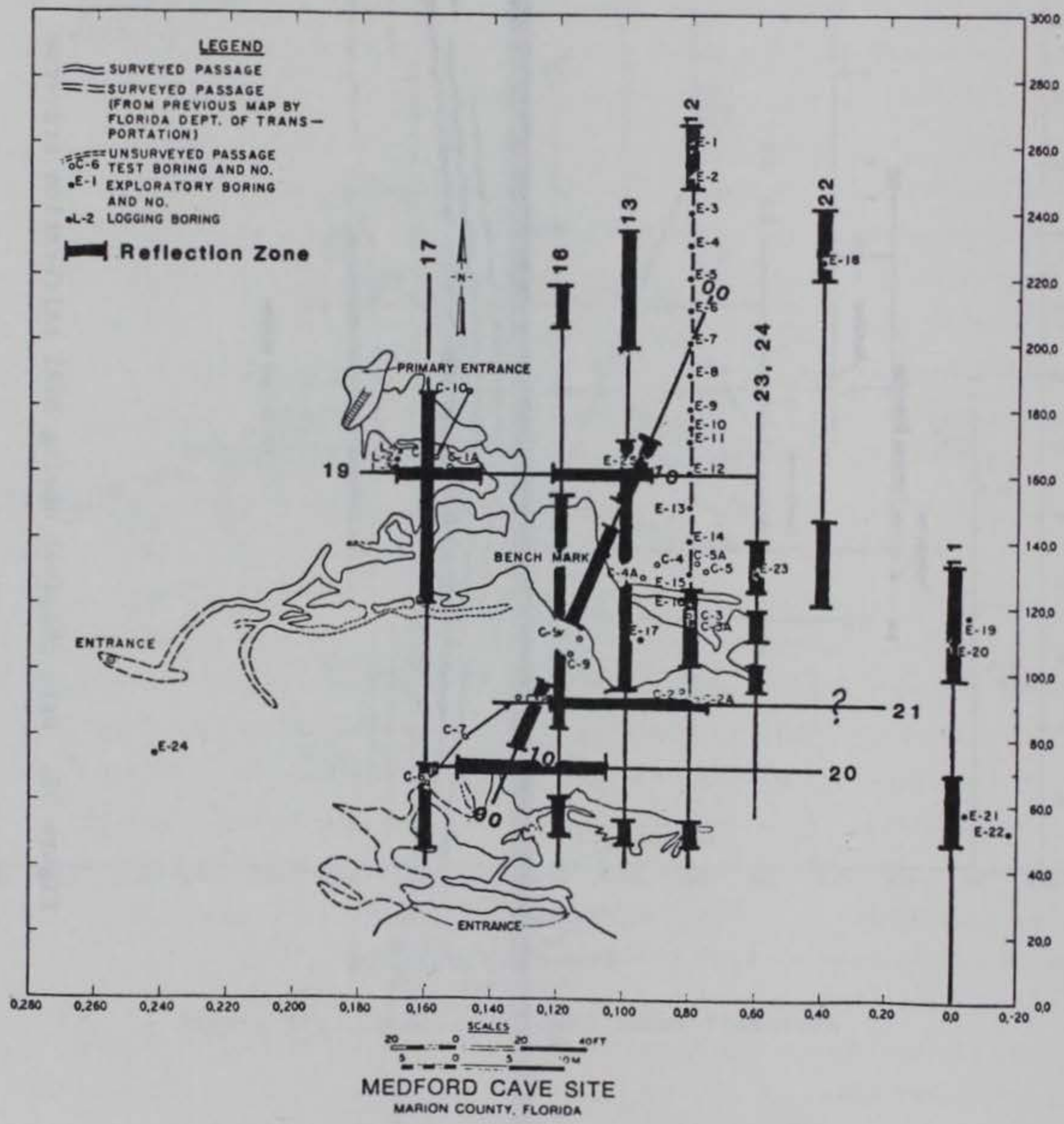

Figure 39. Location of reflection zones interpreted from SwRI data

the presence of the cavity not been known. Strong echo responses were also found in several locations not corresponding to mapped portions of the caverns.

65. Figure 39 could be termed the SwRI anomaly map, but more accurately, a map showing the locations (zones) of prominent reflection returns. It is important to note that this map is a reinterpreted version from that contained in Duff and Suhler (1980). To illustrate how this map was derived, observe Figure 40, which is a reproduction of the record obtained by SwRI along the north-south 0 grid line identified as SwRI line 11. Data were obtained at grid point 0,0 and progressing northward to grid coordinate 130,0. These data represent amplitude of returning signal as a function of time through the time window 50 through 120 nsec. (As explained previously, no data were recorded from 0 through 50 nsec to allow time for the oscillations from the pulse to completely decay before recording the returning signal.) The data existing between grid coordinates 0,0 and 25,0 should be disregarded because gain adjustments were made throughout this segment. Comparing Figure 40 to the anomaly map, Figure 39, observe that reflection zone A extends from grid coordinates 50,0 to about 70,0, centered at about 60,0. This zone is represented in Figure 39 by the heavy black segment of line 11 near boring E-21. Likewise, reflection zone B is shown by the heavy black segment of line 11 near borings E-19 and E-20. The actual length of these reflection zones is somewhat subjective and a perfect match between the SwRI and Technos anomaly maps should not be expected. Comparing Figure 40 to Figure 23, which is the Technos data obtained in the same locale, two prominent reflection zones can also be seen at about the same grid coordinates. Reflection zone A (Figure 23) corresponds to a target centered at about grid coordinate 60,0 and reflection zone B is centered at grid coordinate 120,0. Reflections are readily apparent on both sets of data; however, the variable area display generated by the Technos equipment makes the anomalies more pronounced to visual observation.

66. Since subsurface conditions were better defined along the north-south 80 grid line than at any other site location, a special

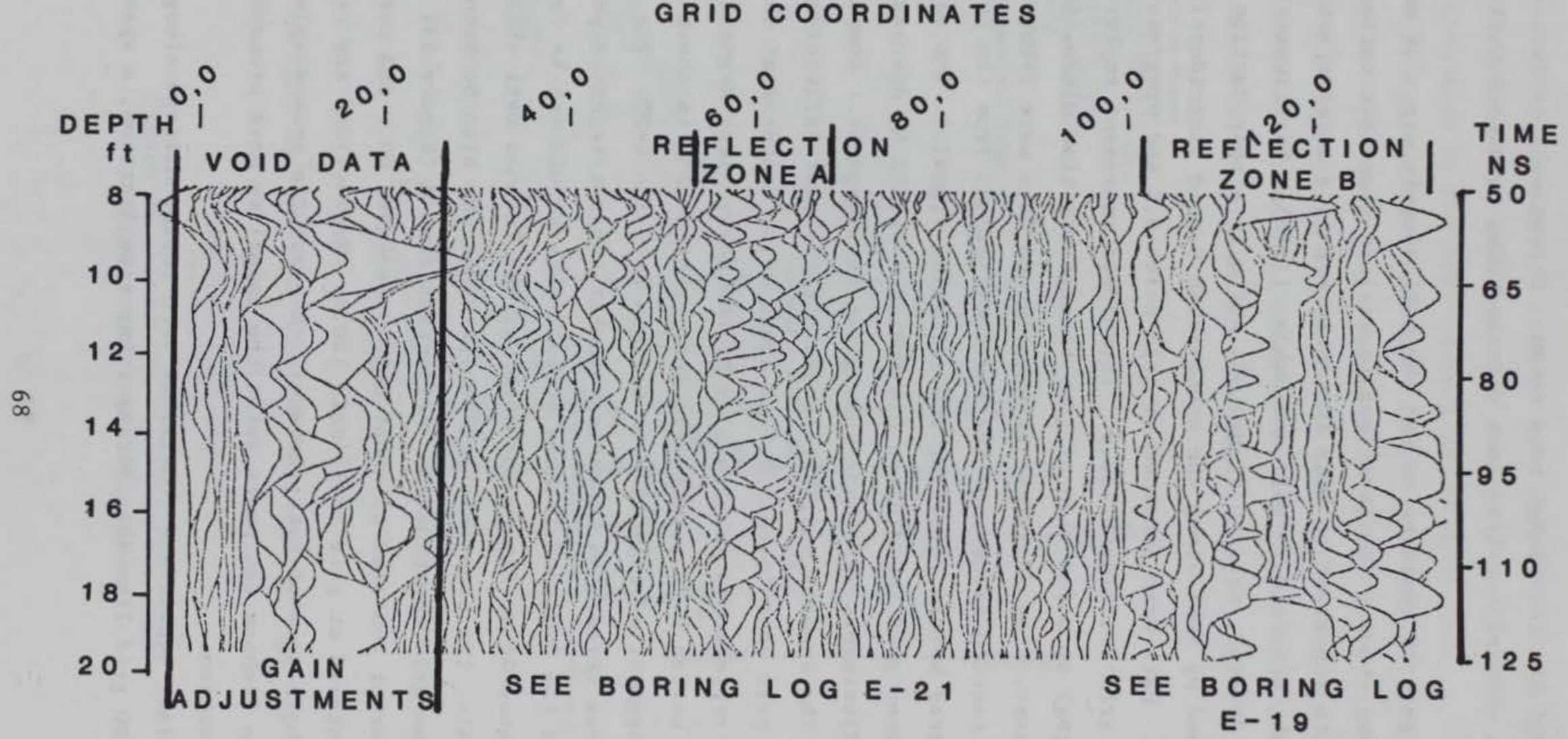

Figure 40. SwRI traverse line 11

effort was made to compare the data obtained by SwRI and Technos along this traverse. Figure 41 shows the data taken by SwRI from coordinates 40,80 to 270,80. Only the time scale window from 50 to 125 nsec is shown. This roughly corresponds to a depth scale from 8 to 20 ft. Three mapped cavity features are shown appropriately scaled in their proper locations. Unfortunately, the tops of cavities 1 and 2 are located below the SwRI time window, but the reflection zone appearing above each is easily recognizable. Cavity 3 also creates some reflection activity, but due to its vertically elongated geometry, is not as apparent. Horizontal layering without anomalous features is evident from coordinates 140,80 to about 240,80. A deep clay pocket (4) beginning at about 240,80 and extending beyond 270,80 and/or a limestone pinnacle is likely responsible for reflections occurring at the extreme northern end of the traverse.

67. Technos data (Figure 42) obtained along the same traverse (R29) were not manipulated in the "time window" fashion. As a consequence, their data presentation is not only more impressive, but contains considerably more usable information from 0 to 200 nsec encompassing a depth range of more than 30 ft. By superimposing the known geologic cross section, pertubations caused by the clay pocket and limestone pinnacles from 160,80 to 230,80 are now explainable. Likewise, cavities 1-3 establish an excellent correlation with the multiple reflections indicated by the arrows. Note the similarity in signatures between cavity 3 and the vertically fissured calibration cave (Figures 13-15). Target 4 was not confirmed, but could be the result of multiple reflections from the limestone pinnacle above the arrow or another small cavity possibly as deep as 30 ft or more. Evidence of horizontal layering can be seen at a depth of about 8 ft (50 nsec), 11 ft (70 nsec), and 17 ft (105 nsec) from grid coordinates 140,80 to 240,80. This is in close agreement with the SwRI data shown in Figure 41.

68. After testing was completed, a recommendation was made by SwRI that exploratory borings be placed at grid coordinates 120,0; 135,50; 125,60; and 160,100. Exploratory borings were later placed at

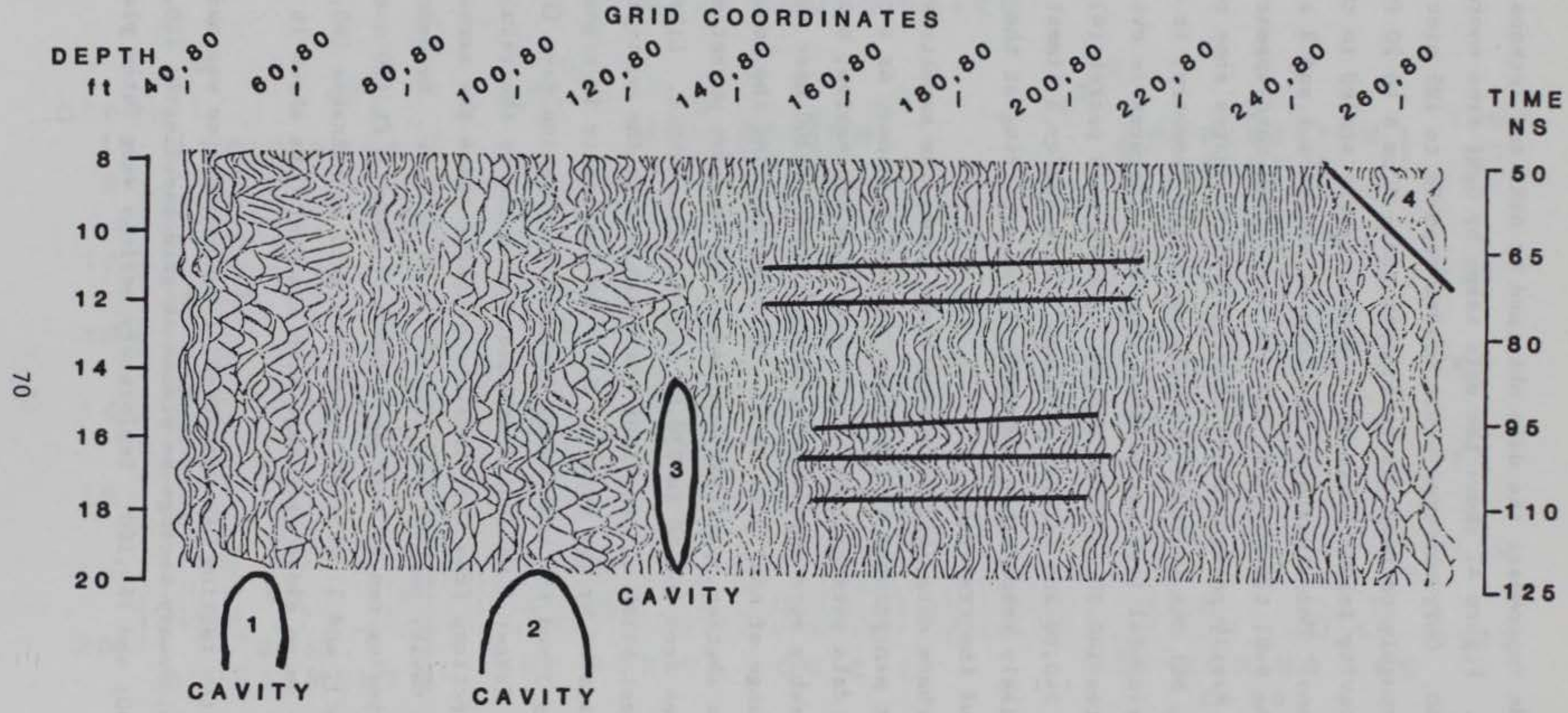

Figure 41. SwRI data obtained along north-south 80 grid line

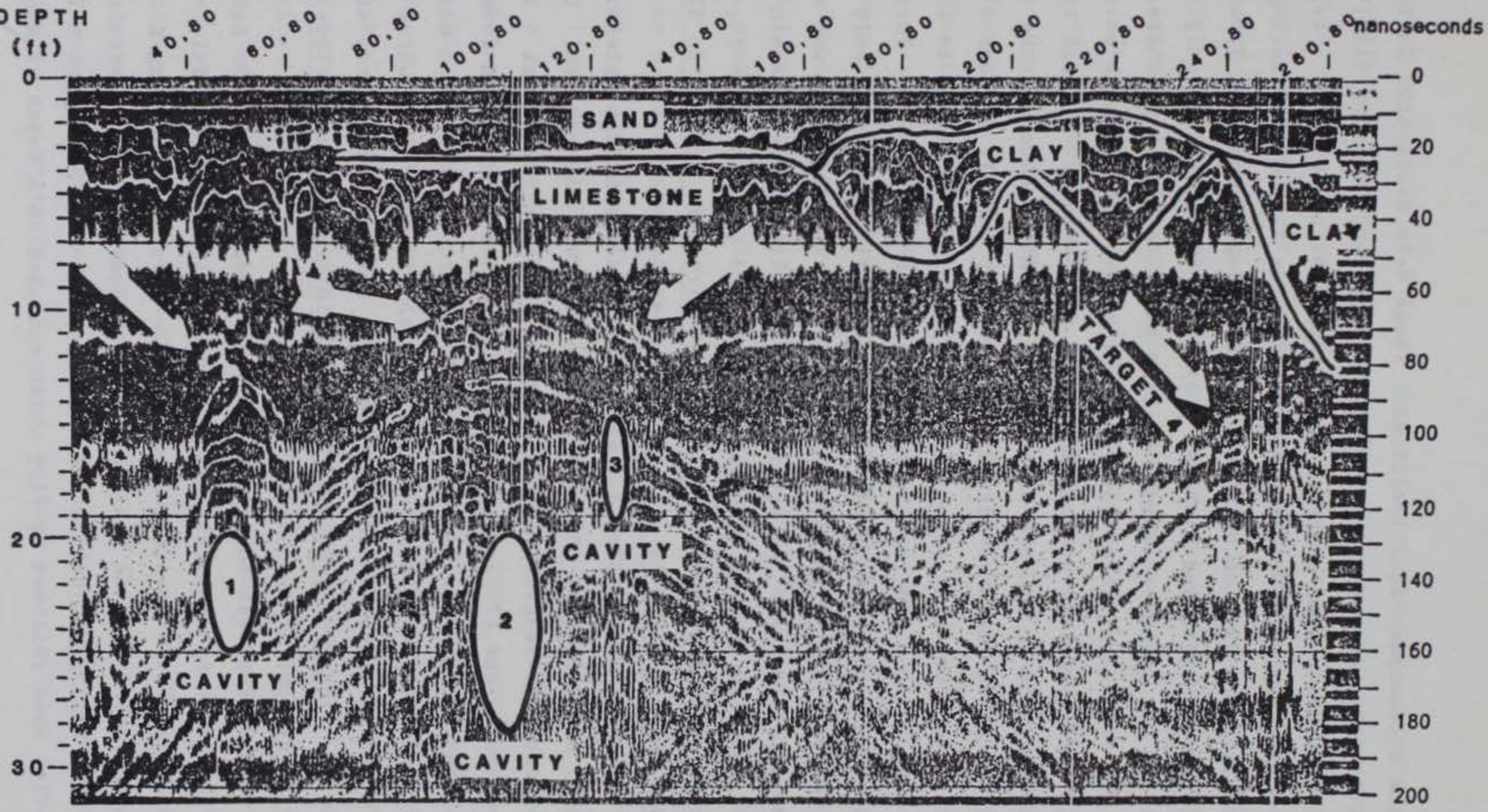

R 29

Figure 42. Technos data obtained along north-south grid line, R29

three of the recommended four locations. These were designated as E-19 (120,0), E-23 (125,60), and E-25 (160,100). The fourth boring (135,40) was not placed due to time and cost limitations for the project. Logs for these borings were previously shown in Figures 35 and 36. Boring E-19, an abbreviated version of which was shown superimposed on Technos line R31 (Figure 23), showed that the overburden thickness was only about 2 ft and was comprised mainly of clay sand. A highly weathered limestone was then encountered to a depth of about 4 ft at which point a medium to hard limestone was encountered. Core recovery through this zone was 100 percent to a depth of about 10 ft. After encountering a thin layer of chert, the core barrel advanced very rapidly through a soft material to a depth of about 17 ft. No core was recovered in this zone, but clay residue was readily apparent in the core barrel. Further attempts at core recovery to a depth of about 25 ft resulted in only 8 percent recovery in the zone from 17 to 22 ft. This material was a gray montmorillonite clay. At a depth of 27 ft, limestone was again encountered and a 70 percent core recovery made to a depth of 34 ft, the maximum depth of the exploratory hole. The entire zone from 10 to 22 ft in depth was characterized as a clay-filled void.

69. Boring E-23 revealed a black silty sand overburden extending to a depth of about 3 ft at which point limestone was encountered. One hundred percent core recovery was experienced to a depth of about 8 ft. A 93 percent core loss (7 percent recovery) was then experienced from 8 to about 12 ft. Only a few pieces of chert were recovered. Even more loss was experienced from that point to a depth of about 18 ft where medium to hard limestone was encountered. The hole was terminated at a depth of 26 ft. The zone from 8 to 18 ft was interpreted as a clay-filled cavity system.

70. Boring E-25 was located in a fringe area where Technos data exhibited little or no anomalous behavior and SwRI data showed only slight indications of a possible anomaly. The location of boring E-25 was determined mainly on the basis of low microgravity and resistivity readings. The boring was drilled to a depth of 25 ft. The upper 3 ft showed a silty sand followed by clay which extended to a depth of about

8 ft. From a depth of 8 ft to the bottom of the hole, a very soft fossiliferous limestone with some chert fragments was encountered. The material was highly fractured. Only a 6 percent core recovery was obtained from a depth of 8 to 20 ft and only a 20 percent core recovery obtained from 20 to 25 ft. No cavity could be confirmed at this location. Presence of the 8-ft clay pocket was determined to be the reason for microgravity and resistivity lows.

71. In the conduct of SwRI crosshole radar tests at the Medford Cave site, some 25 borehole scans were recorded over distances greater than 100 ft. Many were made with transmitter and receiver offset (at different elevations) so that a target could be reconstructed in two dimensions.

72. Fountain and Herzig (1980) showed some 11 crosshole examples of results obtained with the transmitter and receiver located at a common depth. Upon examination of their data, those anomalies indicated by differences in pulse arrival times associated with air-filled cavities caused a high pulse velocity (or short time of flight); whereas, water- or mud-filled cavities caused a slowdown or longer time of flight of the pulse. This change in wave speed is associated with the electrical characteristics of the material; i.e., air has a lower conductivity than limestone, consequently, a higher EM wave speed.

73. Figure 43 shows a crosshole record obtained by SwRI between boreholes C-4 and C-5, 17 ft apart, with no known cavity between the borings. The data are displayed in the form of pulse travel time as a function of depth from the ground surface. Data were processed in the variable area format which assigns a degree-of-gray intensity to the amplitude of the received signal. Observing Figure 43a, the first vertical dark band is analogous to the high-amplitude peak of the incoming wave; whereas, the following white band is the trough of the wave. The second gray band is representative of the second peak, which is of lower amplitude than the first. One will observe that the first-arrival times are approximately equal throughout the entire scan in Figure 43a. Figure 43b is a crosshole record between borings C-2 and C-3 which are 22 ft (6.7 m) apart. In this case, a known air-filled

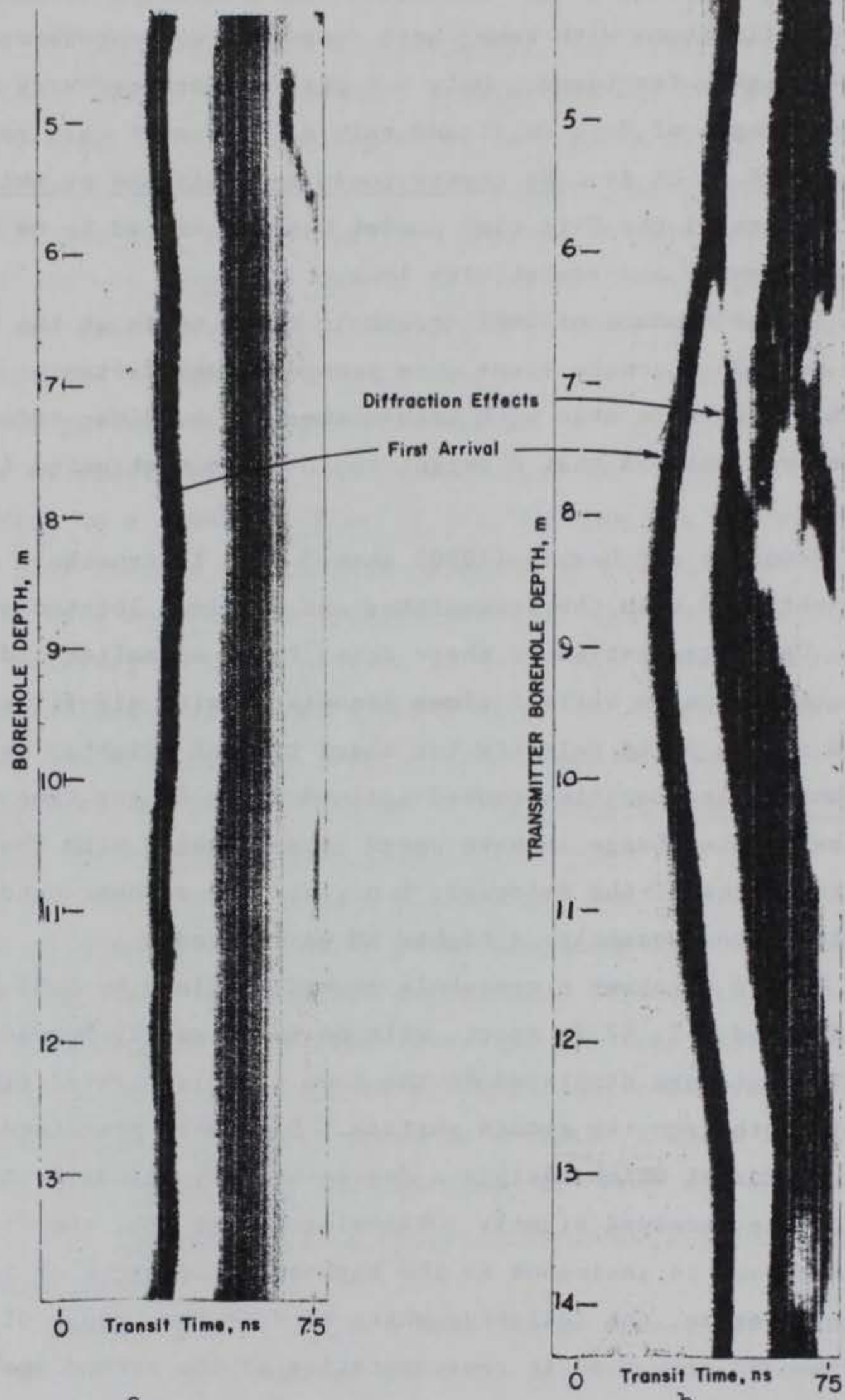

a.

EM Crosshole Record
Boreholes C4-C5, 17ft Apart
Transmitter-Receiver Raised Synchronously
(No known cavity between boreholes)

b.

EM Crosshole Record
Boreholes C2-C3, 23ft Apart
Transmitter-Receiver Offset 1m
Raised Synchronously
(Known Cavity)

Figure 43. Example of SwRI crosshole test (variable area format)

cavity was located between the boreholes centered at a depth of about 29 ft (9 m). Its presence is evidenced with the decreased first-arrival times and the diffraction effects which are also visible on the record above and below the center of the cavity. This example serves to illustrate that the crosshole radar techniques should receive serious consideration for cavity detection.

74. Figure 44 shows the radar scans run between borings C-3 and C-5. Observe that in this display, SwRI chose to process data in an analog format that would show the entire signature of the returning reflections rather than shades of gray. These data were recorded at 39.4-in.- (10-cm-) depth intervals. The small mapped cavity feature (see also cavity 3, Figure 42) between the borings at a depth of 15 to 20 ft (4.6 to 6.1 m) is evidenced by the shorter arrival times occurring at a depth of 15 ft (4.6 m). Signal-arrival times of selected traces are shown opposite the applicable traces on the right-hand side of the SwRI plot. An arrival time of 29 nsec was noted at a depth of 4.6 ft. When comparing this time to the 33 nsec observed at depths of 12.8 and 20 ft (3.9 and 6.1 m, respectively) a difference of 4 nsec would be expected with the presence of an air-filled cavity between the transmitter and receiver having a width of about 3 to 4 ft (1 to 1.2 m). It should also be noted that a decrease in signal amplitude is noticeable at this depth. Other features are apparent on this plot at depths of 23.6 ft (7.2 m), 33.5 ft (10.2 m), and (very slightly) 37 ft (11.3 m). These will be discussed in greater detail later.

75. After all tests had been conducted at the Medford Cave site by the radar contractors, the exploratory borings previously described were undertaken. Final locations of the borings were chosen on the basis of recommendations by the radar contractors and with some consideration given to the results of microgravity, refraction seismic, and resistivity tests conducted in the same areas. Considering the anomalous features found in the boreholes (previously described), one can conclude that the SwRI ground-probing radar tests as well as those conducted by Technos were successful and should be considered for both reconnaissance and high-resolution cavity detection surveys recognizing that the radar's

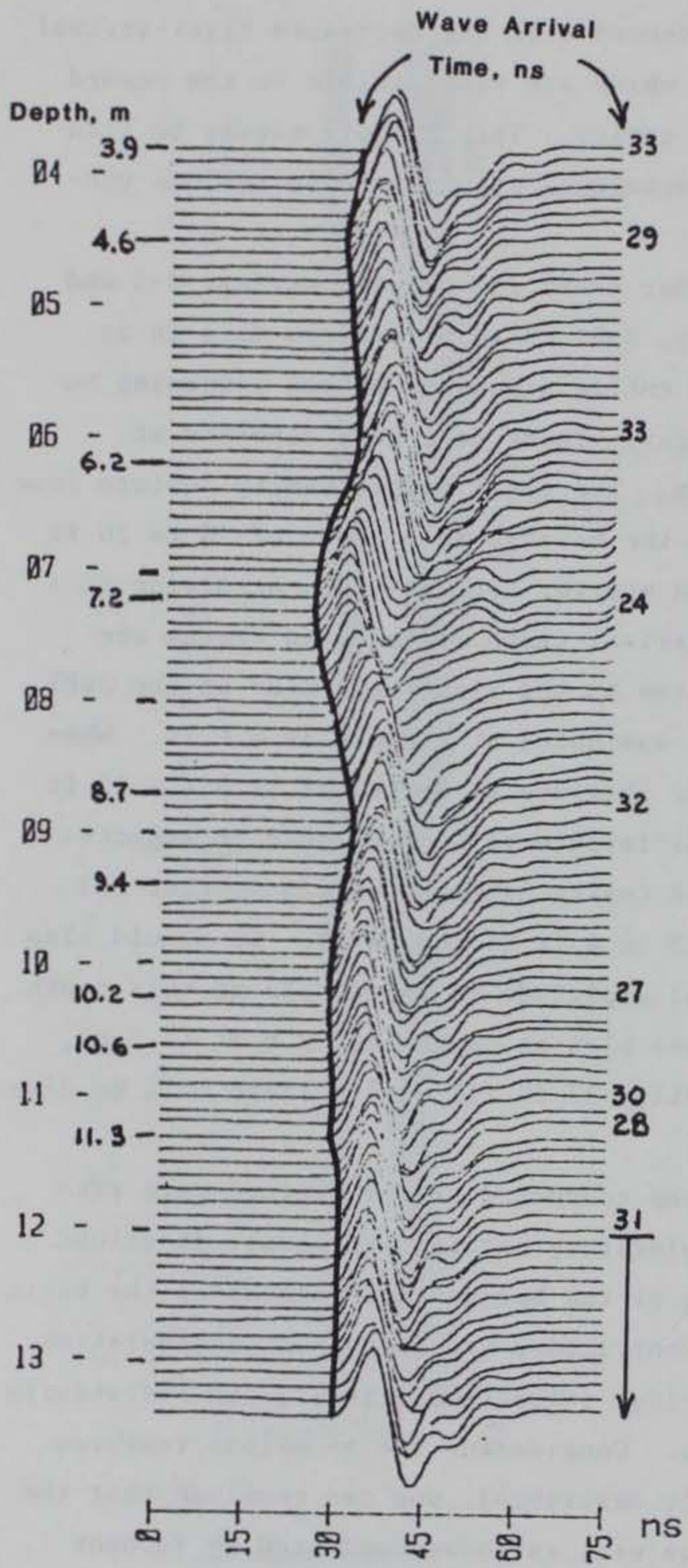

Figure 44. Example of SwRI crosshole test between borings C-3 and C-5

maximum depth of penetration and degree of resolution will be dependent on site conditions.

LLNL

76. Appendix A contains all the information reported by Laine (1980) pertaining to EM tests conducted at both the Medford Cave and Manatee Springs test sites. The report also contains a section on borehole-to-borehole resistivity, which, while not directly related to the scope of this report, is included for reader information.

77. It should be noted again that the radar system devised and operated by LLNL personnel was intended for use within and between boreholes. Consequently, no surface ground-probing tests were conducted by LLNL.

78. Laine states that single-frequency depth scans were made between boreholes C-3 and C-5 at operating frequencies of 1 to 100 MHz. Data were plotted in terms of amplitude of received signal as a function of frequency and borehole depth. At this location, the top and bottom of the small mapped cavity between borings C-3 and C-5 are actually located at 15 and 20 ft (4.6 and 6.1 m, respectively), not at 24 and 32.1 ft (7.3 and 9.8 m, respectively), as stated by Laine. Laine's interpretation of the data shown in Appendix A, Figure A10, states that the top of the cavity is located at a depth of about 23.6 ft (7.2 m) and the bottom at about 34.8 ft (10.6 m) (page A14). Another interesting data display devised by Laine shows a swept frequency plot between boreholes C-3 and C-5 as a function of amplitude and depth (see Figure A11). These data show pronounced signal nulls in the area of the known cavity. Other nulls which were not related to the mapped feature can also be seen.

79. Another more detailed interpretation can be rendered using Laine's swept frequency plot (Figure 45). Bearing in mind that decreasing signal amplitude is in the up direction, by noting curve A, it will become apparent that a pronounced null exists at a depth of 16.4 ft (5 m) in the 30-MHz region and is evident to a depth of more than 19.7 ft (6 m). This effect can be related to the mapped cavity known to exist between 15.1 and 20 ft (4.6 and 6.1 m, respectively). Also, beginning at

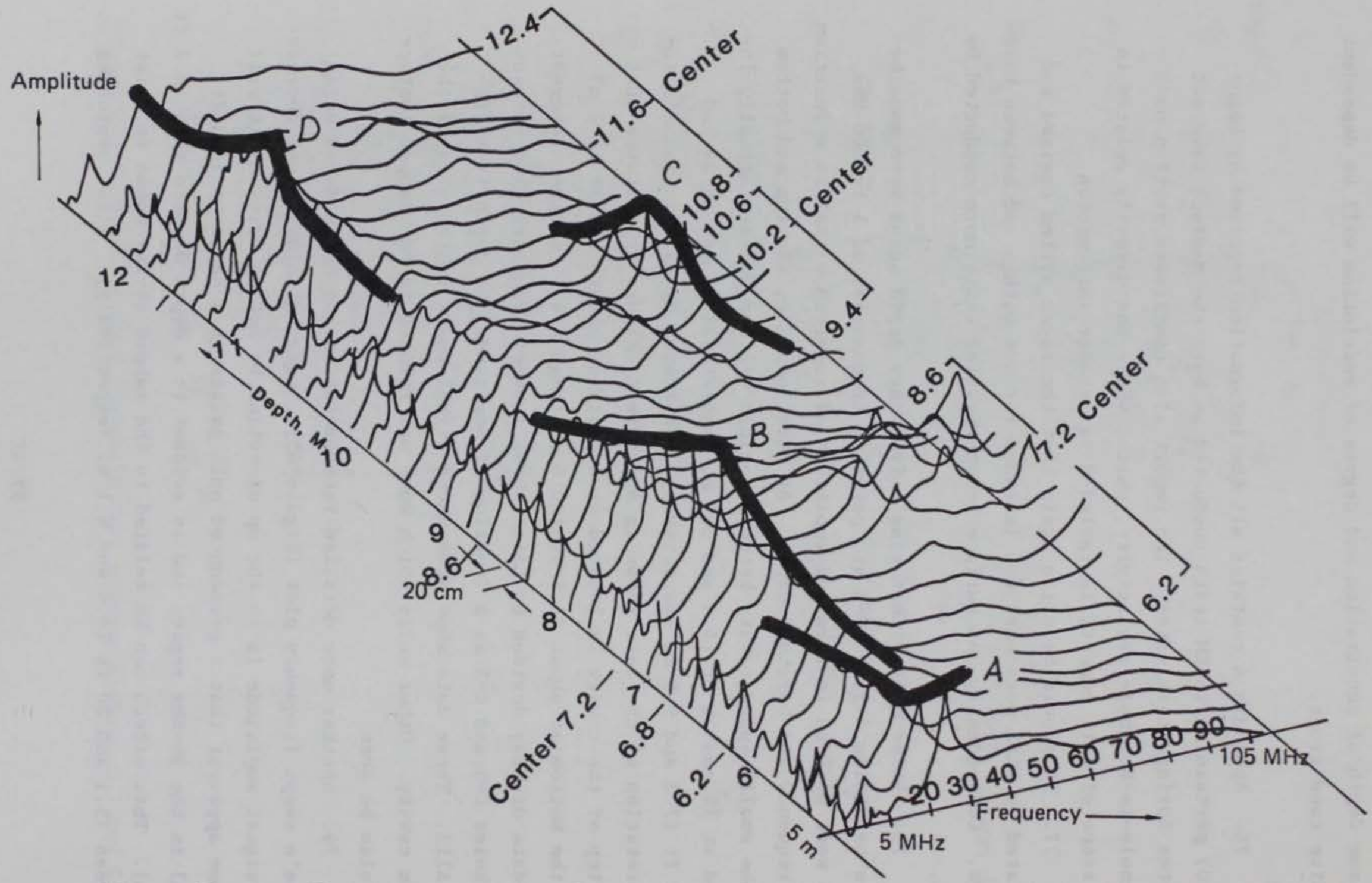

Figure 45. Detailed interpretation of LLNL swept-frequency plot between boreholes C-3 and C-5. Note that the decreasing signal amplitude is in the up direction

a depth of about 19.7 ft (6 m), the effects of a large anomaly appear. The maximum signal loss occurs on curve B at a depth of about 23.6 ft (7.2 m) in the frequency range of about 40 MHz, but the effect is apparent to a depth of about 28.2 ft (8.6 m). A third anomaly can be observed on curve C near the 100-MHz region centered at a depth of about 33.5 ft (10.2 m). Its effect can be seen from 31.5 to 34.8 ft (9.6 to 10.6 m, respectively). Nearing the maximum depth of Laine's investigation, other signal losses can be observed centered at about 38 ft (11.6 m) (curve D) in the 30-MHz range. Its effect can be observed from 35.4 to 40.7 ft (10.8 to 12.4 m, respectively).

80. Even though the test procedure advocated by SwRI acquires and displays data in the time domain, some comparisons can be made with the data obtained by LLNL in the frequency domain (Figures 44 and 45, respectively). Assuming that the "normal" (no anomalies) arrival times between borings C-3 and C-5 are 31 to 33 nsec, as shown in Figure 44, a shorter arrival time occurs at a depth of about 15.1 ft (4.6 m). This can be attributed to the presence of the small mapped cavity, and is based on an inference that if LLNL had acquired shallower data, an even sharper decrease in signal amplitude on curve A would have been observed (Figure 45). The shortest arrival time observed on the entire SwRI record is 24 nsec at a depth of 23.6 ft (7.2 m), which is in excellent agreement with the largest signal loss recorded by LLNL (curve B, Figure 45). Also, the zone influenced by the anomaly is virtually identical to that observed by LLNL, 20.3 to 28.2 ft (6.2 to 8.6 m, respectively). Another similarity occurs at a depth of 33.5 ft (10.2 m). The SwRI arrival time is only 27 nsec (about 5 nsec shorter than the norm) corresponding to the pronounced LLNL signal amplitude loss shown in curve C (Figure 45). The amplitude loss, curve D (Figure 45), observed by LLNL at a depth of 38 ft (11.6 m) is only slightly discernible at a depth of 37.1 ft (11.3 m) in Figure 44. A possible explanation is that if an anomalous condition does exist, it has little effect on the time of flight of the EM signal. However, if the area were highly fractured, signal losses could be expected. Again, the SwRI method of data display concentrates on the enhancement of high-quality data in the time domain

and also uses time-gain amplification which will tend to make their data less sensitive to signal loss. However, obvious signature changes can be seen in the region from 23.6 to 28.5 ft (7.2 to 8.7 m, respectively).

81. Both radar systems have detected the presence of a rather large, unmapped anomalous feature existing beneath the small mapped cavity. The zone extends from a depth of slightly more than 19.7 ft (6 m) to a depth of about 28.2 ft (8.6 m). This zone is apparently related to an extension of the larger cave system. Unfortunately, time and cost limitations prevented an exploratory boring in this area.

82. Further supporting evidence of an anomaly at this location was obtained by surface electrical resistivity. Noting Figure 46 (Butler, 1983), it will be seen that this feature was detected with a high level of confidence using the pole-dipole technique. Additionally, the Wenner array using a 40-ft (12.2-m) electrode spacing also evidenced a pronounced low resistivity at this location (Ballard, 1982).

Manatee Springs, Florida

SwRI

83. A complete documentation of tests conducted by SwRI at the Manatee Springs, Fla., site was reported by Herzig and Suhler (1980). This report is also readily available through the WES Technical Information Center and from SwRI.

84. At the Manatee Springs test site, negative results were obtained by SwRI from two surface traverses located near borings C-5, C-2, C-3, and C-4. Figure 7 is a site map of Manatee Springs. Observing the data from these traverses, no voids or water-filled cavities were discernible by SwRI. There was very little expectation of being able to detect the main water channel at a depth of 105 ft (32 m). This would have required some 210 ft (64 m) of round-trip signal travel in a medium that at certain depths did not permit even 32.8 ft (10 m) of penetration.

85. The principal EM surveys were conducted in crosshole fashion

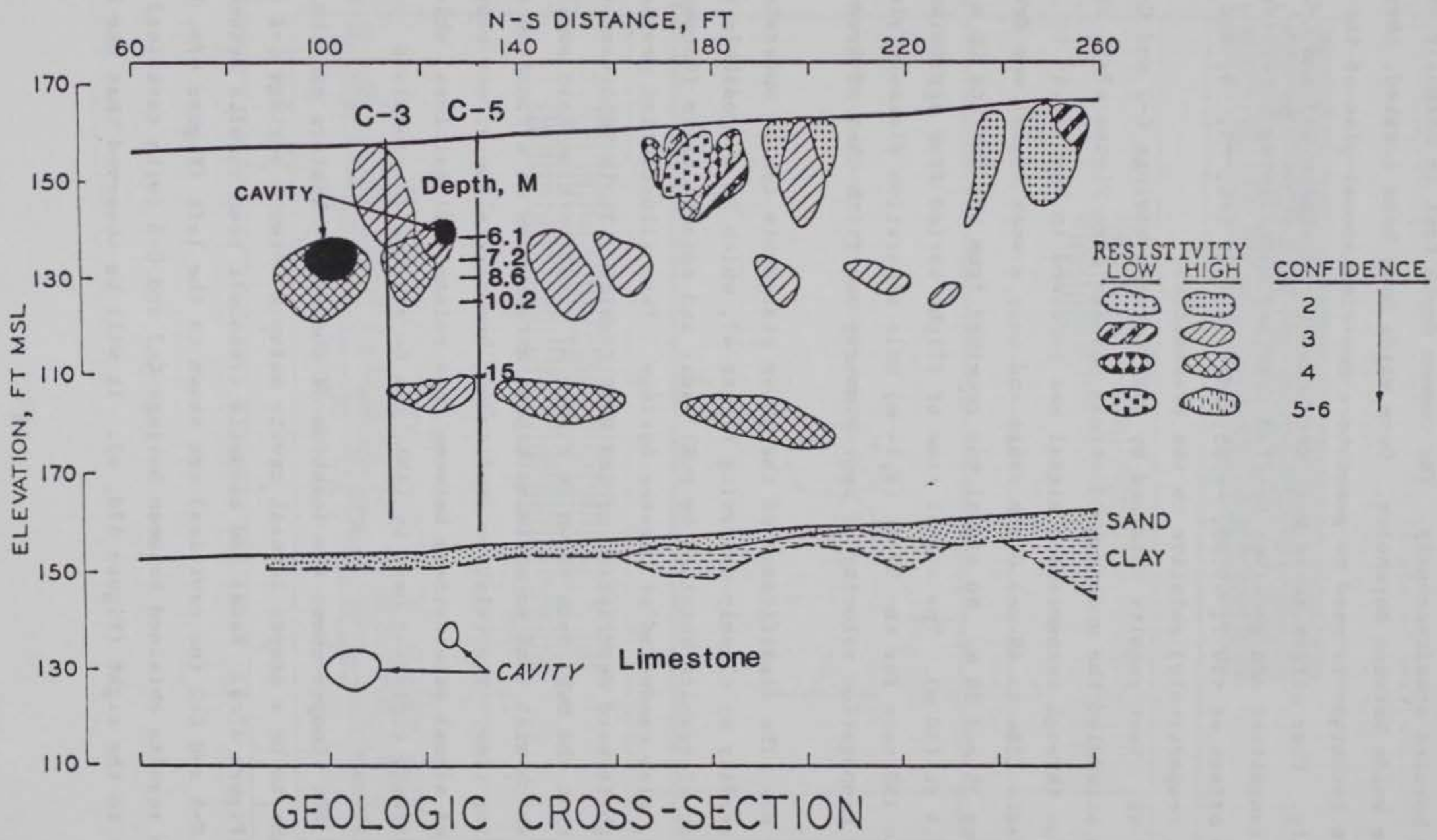

Figure 46. Interpreted pole-dipole resistivity cross section compared with known geology along the 0,80 to 260,80 line at the Medford Cave site (The numbers indicating increase in confidence levels correspond to the number of arc intersections which define the anomaly.) (from Butler, 1983)

with the transmitter and receiver maintained at a common depth while being hoisted simultaneously. The common depth test is normally used to locate voids between boreholes. Once voids have been located, then an offset technique is used to generate a two-dimensional plot of the anomaly. Four offset tests were conducted in boreholes C-3 and C-2 with the transmitter and receiver hoisted together maintaining a receiver depth offset of +19.7, +9.85, -9.85, and -19.7 ft (+6, +3, -3, and -6 m, respectively) relative to the transmitter.

86. Test results obtained by SwRI between borings C-2 and C-3, which straddled the underground stream passage (see Figure 47e), showed that no through transmission signal was received in the 124.6- to 160.7-ft- (38- to 49-m-) depth range and only a weak signal was detected between 35 and 38 m. No signal was received from the surface to a depth of 98.4 ft (30 m). The signal time of flight varied from approximately 120 to 150 nsec for the 30-ft (9.14-m) hole separation distance yielding an EM propagation velocity of approximately one-fifth that of free-air space.

87. The significance of the above statements can be understood more readily by closely observing Figure 47, which is a crosshole comparison of results obtained by SwRI radar and seismic tests (Cooper, 1982), also conducted at Manatee Springs. This illustration provides a straightforward description of the test results. It is important to note that the SwRI data shown in Figure 47 displays time-gain amplification which will tend to minimize signal attenuation as a function of increasing time. The relative amplitudes, however, allow direct comparisons of signal attenuations between data points. Signal loss, which is the primary criterion used by LLNL, can be related to anomalous conditions.

88. Cooper shows the location of the cavity feature and the zone thought to be a deeper lateral cavity network between borings C-2 and C-3 (Figure 47c). Radar and acoustic crosshole test results between borings C-5 and C-2 (no cavities) are shown to the left (Figure 47a, b), while results obtained between borings C-2 and C-3 (with cavities) are shown to the right (Figure 47d, e). It will be observed that the C-5 to

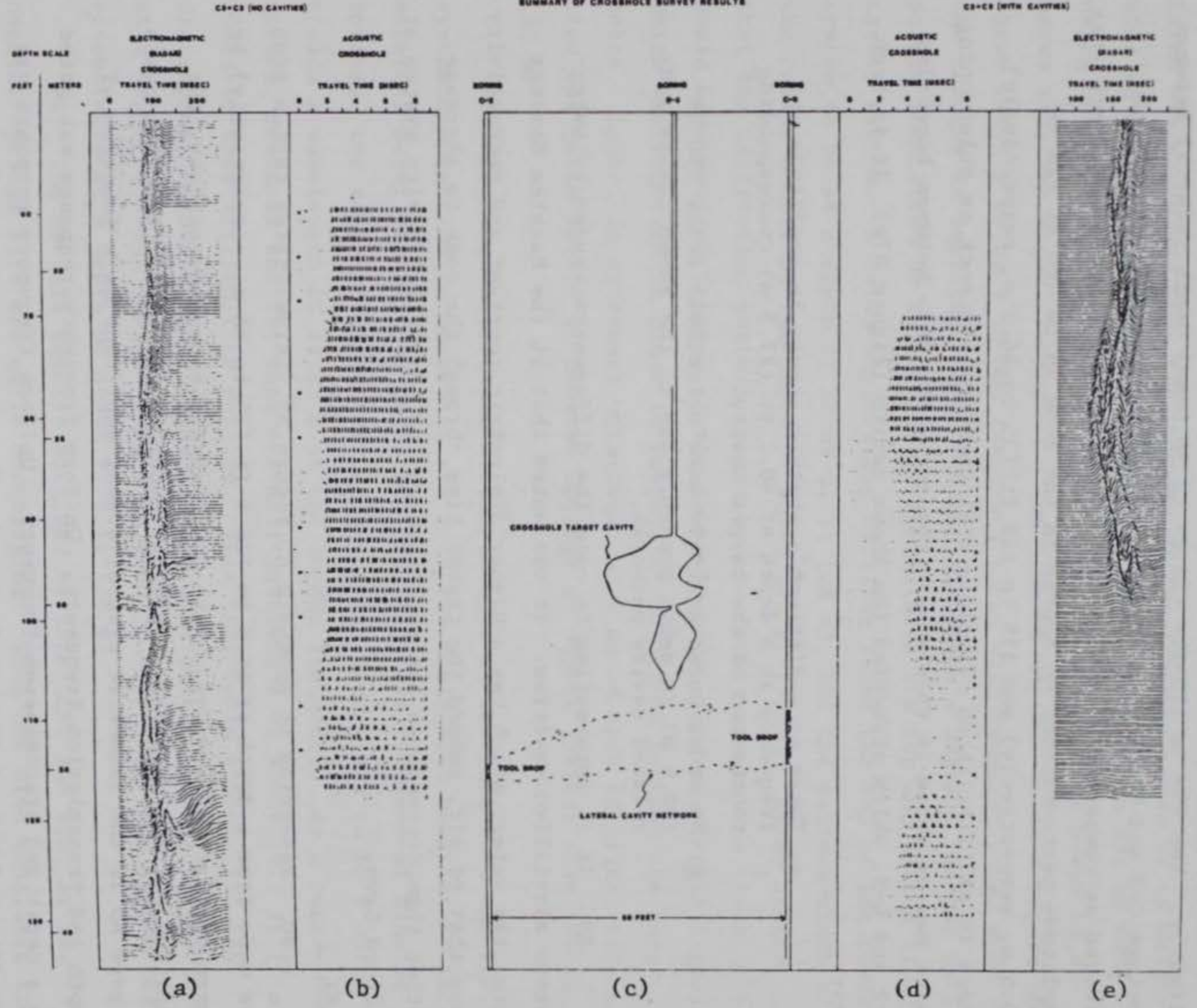

Figure 47. Summary of crosshole results obtained at Manatee Springs (from Cooper, 1982)

C-2 radar first-arrival times are reasonably constant except for one interval between 101.7 and 105 ft (31 and 32 m, respectively) in depth. Here the radar pulse is attenuated and its arrival time increases only slightly. The 40- to 120-ft- (12.2- to 36.6-m-) depth interval between borings C-2 and C-5 is essentially free of cavities and may be considered as competent rock for this site. It is interesting to note that amplitude perturbations do appear in the zone 95 to 100 ft (29 to 30.5 m, respectively) and 115 to 120 ft (35 to 36.6 m, respectively). These in all likelihood correlate with poor-quality rock or solutioning which has occurred in this zone. Observing the data between boreholes C-2 and C-3, which straddled the known cavity (Figure 47e), it is seen that:

a. There is a distinct signature change in amplitude and frequency at a depth of 90.2 ft (27.5 m) corresponding to the top of the target cavity.

b. No radar pulse arrivals were detectable below 100 ft (30.5 m) in depth probably due to the known cavity and related cavity networks.

89. It is interesting to note the differences caused by water- versus air-filled cavities. It was noted that at the Manatee Springs site, the water, which has a higher dielectric constant and conductivity than that of air, caused the travel time through the zone to increase rather than decrease as observed through the air-filled cavity system at Medford Cave.

LLNL

90. Referring to Appendix A, Figure A5, Laine states that a scan was made from a depth of 65.6 to 124.6 ft (20 to 38 m, respectively) between borings C-3 and C-4. With the transmitter power constant, the amplitude of the received signal was recorded at 3.3-ft (1-m) intervals. Figure A5 is the isometric plot of signal amplitude as a function of depth and transmission frequency. Uniform frequency response was noted to a depth and transmission frequency. Uniform frequency response was noted to a depth of 95.1 ft (29 m), but a pronounced high-frequency loss began at 98.4 ft (30 m) and continued to greater depths. This was the same condition found by SwRI when they conducted tests at this location.

Laine pointed out that an interesting feature of that frequency scan was the extremely low amplitude signal level obtained at a depth of about 111.5 ft (34 m), again confirming the results obtained by SwRI. Laine has explained that the purpose of the frequency scan is to determine which frequency propagates best so that a second run can be made using only a single frequency with a constant transmitter power to observe relative signal losses as a function of depth. Laine's Figure A6 shows results using a 10-MHz frequency input with constant power and the changes in amplitude as a function of borehole depth. The two null points identified by Laine closely approximate the top and bottom of the cavity system. A later exploratory drilling found the top of the cavity system to be at a depth of about 91 ft (28 m), but the maximum width of the cavity occurs at the depth of about 105 ft (32 m). Laine stated that the diffraction pattern caused by the cavity was not as clean as he would have desired because of the low-frequency, long-wavelength signal, which was required in order to propagate the signal between the boreholes. Laine, in agreement with SwRI, also noted that EM signal attenuation was quite severe at Manatee Springs at depths greater than 100 ft (30 m).

91. Another observation worthy of note is the fact that the LLNL system can be used to determine the relative dielectric constant of the material being tested (see pages A10 and A11). In the case of Manatee Springs, the relative dielectric constant was determined to be 6 which yields a wavelength of 12.25 m at the 10-MHz frequency. As a consequence, features smaller than one-half wavelength or about 19.7 ft (6 m) would be very difficult to resolve. This fact could account for the discrepancy encountered by Laine when he interpreted the top of the cave at a depth of about 106.6 ft (32.5 m) when in actuality, the system was encountered at a depth of about 91.8 ft (28 m).

92. The overall results obtained by both LLNL and SwRI at the Manatee Springs site are quite encouraging. When one also considers the excellent results obtained at the Medford Cave site, it must be concluded that exploitation of the EM ground-probing concept might produce one of the most powerful exploration tools yet devised for engineering

geophysics applications. Usefulness of the technique will undoubtedly be improved by the evolution of both hardware and software acquisition and evaluation packages.

PART V: CONCLUSIONS

93. Based upon the test results obtained at three test sites by four independent investigators, the following conclusions can be drawn:

a. Surface ground-probing pulse radar systems could not be successfully used at the WES test site by any of the three contractors. This was due to the high dielectric constant and conductivities of the silty material (loess) tested.

b. State-of-the-art surface ground-probing pulsed radar systems of the type used by both Technos and SwRI can detect shallow cavities at sites where electrical properties will permit their use. The maximum depth of penetration confirmed was about 25 ft (7.6 m) at the Medford Cave site. With regard to electrical properties, the area where that penetration was observed was nearly ideal, silty sands over soft limestone. The thinnest cavity confirmed was about 1 ft (0.3 m) thick; its lateral extent was unknown.

c. The shades-of-gray (variable area) method of displaying data was superior to actual signature displays for onsite data interpretation.

d. Crosshole radar tests conducted by both SwRI and LLNL were highly successful at the Medford Cave site. The smallest known air-filled cavity feature easily detected was about 2 ft (0.6 m) thick by 5 ft (1.5 m) in height. Wavelengths associated with the frequencies used to confirm this cavity could likely have detected a cavity approximately half this size.

e. Crosshole radar tests conducted at the Manatee Springs site by SwRI and LLNL were also considered to be successful. The target cavity feature was highly irregular in shape but approximately 10 ft (3 m) in width at the maximum and about 12 ft (3.7 m) in height. Its presence was detected by signal amplitude attenuation accompanied by a lower EM wave velocity. The SwRI crosshole radar system could not receive a transmitted signal below a depth of about 100 ft (30 m). It is not known whether the electrical properties, the highly fractured material encountered in this area, or a combination of both were responsible for lack of signal transmission. The LLNL system, which incorporates an adjustable frequency range, could only send low frequency signals in this zone.

94. Based on the above, it was finally concluded that ground-probing radar, either in the surface or the cross borehole mode, is a viable candidate for site investigations where electrical properties of

the materials under investigation are conducive to the transmission of EM signals. Those sites with desirable electrical properties are:

a. Sites with overburden materials composed mainly of sands or silty sands having low moisture content.

b. Sites with water tables preferably below the area of interest.

c. Sites composed of low-conductivity rock underlying a, such as soft limestone or granite.

REFERENCES

Ballard, R. F., Jr. 1982. "Tunnel Detection," Technical Report GL-82-9, U. S. Army Engineer Waterways Experiment Station, CE, Vicksburg, Miss.

Battelle Laboratories. 1981. "Computer-Enhanced Geophysical Survey Techniques for Location of Underground Objects and Structures," Richland, Wash.

Benson, R. C. 1978. "Radar Subsurface Profiling," prepared for U. S. Army Engineer Waterways Experiment Station, CE, by Technos, Inc., Miami, Fla.

Benson, R. C., and Glaccum, R. A. 1980. "Application of Radar and Seismic Reflection Techniques to Cavity Detection, Medford Cave Site, Florida," Technos No. T-79-053, prepared for the U. S. Army Engineer Waterways Experiment Station, CE, by Technos, Inc., Miami, Fla.

Bowders, J. J., Jr., Lord, A. E., Jr., and Koerner, R. M. 1982. "Sensitivity Study of a Ground Probing Radar System," Geotechnical Testing Journal, Vol 5, No. 3/4, pp 96-100.

Butler, D. K. 1983. "Cavity Detection and Delineation Research; Report 1, Microgravimetric and Magnetic Surveys: Medford Cave Site, Florida," Technical Report GL-83-1, U. S. Army Engineer Waterways Experiment Station, CE, Vicksburg, Miss.

Butler, D. K., and Murphy, W. L. 1980. "Evaluation of Geophysical Methods for Cavity Detection at the WES Cavity Test Facility," Technical Report GL-80-4, U. S. Army Engineer Waterways Experiment Station, CE, Vicksburg, Miss.

Butler, D. K., Whitten, C. B., and Smith, F. L. 1983. "Cavity Detection and Delineation Research; Report 4, Microgravimetric Survey: Manatee Springs Site, Florida," Technical Report GL-83-1, U. S. Army Engineer Waterways Experiment Station, CE, Vicksburg, Miss.

Cook, J. C. 1981. "Radar and Seismic Tunnel Locating Techniques," Proceedings of the Symposium on Tunnel Detection, 21-23 July 1981, Colorado School of Mines, Golden, Colo.

Cooper, S. S. 1982. "The Use of Downhole Geophysical Methods to Detect Zones of Poor-Quality Rock or Voids," Miscellaneous Paper GL-82-15, U. S. Army Engineer Waterways Experiment Station, CE, Vicksburg, Miss.

Curro, J. R., Jr. 1983. "Cavity Detection and Delineation Research; Report 2, Seismic Methodology: Medford Cave Site, Florida," Technical Report GL-83-1, U. S. Army Engineer Waterways Experiment Station, CE, Vicksburg, Miss.

Duff, B. M., and Suhler, S. A. 1980. "Ground-Penetrating Electromagnetic Tests at Medford Cave, Florida," prepared for the U. S. Army Engineer Waterways Experiment Station, CE, by Southwest Research Institute, San Antonio, Tex.

Fountain, L. S., and Herzig, F. X. 1980. "Earth Resistivity and Hole-to-Hole Electromagnetic Transmission Tests at Medford Cave, Florida," Technical Report No. 14-5940, prepared for the U. S. Army Engineer Waterways Experiment Station, CE, by Southwest Research Institute, San Antonio, Tex.

Fowler, J. C., Rubin, L. A., and Sill, W. L. 1980. "Synthetic Pulse Radar Including a Microprocessor Based Controller, U. S. Patent 4,218,678."

Herzig, F. X., and Suhler, S. A. 1980. "Ground Penetrating Electromagnetic Tests at Manatee Springs, Florida," Final Technical Report, prepared for the U. S. Army Engineer Waterways Experiment Station, CE, by Southwest Research Institute, San Antonio, Tex.

Kraichmann, M. B. 1970. Handbook of Electromagnetic Propagation in Conducting Media, Document NAVMAT, U. S. Government Printing Office, Washington, D. C.

Laine, E. F. 1980. "Detection of Water-Filled and Air-Filled Underground Cavities," Report No. UCRL-53127, Lawrence Livermore National Laboratory, University of California, Livermore, Calif.

Lundien, J. R. 1966. "Terrain Analysis by Electromagnetic Means; Report 2, Radar Responses to Laboratory-Prepared Soil Samples," Technical Report 3-693, U. S. Army Engineer Waterways Experiment Station, CE, Vicksburg, Miss.

_____. 1972. "Determining Presence, Thickness, and Electrical Properties of Stratified Media Using Swept-Frequency Radar," Technical Report M-72-4, U. S. Army Engineer Waterways Experiment Station, CE, Vicksburg, Miss.

_____. 1978. "Feasibility Study for Railroad Embankment Evaluation with Radar Measurements," Miscellaneous Paper S-78-10, U. S. Army Engineer Waterways Experiment Station, CE, Vicksburg, Miss.

Morey, R. M. 1974. "Continuous Subsurface Profiling by Impulse Radar," presented at Engineering Foundation Conference on Subsurface Exploration for Underground Excavation and Heavy Construction, held at Henniker, N. H.

Unterberger, R. R. 1977. "Radar and Sonar Probing of Subsurface at U. S. Army Corps of Engineers Waterways Experiment Station," prepared for the U. S. Army Engineer Waterways Experiment Station, CE, by Texas A&M, College Station, Tex.

_____. 1978. "Radar Propagation in Rock Salt," Geophysical Prospecting, Vol 26, p 312.

Von Hippel, A. R. 1954. Dielectric Materials and Applications, John Wiley & Sons, New York.

Wait, J. R. (Ed.) 1971. Electromagnetic Probing in Geophysics, Golem Press, Boulder, Colo.

APPENDIX A: DETECTION OF WATER-FILLED AND AIR-FILLED UNDERGROUND CAVITIES

by

Edwin F. Laine
Lawrence Livermore National Laboratory
University of California
Livermore, Calif.

DETECTION OF WATER-FILLED AND AIR-FILLED UNDERGROUND CAVITIES

ABSTRACT

Tunnel and cavern detection methods were tested at two experimental sites in Florida. Cross-borehole methods using high-frequency electromagnetic wave diffraction techniques were used over a frequency range of 1 to 100 MHz. A new cross-borehole method using direct current was also used. The experimental sites are karstic. The caverns and tunnels were water-filled at one site and dry at the other site.

INTRODUCTION

In 1980, LLNL carried out an experimental program at Manatee Springs State Park, Florida and at Medford Caves, Florida. Both sites were under the supervision of the U.S. Army Corps of Engineers. The objective of this experimental program was to develop geophysical methods to detect cavities or tunnels in karstic media; this is part of a long-range program to develop techniques for detecting hazards near mining activity. Such hazards range from abandoned mines to geologic faults.

To accomplish this objective, Lawrence Livermore National Laboratory used a high-frequency, electromagnetic cross-borehole probing system which can operate between 100 kHz to 1 GHz. This system can be used to detect high-contrast anomalies by the diffraction effect,[1] or it can be used to produce a pseudocolor, geotomographic image of a plane between boreholes.[2]

---

1. R. J. Lytle, E. F. Laine, D, L. Lager and D. T. Davis, "Cross-borehole Electromagnetic Probing to Locate High-Contrast Anomalies," *Geophysics* 44 (10), 1667-1676 (1979).
2. K. A. Dines and R. J. Lytle, "Computerized Geophysical Tomography," in *Proc. of the IEEE* 67 (7), 1065-1073 (1979).

In addition, LLNL also used a new method of high-contrast anomaly detection using direct-current resistivity measurements between two boreholes.

ELECTROMAGNETIC TECHNIQUE

Figure 1 is a simplified block diagram of the cross-borehole, high-frequency electromagnetic system. A winch holding adequate coaxial cable for the hole depth has a vertical coaxial dipole transmitting antenna attached to the cable end. The length of the antenna is determined by the operating frequencies to be used and the velocity of propagation in the media (relative dielectric ε_r). The antenna is not resonant and is generally made shorter than the highest operating frequency. Therefore, the antenna is not very efficient. The other cable end exits the cable drum through a coaxial rotary

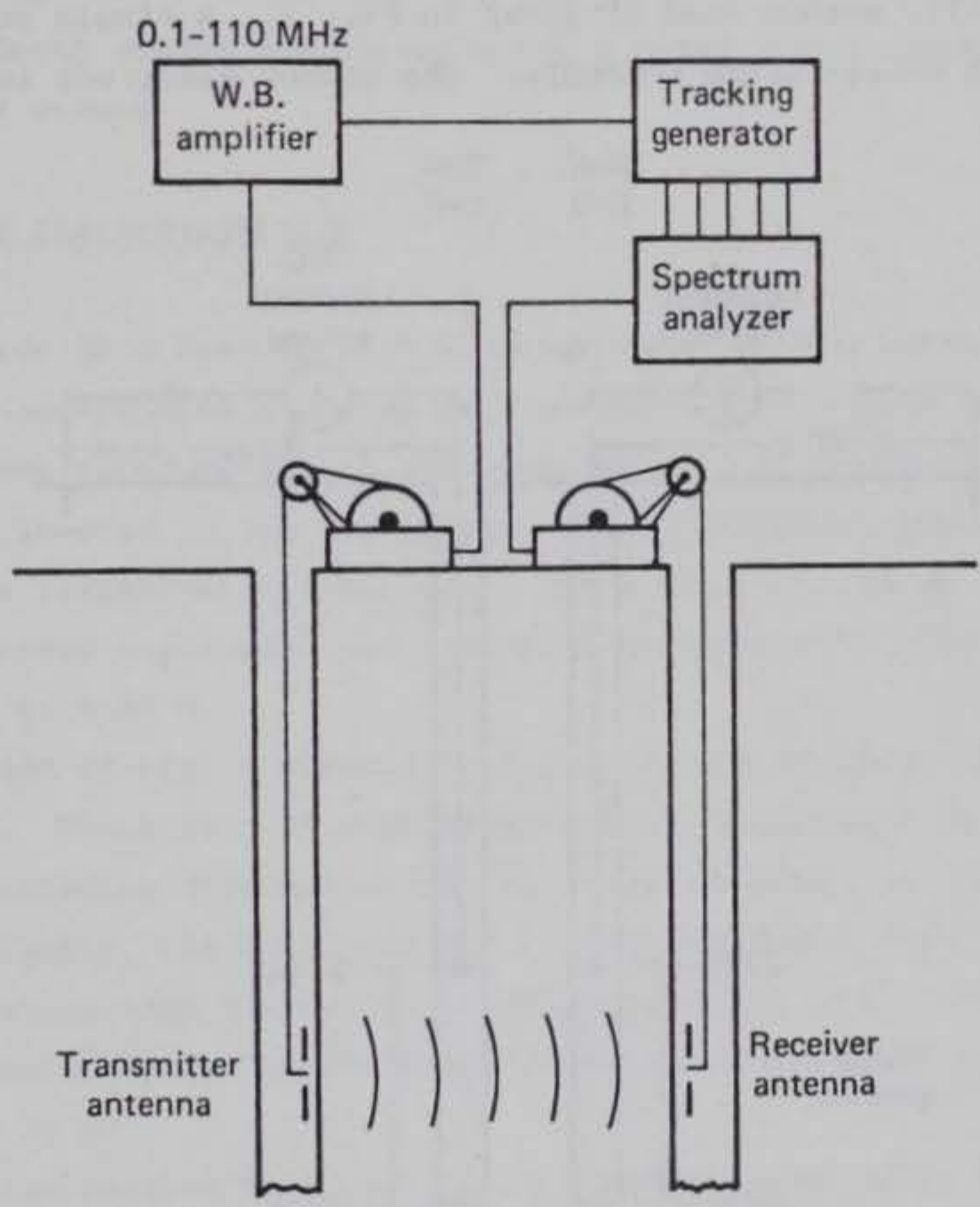

FIG. 1. Block diagram of the high-frequency, cross-borehole EM System.

joint and connects to the output of a 100-Watt (W) wide band amplifier. The amplifier can be driven by an oscillator, tracking generator, synthesizer or whatever is convenient. The second drum is similarly equipped, except the downhole end has a receiving probe installed in it.

The receiving antenna probe is approximately 25 cm long and incorporates active elements to achieve the proper impedance transformation. The rotary joint output then goes to a spectrum analyzer. During operation, the transmit-and-receive antennas are positioned at a specified depth. The transmitted power is read from a power meter and the received power is read from the spectrum analyzer. With constant transmitted power, the received power will vary according to the transmissivity of the media at the operating frequency. Straight-line ray optics are generally used to analyze the results obtained.

RESISTIVITY TECHNIQUE

The resistivity method used is shown in Fig. 2. A single probe is lowered into each water-filled borehole. The second electrode is positioned

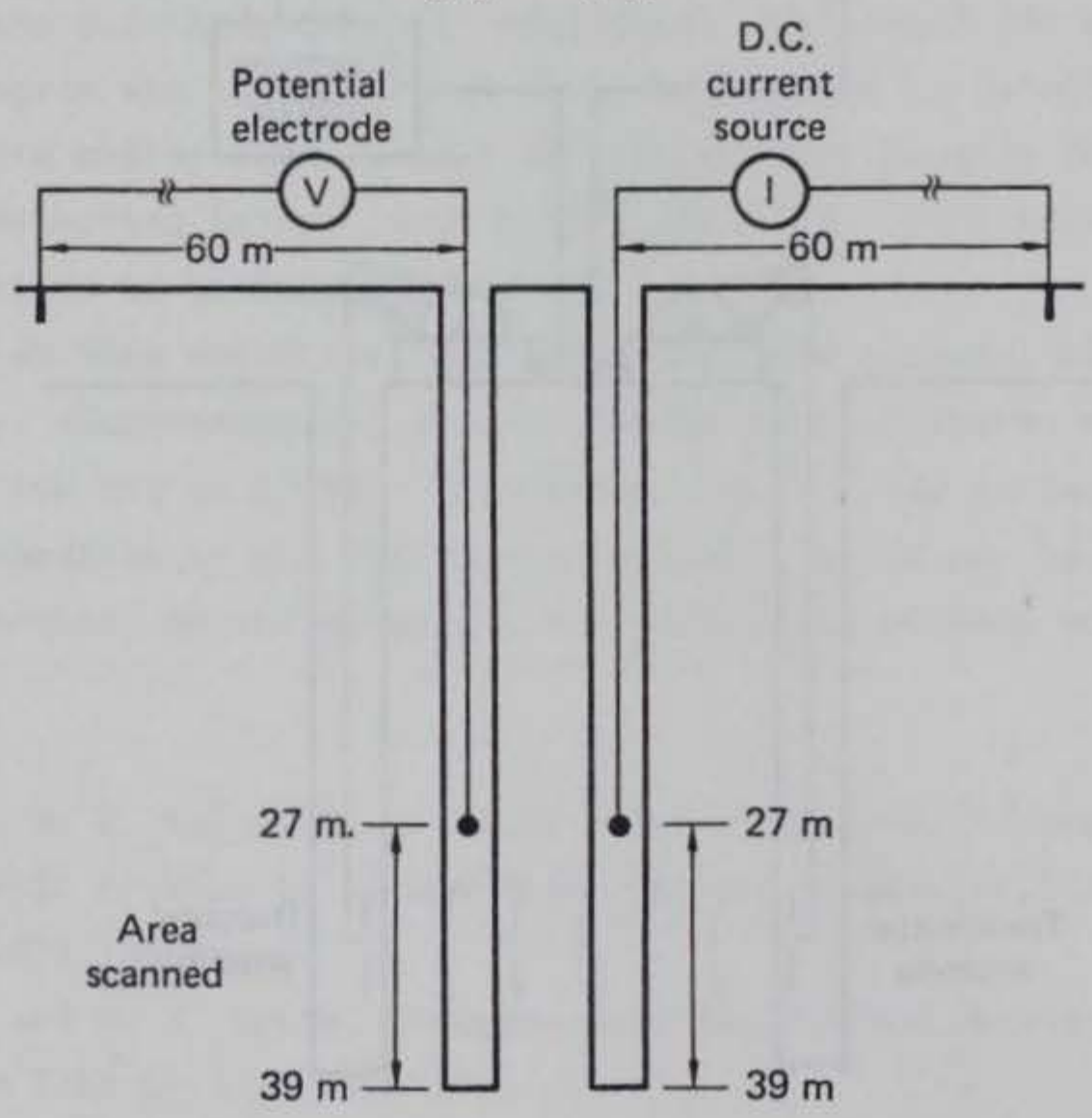

FIG. 2. Block diagram of cross-borehole resistivity system.

about 60 m away. One electrode is energized with commutated DC current; the other electrode is connected to a voltmeter to record the resultant voltage. The probes are positioned incrementally to cover the area to be investigated. At each position, the injected current and resultant voltage are recorded.

EXPERIMENTS AT MANATEE SPRINGS STATE PARK

Manatee Springs is a Florida State Park near Chiefland, Florida. It has an extensive system of underground tunnels. The water-filled tunnels in the area we investigated are about 35 m below the ground surface. This opportunity to experimentally study water-filled tunnels was ideal, as our previous experiments had all been confined to dry tunnels. Figure 3 is a section of a map showing the location of Manatee Springs. Figure 4(a) shows a plan view of the boreholes and Fig. 4(b) shows a section view through boreholes C2 through C5. The tunnel depth of 35 m was obtained from cave divers using depth gauges and allowing for a water level about 3 m below the surface of the ground.

Cross-Borehole Electromagnetics

A scan from 20 m deep to 38 m deep was made between boreholes C3 and C4. Both transmit-and-receive antennas were positioned at a 20-m depth and the amplitude of the received signal was recorded at 1-m intervals, as both antennas were lowered in 1-m increments. The transmitter power was kept constant. The transmission results are shown in Fig. 5 as an isometric plot of depth, received amplitude, and transmission frequency. The spacing between the boreholes is 4.88 m.

Examination of Fig. 5 shows a fairly uniform frequency response down to a depth of 29 m. There is a very pronounced high-frequency loss beginning at 30 m and a continuing degradation of the received signal as one progresses deeper. Apparently, the Williston and Inglis formations have a much greater clay concentration than the Ocala formation (see Fig. 4b). Core samples show a very light-colored rock in the Ocala formation which turns to a brown color at a depth of 30 m.

Another interesting feature of this frequency scan (Fig. 5) is the minimum signal obtained at a depth of 34 m. We could only propagate a very weak signal between 5 to 15 MHz. The signal amplitude and frequency response

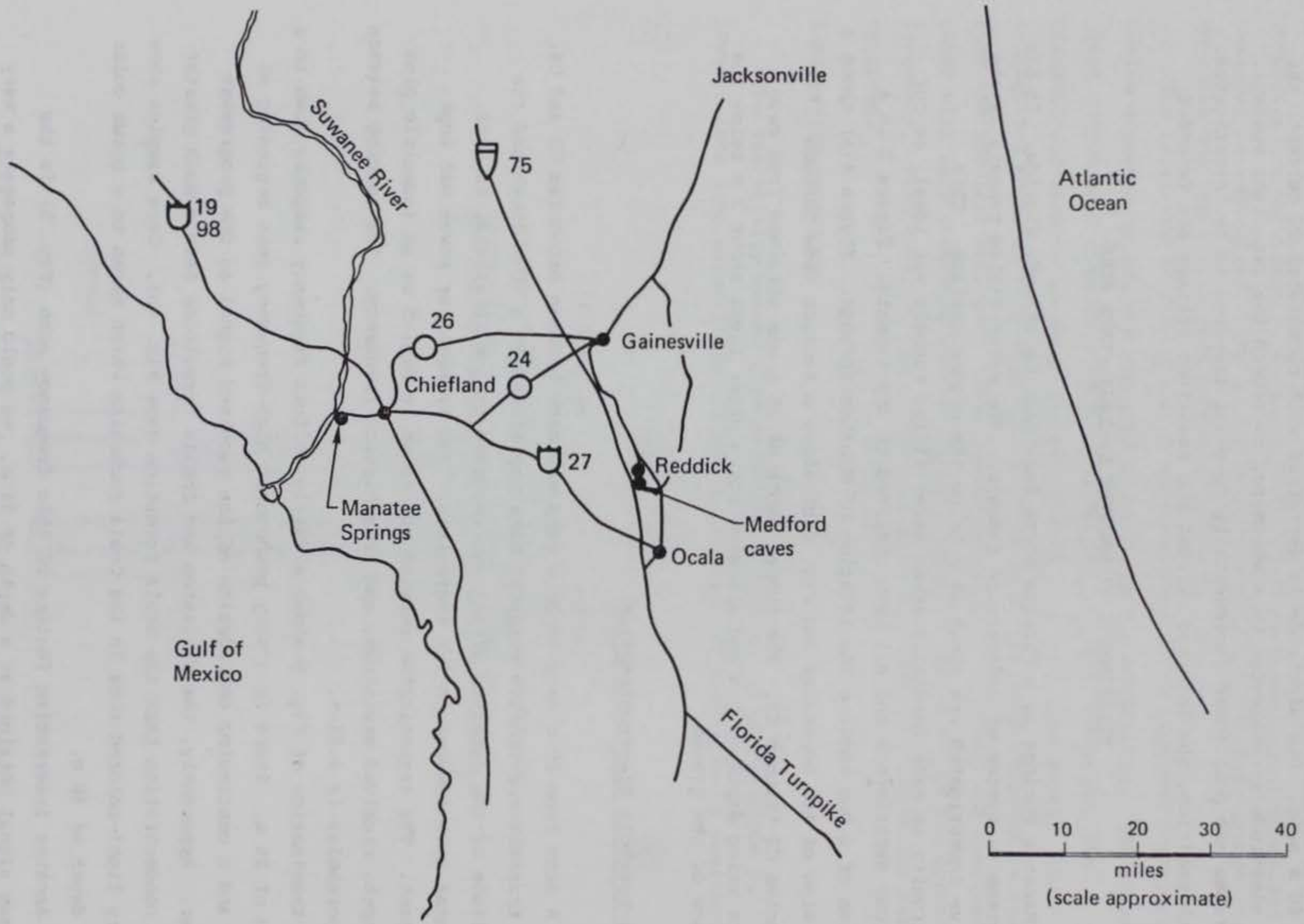

FIG. 3. Map of north central Florida.

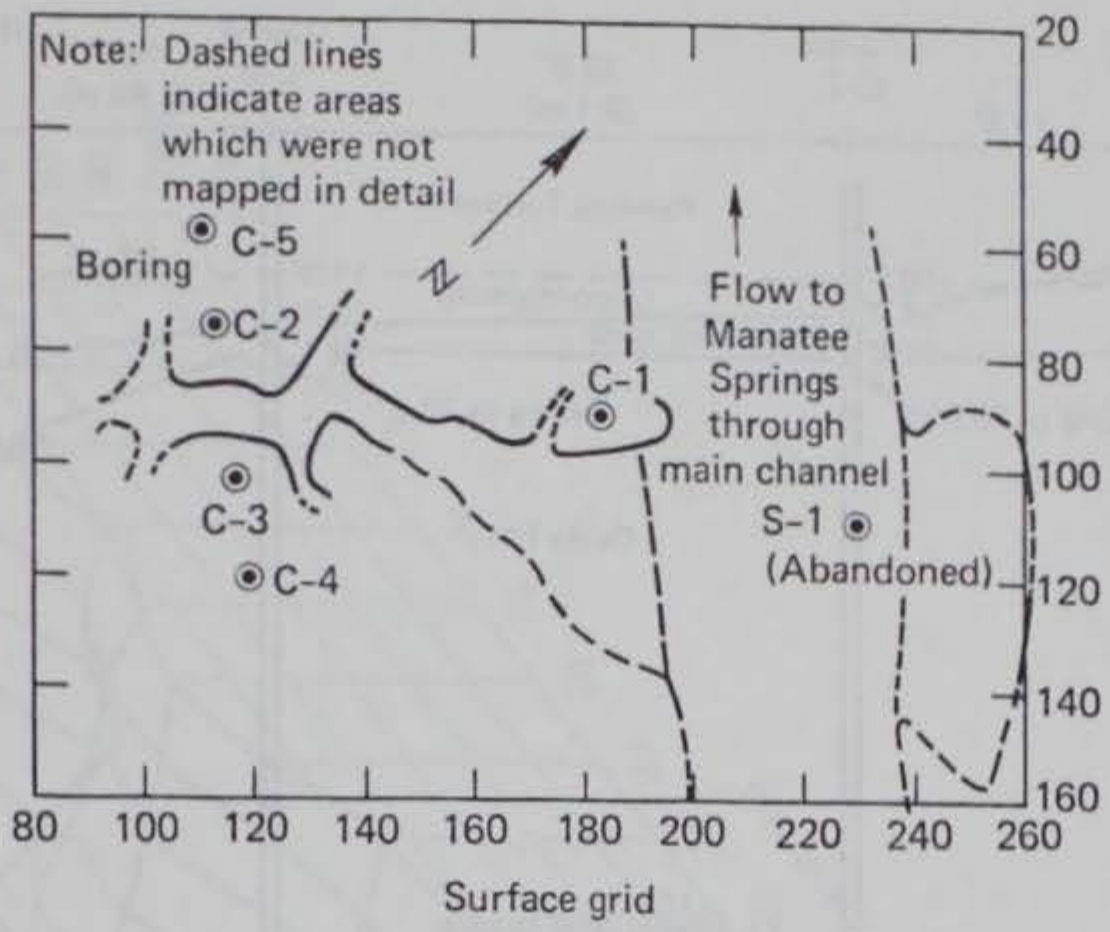

FIG. 4(a). Plan view of boreholes, Manatee Springs State Park, Florida.

increase rapidly (within 1 m) on either side of the 34 m depth. This leads one to suspect either a clay layer or a cavity between these two holes. We suspect there may be a small branch cavity less than 1 m wide in this area.

The purpose of the frequency scan is to determine what frequency is best suited for probing the area between boreholes in greater detail. The sweep-frequency method is limited because of the necessarily wide bandwidth of reception required to allow sweep times that would not be too time-consuming. One can use a narrow, restricted bandwidth to increase the dynamic range, but the sweep times last many minutes for just one scan time. A single frequency restricted to a narrow bandwidth, typically 1 kHz, brings system noise levels down low enough so that one can measure signals as low as -110 dbm with a spectrum analyzer (0 dbm = 1 milliwatt into 50 ohms).

Figure 6 shows a plot of a depth scan made at 10 MHz. The scan was made between boreholes C3 and C2, with the transmitter in C3 and the receiver in C2. Both antennas were positioned at 25 m deep and both antennas were incremented in 20-cm steps. The transmitted incident power was constant at 64 W with 24 W reflected (this is because of antenna impedance mismatch). The resultant received power is then plotted versus depth. The diffraction pattern of the cave is visible in Fig. 6. It is not as clean as one would desire because of the low frequency necessary to propagate the distance

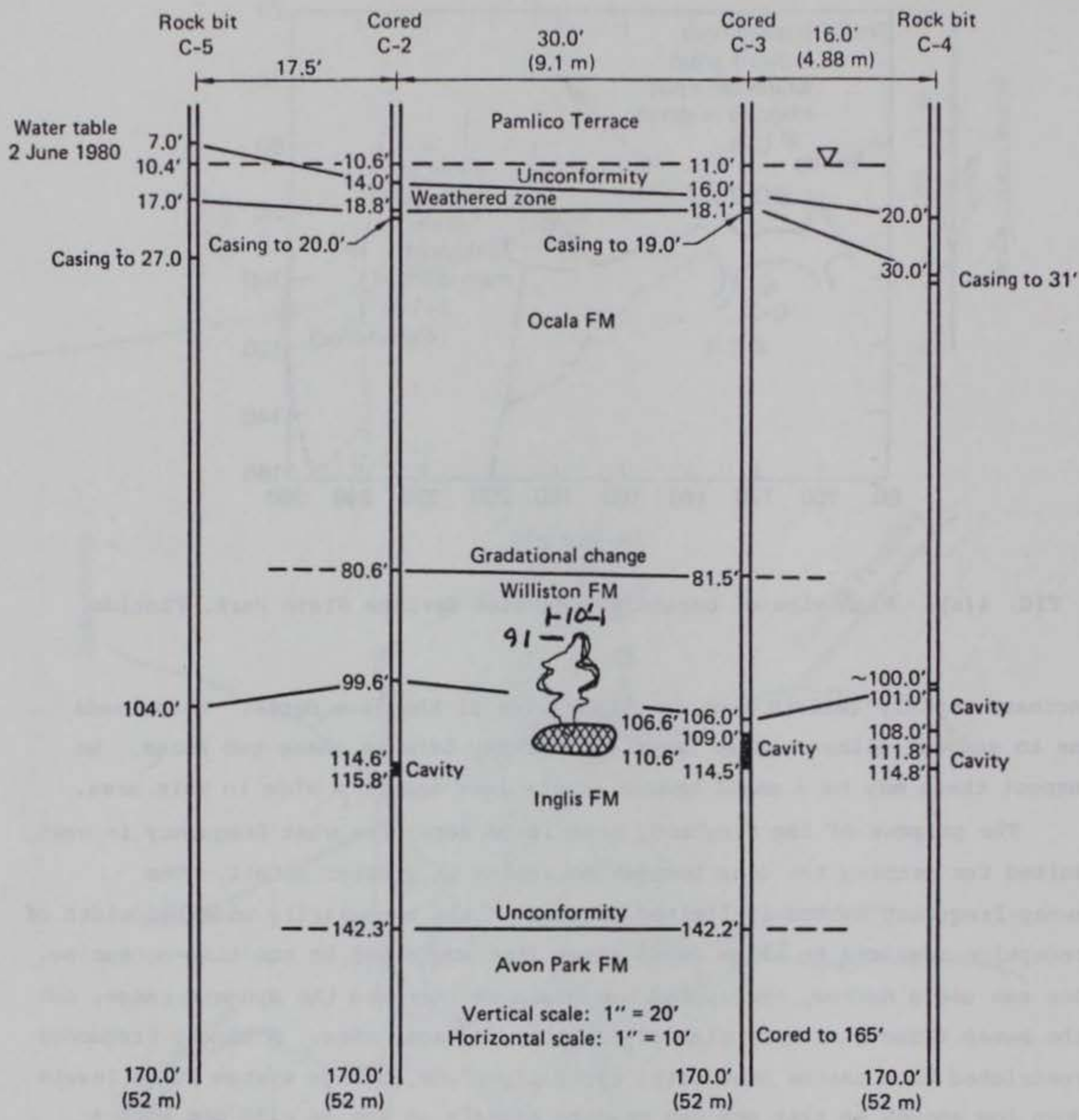

Note: Cavity depth data from diver's depth meter.

FIG. 4(b). Cross-sectional view of boreholes, Manatee Springs State Park, Florida.

between boreholes (9.2 m). The signal in the cave area varies between -80 to -100 dbm. If we go higher in frequency to give sharper nulls produced by the top and bottom of the cave, the signal levels would be too low to be useful.

Manatee Springs is difficult to probe at high frequencies because of the high-conductivity media at the cave depths. To achieve transmission, one has

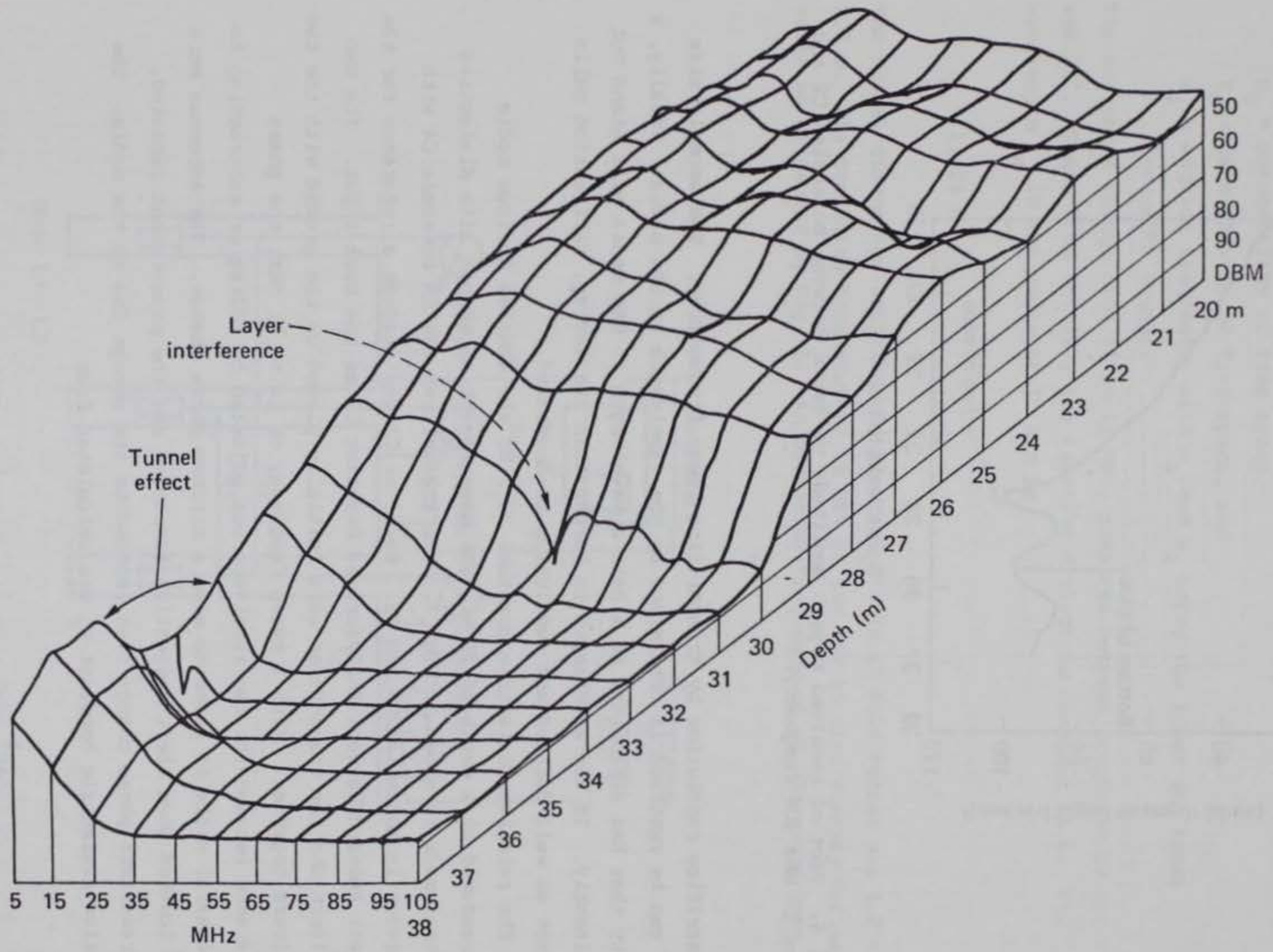

FIG. 5. Swept frequency display of high-frequency electromagnetic transmission between boreholes C4 and C3.

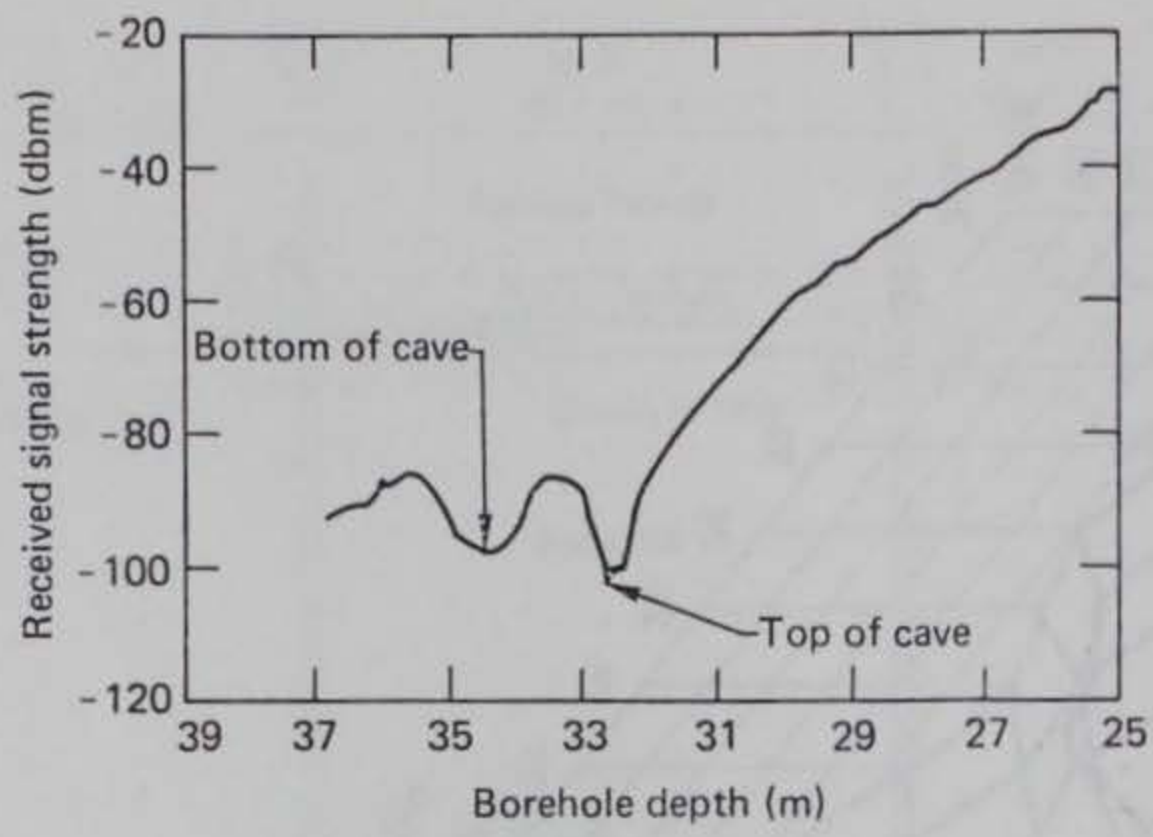

FIG. 6. Plot of received signal amplitude vs depth between boreholes C2 and C3 at 10 MHz (CW frequency).

to sacrifice resolution by transmitting lower frequencies. The anomaly size that can be resolved is determined by the wavelength in the media. Ideally, a cavity that has dimensions of a half a wavelength in the media will stand out prominently. If the wavelength is larger than the cavity, diffraction nulls are not as well-defined and resolution is decreased.

The relative dielectric constant (ε_r) at the Manatee Springs media was measured at a depth of 25 m. The measurement of the *in situ* dielectric constant made is shown in Fig. 7. The transmitter was in borehole C4 with receivers in boreholes C3 and C2. Receiver C3 was used as a reference for the Hewlett Packard Network Analyzer and Receiver C2 as the test input. The two receivers and the transmitter were initially placed on the ground with the two receivers together. With a sweep frequency of 10 to 11 MHz, the phase difference between the two receivers was adjusted by adding or subtracting to the coaxial cable in order to give a minimum phase change. The antennas were then lowered down their respective boreholes and the measurement repeated. The resultant phase change then represents the change due to the media. The relative dielectric constant ε_r was calculated from

$$\varepsilon_r = \frac{(\Delta\phi)^2}{(\omega_2 - \omega_1)^2 \mu_0 \varepsilon_0 R^2} \qquad (1)$$

where $\Delta\phi$ = phase change in radian,

R = distance between holes-meters,

μ_0 = permeability of free space,

ϵ_0 = permittivity of free space, and

ω_i = angular frequency, with ω_1 and ω_2 being the lower and upper frequency bounds.

The net phase change from 10 to 11 MHz, measured between boreholes C2 and C3, was.27°. Then, from Eq. (1), the relative dielectric constant is 6. The wavelength λ_m in the media at 10 MHz is

$$\lambda_m = 12.25 \text{ m} \tag{2}$$

The tunnel dimensions estimated by the cave divers in this region are 1.2 × 2.5 m. The operating frequency of 10 MHz is too low to give sharply defined nulls as evidenced by Fig. 5. An operating frequency of 60 MHz would have

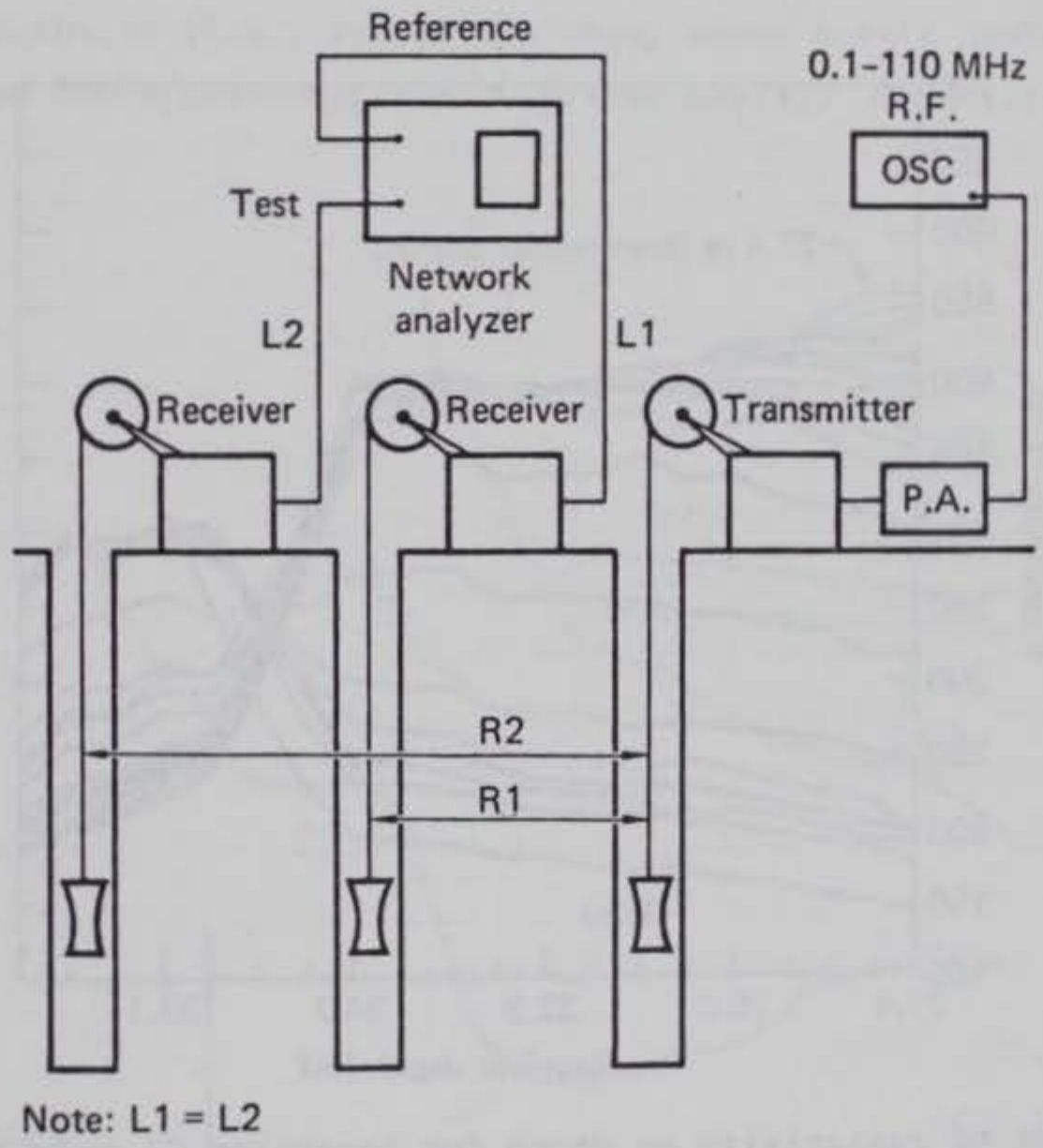

FIG. 7. Block diagram of the three-hole differential system to measure absolute transmission loss or phase change between boreholes.

been more desirable. Unfortunately, 60 MHz would not propagate through the high-conductivity media.

Borehole-to-Borehole Resistivity

Borehole-to-borehole resistivity measurements were made between C2 and C3. A single current injection electrode was placed in C2 and a single potential electrode in C3. Long lines were placed on the ground opposite from the boreholes and a ground electrode was placed on the surface for the return contacts. The electrode positions started at a depth of 27 m and were incremented 0.3 m in depth to 39 m. Figure 8 shows a plot of depth versus the ratio V/I.

Comparing the cross-borehole resistivity (Fig. 8) with the cross-borehole, high-frequency data (Fig. 6) shows good agreement with the depth location of the tunnel. The general change in conductivity with depth is also in good agreement.

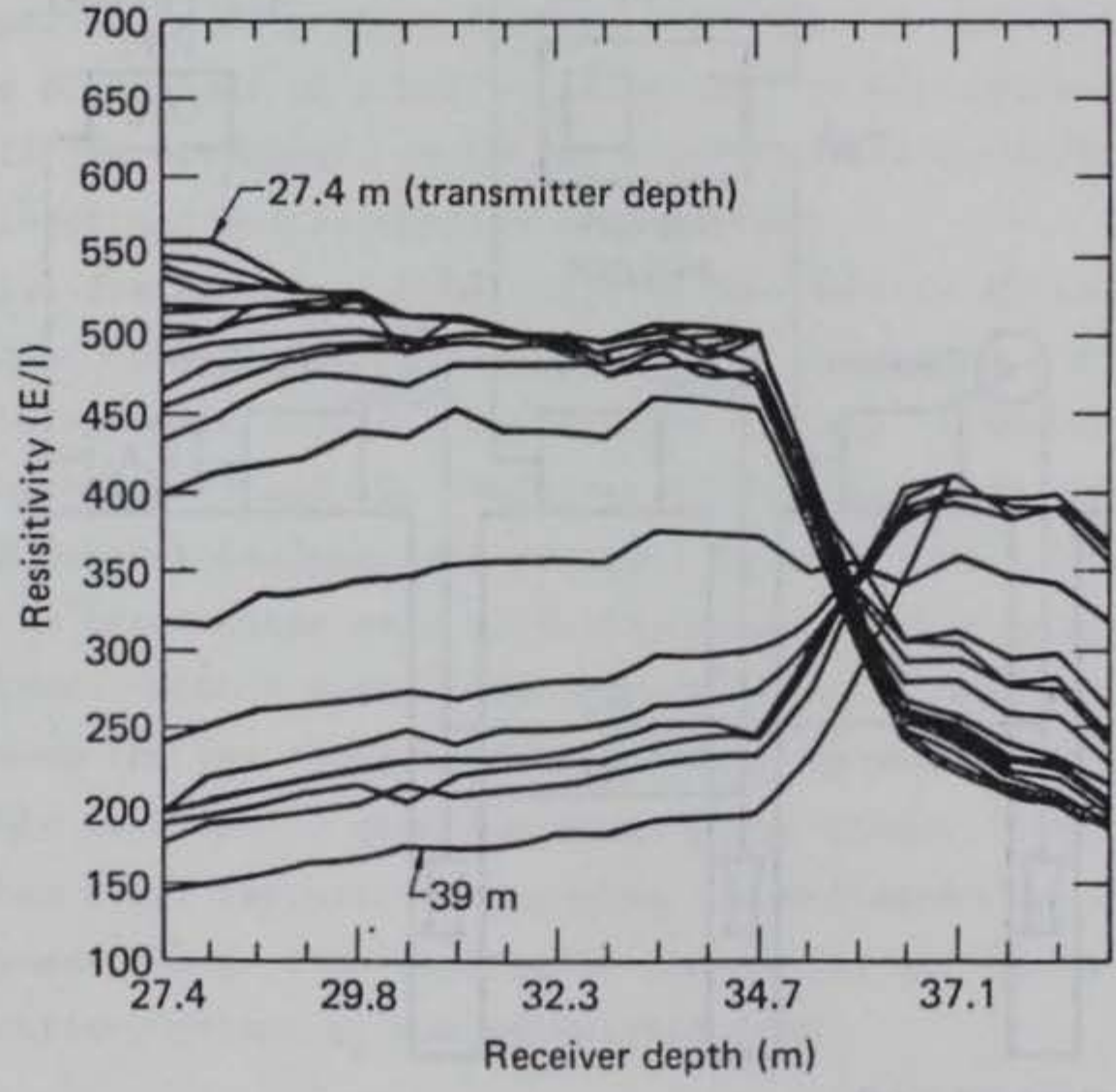

FIG. 8. Plot of resistivity vs depth for boreholes C2 and C3 at Manatee Springs State Park, Florida. Transmitter curves every 2 ft from 90 ft to 128 ft. The transmitter probe is held fixed as the receiver probe depth varied.

MEDFORD CAVES

Medford Caves is a complex of limestone tunnels and caves on private property about 16 km north of Ocala on Old Highway 441 near the small town of Reddick, Florida (see Fig. 3). The caves are shallow (3 to 10 m below ground level), dry, and the interiors are accessible (for younger and more agile experimenters). The interiors are quite irregular with some steep narrow passageways. A plan view of boreholes at Medford Caves is shown in Fig. 9.

Cross-Borehole Electromagnetics

At Medford Caves, we repeated the cross-borehole method used at Manatee Springs. Cross-borehole, high-frequency electromagnetic measurements were made in two different locations. We made single-frequency depth scans between two boreholes as shown in Fig. 10. The scan was made between boreholes C3 and C5 at an operating frequency of 100 MHz. Physical examination of the area between the boreholes (i.e., inside the cave) shows a very broken and irregular shape for a cut-away section of the cavity. This irregular shape,

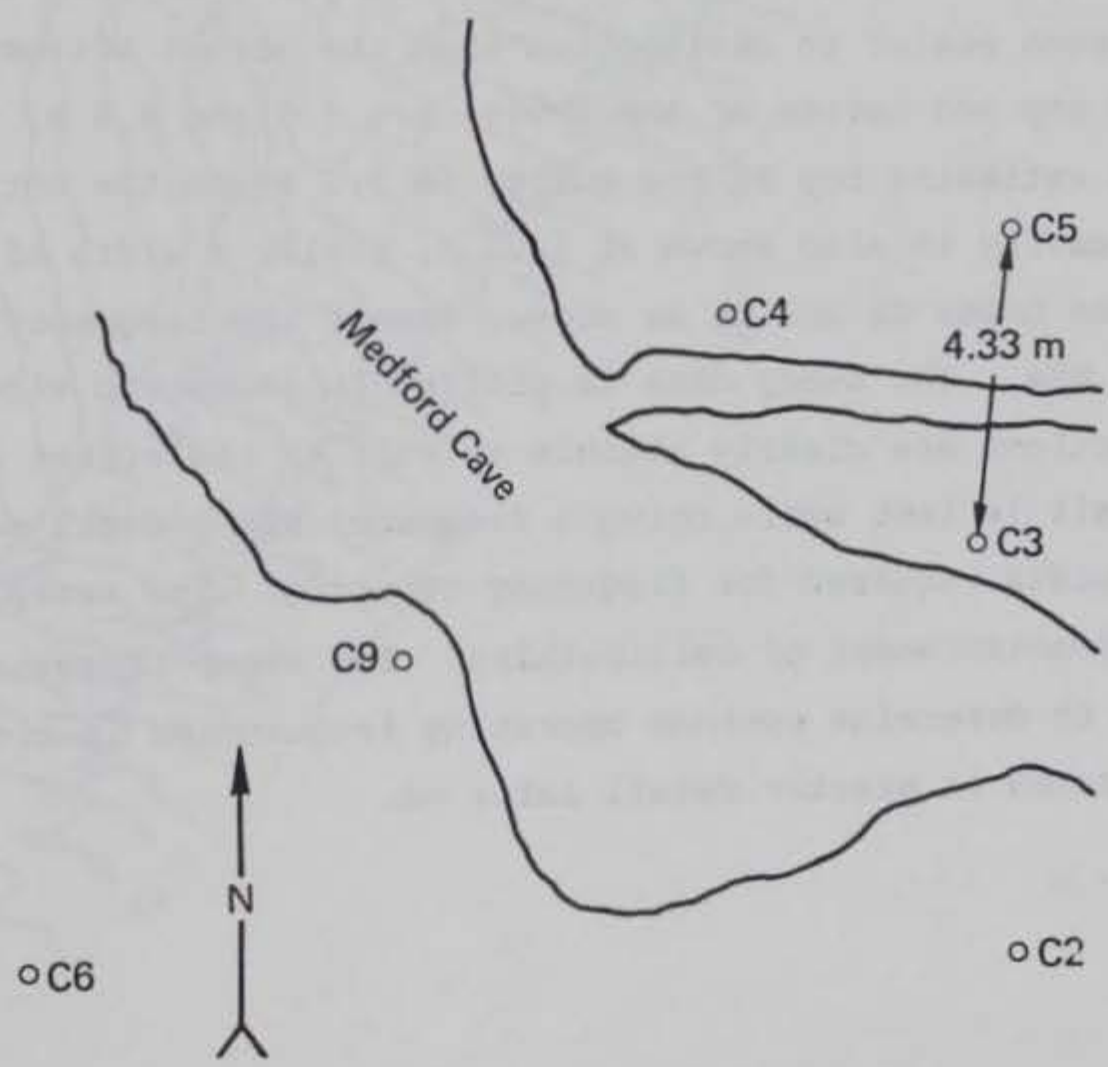

FIG. 9. Plan view of boreholes at Medford Caves, Florida.

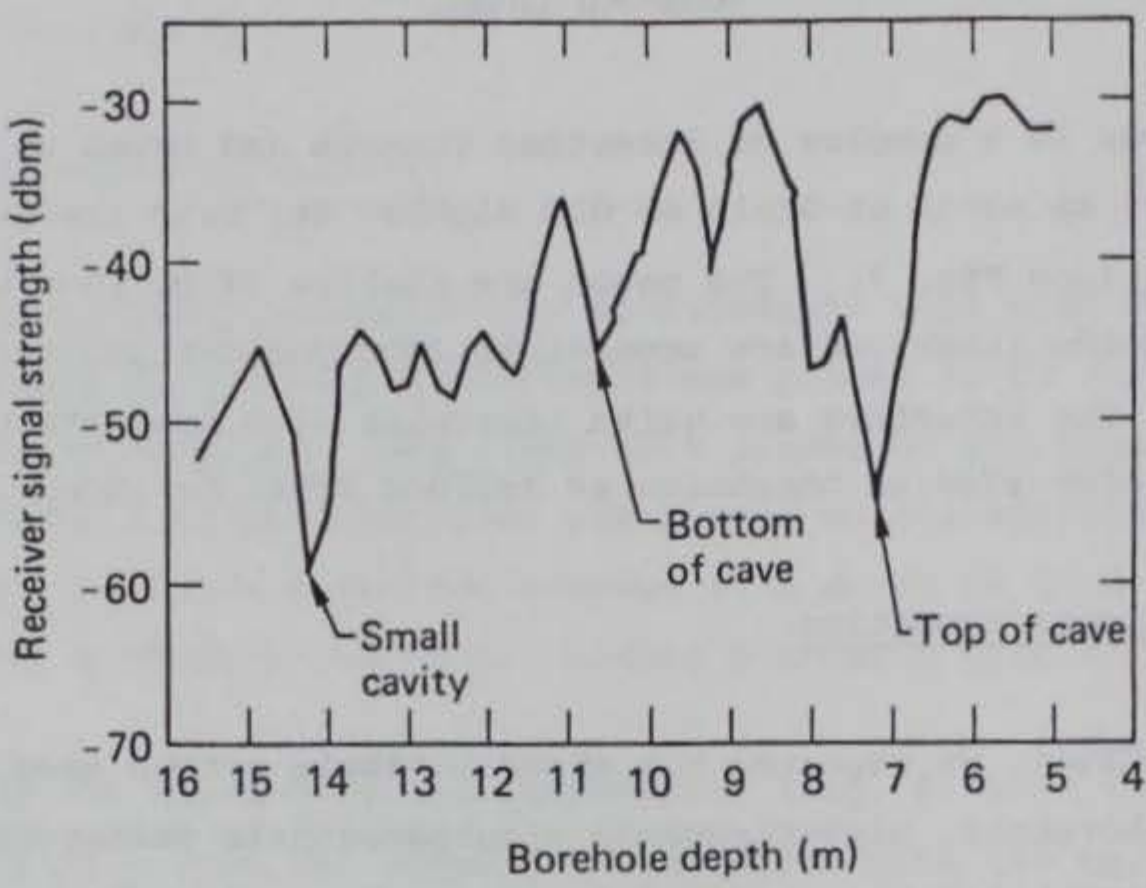

FIG. 10. Plot of high-frequency EM transmission between boreholes C3 and C5 at Medford Caves. The frequency is fixed at 100 MHz.

we believe, causes a complicated diffraction pattern than can easily confuse the diagnosing of the cavity location. For this particular cave area, the top of the cavity is much easier to distinguish than the actual bottom.

The measured top and bottom of the cavity are 7.3 and 9.8 m, respectively. From Fig. 10, the estimated top of the cavity is 7.2 m and the bottom is 10.6 m. A small cavity is also shown at 14.2 m, having a width of about 50 cm. We scanned the same holes C3 and C5 as above, except the frequency was swept from 5 MHz to 105 MHz. The sweep data is plotted in isometric view in Fig. 11. The surface reflections are clearly visible as well as the effect of the tunnel. Some detail is lost while doing a frequency sweep depth scan because of the wider bandwidth required for frequency sweeping. The sweep is a very useful preliminary measurement of multipathing. The sweep frequency technique is generally used to determine optimum operating frequencies in order to make single-frequency scans in greater detail later on.

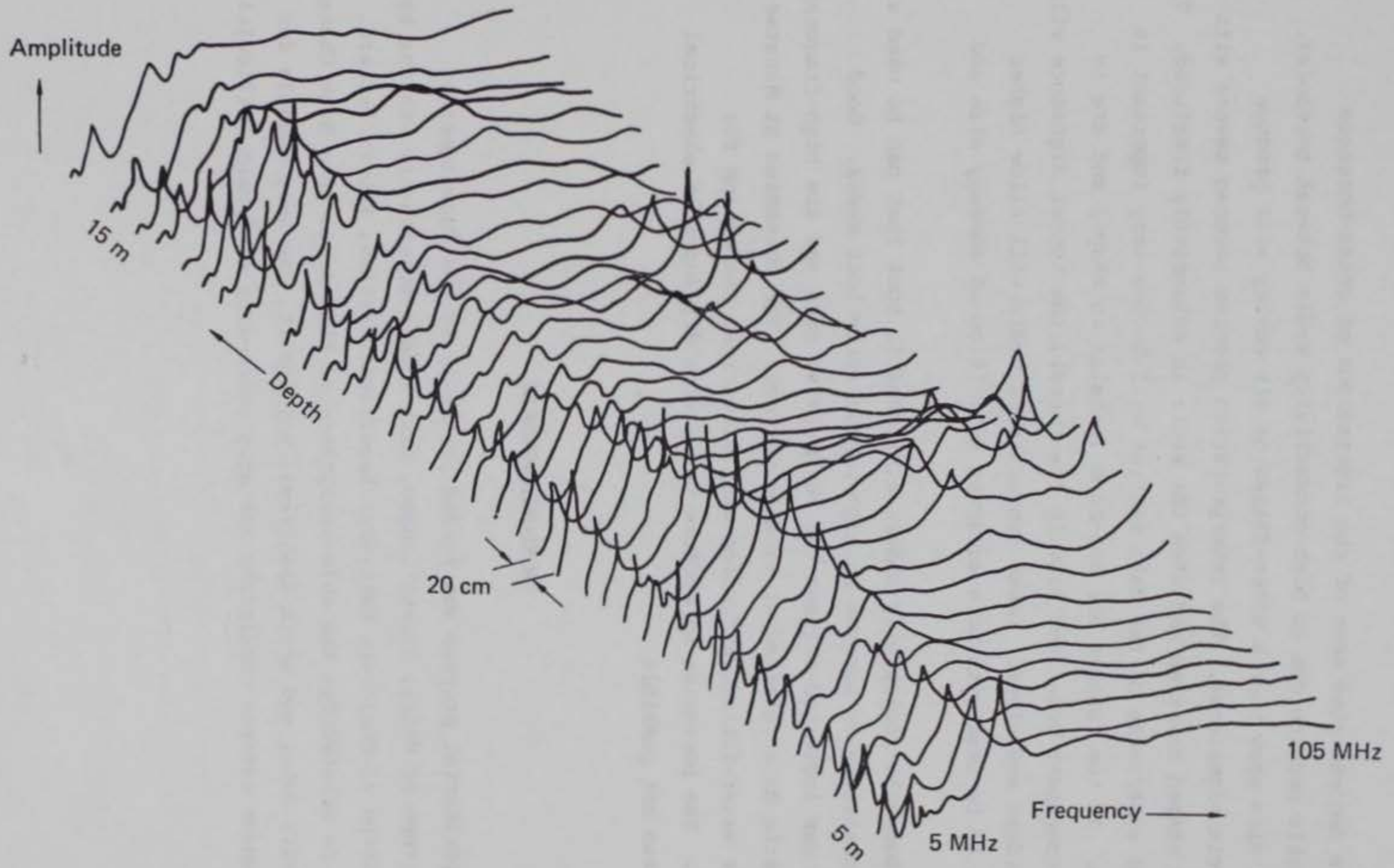

FIG. 11. Swept frequency plot between boreholes C3 and C5 at Medford Caves, Florida. The decreasing signal amplitude is in the up direction.

CONCLUSIONS

We have demonstrated some of the limitations of cross-borehole electromagnetic probing due to high-conductivity media between boreholes. These tests also show that a water-filled or air cavity will produce characteristic signatures. The interpretation problem becomes severe with irregularly shaped cavities and when the media is extensively fractured. The judgment and experience of the data analyst will become very important in these cases. If the tunnels are man-made (regular in shape) and are in reasonably competent rock (not heavily fractured), the tunnel signature will be quite evident and clear. Lower conductivity media will allow higher frequencies to be used with more accurate definition of anomaly size and position.

Cross-borehole resistivity offers a diagnostic tool that can be used with a higher probability of success in high-conductivity host media. Good correlation was indicated between the resistivity data and the high-frequency electromagnetic data obtained at Manatee Springs. The boreholes at Manatee Springs were water-filled, affording easy electrical connection for resistivity. The boreholes at Medford Caves were dry and thus electrical connection was not possible.

ACKNOWLEDGMENTS

The experimental program was funded primarily by the Department of Interior, Bureau of Mines, Joseph Condon, with some supplementary funding by U. S. Army Corps of Engineers Waterways Experiment Station, Robert Ballard. I also wish to acknowledge the able assistance of LLNL personnel, Nick Chakakis, for the resistivity data; and Keith Kishiyama, Ray Egbert, and Doug Nuchols for performing under adverse conditions and ably overcoming equipment difficulties.